POLITECNICO
MILANO 1863

SCUOLA DI INGEGNERIA INDUSTRIALE
E DELL'INFORMAZIONE

# Love Dynamics and the Transition to Parenthood: a Modeling Approach

Tesi di Laurea Magistrale in
Mathematical Engineering - Ingegneria Matematica

Author: **Matilde Polizzi**

Student ID: 258749
Advisor: Prof. Alessandra Gragnani
Academic Year: 2025-26

# Abstract

The transition to parenthood is widely recognized as a major life event that may profoundly reshape the emotional dynamics of a couple. While empirical research highlights both positive and negative relational outcomes, attachment theory suggests that individual differences play a crucial role in determining how couples adapt to caregiving demands. This thesis develops a nonlinear dynamical system framework to model the impact of parenthood on romantic relationships. Building upon an established model of love dynamics described by a system of two ordinary differential equations, we introduce two additional parameters representing caregiving intensity and the distribution of responsibilities between partners. These extensions allow us to investigate how childcare demands modify the long-term average levels of emotional involvement and the qualitative structure of relational dynamics. The analysis is conducted across different attachment configurations, including secure–secure and secure–insecure couples, under constant caregiving demands. In configurations composed of two secure partners, increasing caregiving intensity generally reduces equilibrium involvement, while responsibility allocation generates trade-offs between equity, total emotional engagement, and robustness. In configurations involving one insecure and one secure partner, especially in the presence of synergism, constant caregiving may generate or suppress cyclic dynamics, showing how attachment asymmetry can qualitatively reshape the system's behavior. Moreover, when caregiving demands vary periodically, the interaction between intrinsic nonlinear dynamics and external modulation may produce quasi-periodic regime or chaotic attractors. These findings show that both the intensity and temporal variability of caregiving demands contribute to shaping couple dynamics. Overall, the thesis illustrates how parenthood acts as a structural perturbation of love dynamics, generating multiple possible relationship regimes depending on attachment styles and caregiving structure.

**Keywords:** Nonlinear dynamical systems, bifurcation analysis, love dynamics, transition to parenthood, attachment theory

# Abstract in lingua italiana

La transizione alla genitorialità rappresenta uno dei passaggi più significativi della vita adulta e può incidere profondamente sulle dinamiche emotive all'interno della coppia. La letteratura empirica evidenzia esiti eterogenei, talvolta positivi e talvolta critici, mentre la teoria dell'attaccamento sottolinea il ruolo delle differenze individuali nel determinare il modo in cui i partner affrontano le nuove responsabilità legate all'arrivo di un figlio. La presente tesi propone un modello nell'ambito dei sistemi dinamici non lineari per analizzare l'impatto della genitorialità sulle relazioni romantiche. A partire da un modello preesistente delle dinamiche amorose, descritto tramite un sistema di equazioni differenziali ordinarie, vengono introdotti due parametri aggiuntivi: l'intensità delle esigenze di accudimento del bambino e la distribuzione delle responsabilità tra i partner. Ciò consente di studiare come tali fattori influenzino i livelli di coinvolgimento emotivo all'equilibrio e la struttura qualitativa delle dinamiche relazionali. L'analisi viene condotta su diverse configurazioni di coppia (sicuro–sicuro, sicuro–insicuro e sicuro–insicuro con sinergismo), considerando sia esigenze di accudimento costanti sia, in un caso specifico, variabili nel tempo. I risultati mostrano che l'aumento delle responsabilità genitoriali tende generalmente a ridurre il coinvolgimento emotivo, ma che la distribuzione dei compiti introduce un delicato equilibrio tra equità, intensità del legame e robustezza dinamica della relazione. In configurazioni composte da un individuo insicuro e uno sicuro, in presenza di sinergismo, la genitorialità può generare o sopprimere regimi ciclici, evidenziando come l'interazione tra attaccamento e accudimento riorganizzi qualitativamente il sistema. Quando le esigenze di accudimento presentano una variabilità periodica, emergono comportamenti più complessi, quali dinamiche quasi-periodiche e caotiche. Nel complesso, la genitorialità si configura come una perturbazione strutturale delle dinamiche di coppia, capace di generare molteplici esiti relazionali in funzione delle caratteristiche individuali e delle scelte organizzative adottate dai partner.

**Parole chiave:** Sistemi dinamici non-lineari, analisi di biforcazione, dinamiche d'amore, transizione alla genitorialità, teoria dell'attaccamento

# Contents

# Introduction

The birth of a first child is widely recognized as one of the most significant transitions in adult life. It is often associated with profound joy and meaning, but also with substantial stress and adjustment demands for new parents, as it entails a deep reorganization of daily routines, personal identities, and relational roles, making it a critical phase in the life of a couple. Early studies described this transition as a genuine "crisis" for the couple [15, 31], an idea that stimulated decades of empirical research. A large body of literature has since documented that, on average, the transition to parenthood is accompanied by a decline in marital satisfaction and relationship quality [3, 24], a reduction in sexual satisfaction [23], and an increase in conflicts and disagreement [11, 27, 28]. At the same time, other studies have emphasized the positive aspects of becoming a parent, highlighting increased meaning in life, personal growth, shared goals and enhanced well-being within the couple [10, 39]. Rather than representing a uniformly negative or positive experience, parenthood therefore appears as an intrinsically ambivalent transition. One possible reason for the observed deterioration in some relationships lies in the contrast between the often idealized cultural representation of parenthood and the concrete demands it imposes, since new parents may enter this phase with unrealistic expectations about caregiving, intimacy, and relational balance, only to face fatigue, time constraints, and competing responsibilities. As a result, the need to renegotiate roles and redistribute emotional and practical resources can place the couple under considerable strain [10].

One of the most influential frameworks for explaining these heterogeneous outcomes is attachment theory. A substantial amount of research has examined how attachment style affects the transition to parenthood, showing that it is associated with more or less desirable relational outcomes [29, 34, 42, 48]. In this work, attachment styles are grouped into two broad categories: secure and insecure. Secure individuals are characterized by a positive view of themselves and others and are generally comfortable with intimacy and emotional closeness. Insecure individuals, by contrast, tend to experience difficulties with closeness and may fear dependency on their partner, particularly in emotionally demanding situations [1, 6]. Moreover, individuals may exhibit synergism, meaning that their reaction to their partner's appeal or their response to the partner's love can be amplified

by the level of involvement they already experience [43]. Building on this distinction, several studies have reported that high levels of attachment insecurity are associated with greater difficulties during the transition to parenthood, including increased stress and poorer relational adjustment (see, e.g., [29, 42]). These findings suggest that attachment style plays a central role in shaping how couples respond to caregiving demands and reorganize their emotional dynamics following the birth of a child.

This thesis proposes an application of dynamical systems theory to social psychology, with a particular focus on the dynamics of romantic relationships. One of the earliest attempts to describe love affairs using mathematical models was introduced by Strogatz [46], and was subsequently followed by several publications on couple dynamics and romantic interactions [18–20, 38, 44]. More recently, mathematical approaches have been applied to the impact of the transition to parenthood on couples [16], where individual emotions are represented as oscillatory systems. This work is based on the model introduced in [38], where a romantic couple is described by a system of ordinary differential equations. Each partner is associated with a state variable measuring their emotional involvement toward the other, and the dynamics are governed by three fundamental mechanisms: oblivion process, representing the spontaneous decay of feelings in the absence of interaction; reaction to appeal, which captures sensitivity to the partner's attractiveness; and reaction to love, describing how an individual responds to the partner's emotional involvement. Depending on individual characteristics, couples may exhibit either robust or fragile dynamics: robust couples are characterized by a single stable equilibrium, while fragile couples display bistability, with two stable equilibria separated by a saddle point.

Against this background, this thesis proposes a dynamical model aimed at explaining how the birth of a child may impact the emotional dynamics of a couple, highlighting the role of individual traits and caregiving demands in shaping stability and long-term relationship outcomes.

In Chapter 1, we introduce the couple's model and a modified version in which the presence of a child is represented by two additional parameters: $N$, measuring the overall caregiving demand, and $\epsilon$, describing how caregiving responsibilities are divided between the partners. The dynamical consequences of this extension are then systematically investigated. In Chapter 2, we analyze couples composed of two secure and non-synergic individuals, focusing on how caregiving demands affect robustness, bifurcation structure, and equilibrium levels of emotional involvement. In Chapter 3, a similar analysis is carried out for couples composed of one secure and one insecure individual, both non-synergic, highlighting the role of different attachment styles in shaping the effects of parenthood. Finally, in Chapter 4, we complete the analysis by introducing synergism, which, when

combined with insecure attachment, may give rise to cyclic dynamics. This allows us to explore a broader range of qualitative behaviours and to further investigate the complex interplay between emotional responsiveness, caregiving demands, and relational stability.

# 1 | The Model

In this chapter, we introduce the notation and mathematical framework used throughout the thesis. After presenting the original model of love dynamics, we develop its modified formulation, in which caregiving intensity and responsibility allocation are incorporated as additional parameters. The analysis is based on one of the models proposed in *Modeling Love Dynamics* [38] and in [21, 35–37], which describes the evolution of romantic relationships in accordance with basic principles from the psychology of love and attachment theory [e.g., Bowlby [6], [7], [8]]. The model assumes that the dynamics of love result from a balance between production and consumption processes. Consumption is represented by an oblivion process, which accounts for the fading of feelings following the end of a romantic relationship, either through abandonment or being abandoned by the partner. Production, instead, arises from an individual's response to the care expected from the partner. This mechanism is divided into two components: the first depends on the intrinsic characteristics of the partner and describes the individual's reaction to appeal; the second depends on the partner's emotional involvement and represents the reaction to love. These components will be discussed in detail in the following sections. Starting from these basic definitions, different categories of individuals can be identified, whose distinct behavioural traits give rise to different asymptotic dynamics of the system. In this sense, once the characteristics of the individuals involved are specified, the long-term evolution of the love relationship can be qualitatively predicted.

The models considered in this work are based on finite systems of $n$ first-order Ordinary Differential Equations (ODEs) of the form:

$$\dot{\boldsymbol{x}}(t) = \boldsymbol{f}(\boldsymbol{x}(t)), \tag{1.1}$$

where $\boldsymbol{x}(t) = (x_1(t),\ x_2(t),\ ...,\ x_n(t))$ is the state of the system and $\dot{\boldsymbol{x}}(t)$ stands for $\frac{d\boldsymbol{x}(t)}{dt}$. Given an initial condition $\boldsymbol{x}(0) \in \mathbb{R}^n$, the equation (1.1) can be integrated in time to obtain the time evolution of the state vector $\boldsymbol{x}(t)$.

In this study, we focus on simple models, also referred to as *minimal* models [38], characterized by $n = 2$ equations, one describing the dynamics of partner 1 and the other of partner 2 in a couple. Before introducing the explicit form of the model, some clarifications are necessary. First, minimal models represent a significant simplification of reality, which is inherently much more complex. Romantic love is a multilayered phenomenon, encircling different components such as friendship, esteem, emotional attachment, and sexual compatibility, and it is therefore difficult to provide a unique and exhaustive definition. The model captures the main qualitative aspects of love dynamics, while neglecting many other factors that could, in principle, be taken into account. Second, there is not any objective and unique way to quantitatively measure love between two individuals. Although several attempts to quantify emotional involvement have been proposed in the literature ([32]. [45]), we adopt an abstract modeling approach. In this context, each partner is described by a state variable $x_i(t)$ representing a qualitative measure of emotional involvement: positive values correspond to positive feelings, while negative values represent negative feelings. The magnitude of $x_i(t)$ does not provide an exact intensity of love, but rather indicates the level of involvement in a qualitative sense. Moreover, we restrict our analysis to the interaction between the two individuals only, neglecting external influences. In reality, exogenous factors such as social pressure, family, or life events may significantly affect the evolution of a relationship; however, these effects are not included in the present model. Accordingly, we consider a system composed of two coupled first-order ODEs, given by:

$$\begin{aligned} \dot{x}_1(t) &= f_1(x_1(t), x_2(t)), \\ \dot{x}_2(t) &= f_2(x_1(t), x_2(t)), \end{aligned} \tag{1.2}$$

Here, $x_i(t)$, with $i = 1, 2$, represents the emotional *involvement* or *feeling* of partner $i$ toward the other partner, while $\dot{x}_i(t)$ denotes its rate of change over time. The functions $f_i$ in the model (1.2) are defined as the balance between consumption and production of love. The consumption term is represented by the *oblivion* process $O_i$. The production term consists of two contributions: the *reaction to love*, denoted by $R_i^L$, and *reaction to appeal*, denoted by $R_i^A$. As a result, the evolution of the involvement variable $x_i$ can be written in the form:

$$\dot{x}_i = O_i + R_i^A + R_i^L, \tag{1.3}$$

where the explicit dependence on $t$ has been omitted for notational simplicity, while the

detailed expressions of each term will be provided in Sections 1.1, 1.2, 1.3.

Although the proposed model represents a strong simplification of reality, it is able to capture the essential mechanisms underlying the dynamics of romantic relationships, as we can see in the results of [38]. By focusing on a limited number of key variables, the model allows for a clear qualitative analysis while retaining meaningful interpretability.

## 1.1. Oblivion process

The oblivion process can be studied by considering an individual who has abandoned or has been abandoned by the partner, i.e., $R_i^A = R_i^L = 0$. In this situation, the *feeling* $x_i(t)$ is expected to decay in time as the emotional attachment fades. A common and mathematically convenient assumption is that this decay is proportional to the current level of involvement, leading to an exponential relaxation. Therefore, we assume that $x_i(t)$ decays exponentially to zero at a rate $\alpha_i$, called the *forgetting coefficient*, so that:

$$\dot{x}_i = -\alpha_i x_i, \tag{1.4}$$

where the linear dependence of the consumption term is inspired by analogous relaxation processes in physics and chemistry (e.g., radioactive decay, cooling, first-order chemical reactions). In this case, the oblivion term is: $O_i = -\alpha_i x_i$. The solution of (1.4) is:

$$x_i(t) = x_i(0)\exp(-\alpha_i t), \tag{1.5}$$

where $\alpha_i$ is the inverse of the time needed to forget a former partner after the breakup and its interpretation is shown in Figure 1.1.

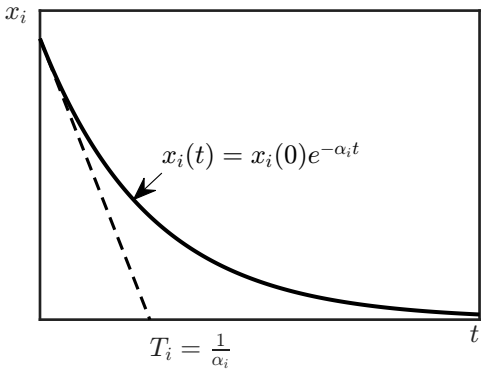


Figure 1.1: Exponential decay of interest in the partner after the separation.

## 1.2. Reaction to appeal

The appeal of partner $j$ perceived by partner $i$ is denoted by $A_j$ [38]. In general, appeal cannot be reduced to physical attractiveness alone, but rather represents a multidimensional concept embracing several personal and social characteristics. These may include, for instance, physical appearance, intelligence, age, education level, social status, and other individual traits that can influence attraction. The perceived appeal is assumed to be independent of the emotional involvement $x_i(t)$. To account for this multidimensional nature, the appeal $A_j$ is described through a set of $h$ components $A_j^h$, each corresponding to a specific aspect of attraction. Individual $i$ assigns a weight $\lambda_i^h$ to each component, reflecting the relative importance of the $h$-th characteristic in shaping their perception. The total appeal of partner $j$, perceived by partner $i$, is then defined as the weighted sum:

$$A_j = \sum_h \lambda_i^h A_j^h, \tag{1.6}$$

This formulation highlights that appeal is not an intrinsic property of an individual, but rather it depends on how the partner's characteristics are perceived and evaluated. On the basis of this definition, we can introduce the production term associated with the reaction to appeal, $R_i^A$:

$$R_i^A = \gamma_i A_j \tag{1.7}$$

where $\gamma_i$ is the sensitivity of individual $i$ to the partner's appeal. In the present model, the reaction to appeal is assumed to be time-invariant. Although perceived appeal may evolve over time, this assumption is justified by restricting the analysis to time scales over which both the components of appeal and the individual sensitivity $\gamma_i$ can be considered approximately constant.

## 1.3. Reaction to love

The reaction to love $R_i^L$ necessarily depends on the emotional involvement of the partner $x_j(t)$. According to well-established results in attachment theory (e.g. Bolwby [6]), individuals can be broadly classified into two main categories: *secure* and *insecure* attached individuals.

Secure individuals are characterized by a positive representation of both themselves and others [1, 6]. Their romantic relationships typically involve emotional closeness, intimacy, mutual respect, and stable involvement. Consequently, secure individuals tend to respond positively to increases in their partner's emotional involvement, without experiencing fear of closeness or intimacy. From a modeling perspective, these psychological traits suggest that the reaction to the partner's emotional involvement should be monotonically increasing: as the partner's level of engagement rises, a secure individual tends to respond with increasingly positive involvement. For this reason, for *secure* individuals, we adopt the following reaction function:

$$R_i^L(x_j) = \frac{e^{x_j} - e^{-x_j}}{\frac{e^{x_j}}{R_i^+} - \frac{e^{-x_j}}{R_i^-}}, \tag{1.8}$$

where $R_i^+ > 0$ and $R_i^- < 0$ are the asymptotic limits for $R_i^L(x_j)$ for $x_j \to +\infty$ and $x_j \to -\infty$ respectively, as shown in Figure 1.2.

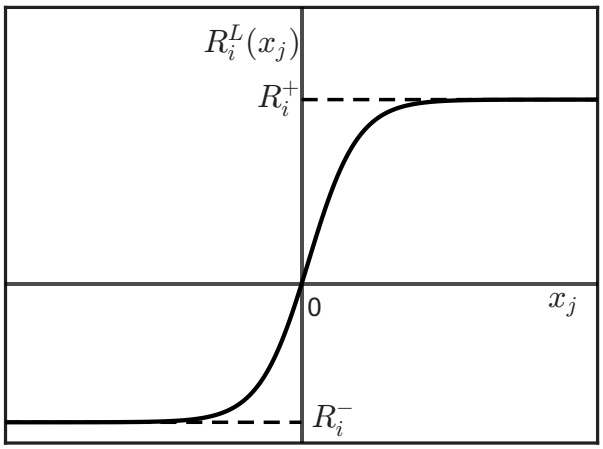


Figure 1.2: Reaction to love for a secure individual.

Conversely, *insecure* individuals typically experience difficulties in tolerating emotional closeness and may fear dependency on their partner [1, 6]. In romantic relationships, this can manifest as discomfort with intimacy, difficulty in trusting the partner, and a tendency to withdraw emotionally when the level of closeness becomes too intense. As a result, insecure individuals are unlikely to respond with increasing involvement when their partner becomes more emotionally engaged. Instead, their reaction tends to weaken beyond a certain threshold, as higher levels of closeness trigger fear of losing independence or of being overwhelmed by the relationship. For these reasons, insecure individuals

are modeled following [38]; however, the functional form has been modified to ensure a saturated behavior for negative values of $x_j$:

$$R_i^L(x_j) = \begin{cases} \beta_i x_j e^{-k_i x_j} & \text{if } x_j \geq 0 \\ \frac{e^{x_j} - e^{-x_j}}{\frac{e^{x_j}}{R_i^+} - \frac{e^{-x_j}}{R_i^-}} & \text{if } x_j < 0 \end{cases} \tag{1.9}$$

where $\beta_i$ measures the reactivity of individual $i$ to the partner's love and $k_i$ determine the values of the partner's involvement $x_j^*$ at which the reaction reaches its maximum (see Figure 1.3). Moreover, in order to ensure that the derivative of $R_i^L(x_j)$ is continuous at $x_j = 0$, the asymptotic value $R_i^+$ must satisfy the relation:

$$R_i^+ = \frac{1}{\frac{1}{R_i^-} + \frac{2}{\beta_i}}$$

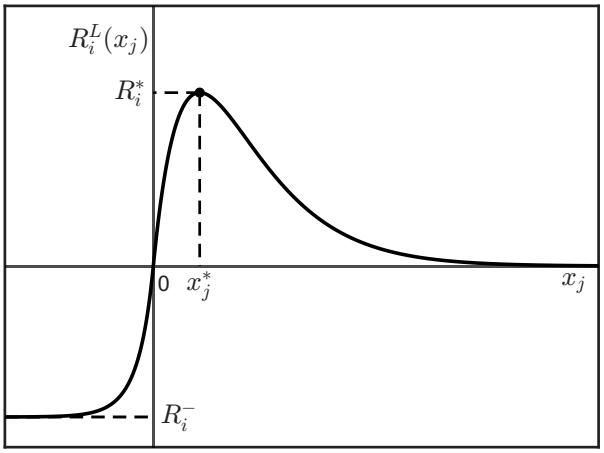


Figure 1.3: Reaction to love for an insecure individual. ($x_j^* = \frac{1}{k_i}$, $R_i^* = \frac{\beta_i}{e k_i}$)

## 1.4. Synergism

Sometimes, when strong emotional involvement is present, the perception of the partner may no longer remain fully objective, but instead be enhanced by love itself. This phenomenon, referred to as *synergism*, was first observed in a study comparing the perception of attractiveness between individuals involved in a romantic relationship and individuals who were not [43]. From a modeling perspective, synergism can reasonably be assumed to affect both the reaction to love $R_i^L(x_j)$ and the reaction to appeal $R_i^A$, as discussed in [38].

Taking these effects into account, the reactions to appeal and to love can be rewritten as:

$$R_i^A(x_i) = (1 + s_i^A S_i^A(x_i))\gamma_i A_j,$$
$$R_i^L(x_i, x_j) = (1 + s_i^L S_i^L(x_i))R_i^L(x_j),$$

where $R_i^L(x_j)$ denotes the reaction to love of a non-synergic individual. The functions $S_i^A(x_i)$ and $S_i^L(x_i)$ are equal to zero for $x_i \leq 0$ and increase monotonically from 0 to 1 for $x_i > 0$, as shown in Figure 1.4. Parameters $s_i^A$ and $s_i^L$ represent the synergism coefficients associated, respectively, with the reaction to appeal and the reaction to love: they vanish for non-synergic individuals, while they take positive values for synergic individuals. The synergism is modeled through the function:

$$S_i(x_i) = \begin{cases} 0 & \text{if } x_i < 0 \\ \frac{x_i^m}{\sigma_i^m + x_i^m} & \text{if } x_i \geq 0 \end{cases} \tag{1.10}$$

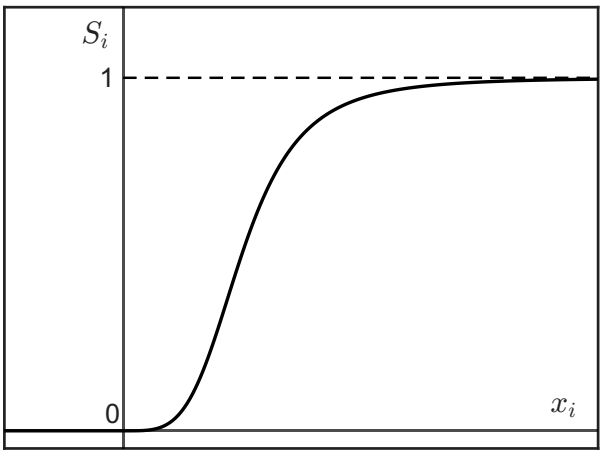


Figure 1.4: The graph of a typical synergism function $S_i(x_i)$ for a synergic individual.

## 1.5. Resulting model for couples

In the previous sections, we have discussed the individual behavioral characteristics that influence the emotional dynamics between two partners. By incorporating all these features into the general system (1.3), and assuming that synergism acts exclusively on the appeal term, we obtain the following two-dimensional model:

$$\begin{cases} \dot{x}_1 = -\alpha_1 x_1 + (1 + s_1^A S_1^A(x_1))\gamma_1 A_2 + R_1^L(x_2) \\ \dot{x}_2 = -\alpha_2 x_2 + (1 + s_2^A S_2^A(x_2))\gamma_2 A_1 + R_2^L(x_1) \end{cases} \tag{1.11}$$

All parameters are assumed to be constant in time, thereby neglecting possible long-term changes in individual characteristics, which may occur over much longer time scales [40]. The functional form of the reaction to love must be chosen according to the attachment style of each individual: Equation (1.8) is adopted for secure individuals, while Equation (1.9) is used for insecure ones. Moreover, it is necessary to specify whether the synergistic term given in Equation (1.10) is included.

In the case of non-synergic individuals, two qualitatively different behaviours can arise [38]. The system may admit either a single stable equilibrium, or two stable equilibria. Couples characterized by the presence of a single equilibrium are referred to as *robust couples*: in this case, perturbations of the system do not alter the long-term outcome ($E^*$), and the dynamics always return to the same equilibrium state (see Figure 1.5a). Conversely, couples displaying two stable equilibria are said *fragile couples*: for these couples, some perturbations may lead to a transition from mutual attraction ($E_1^*$) to hostility ($E_2^*$), or vice versa 1.5b.

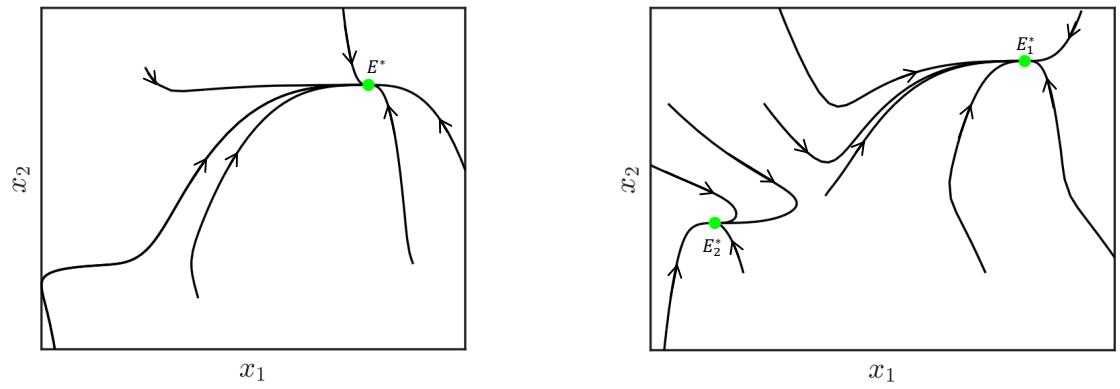


(a) Robust couple (b) Fragile couple

Figure 1.5: Comparison between robust and fragile configurations.

If instead we consider couples characterized by insecurity and synergism, a different qualitative behaviour may emerge. In this case, the system can exhibit *cyclic* dynamics [21, 38], in which the emotional involvement of the two partners does not converge to a stationary state but instead displays recurrent and periodic oscillations. An example of such periodic behaviour is shown in Figure 1.6.

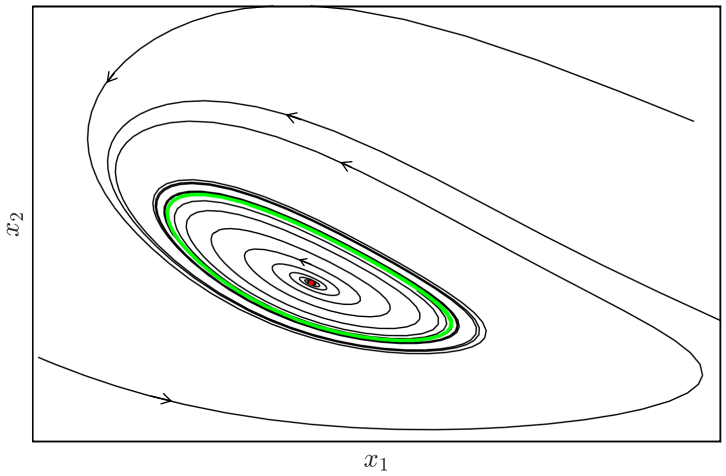


Figure 1.6: Example of cyclic regime in the phase plane.

## 1.6. Caregiving

After introducing the basic notation and the main mechanisms governing love dynamics, we now present a modified version of the model. In this work, the original couple model is extended to describe how relational dynamics may change following the transition to parenthood.

The birth of a child represents a major life event for a couple and has been shown to significantly affect relationship dynamics. Several empirical studies report that this transition is often associated with increased stress and changes in intimacy and communication patterns [4, 13, 14, 26]. While many works document an average decline in relationship satisfaction, it is important to note that this outcome is not universal: for some couples, parenthood may also strengthen emotional bonds, increase cooperation, or foster a renewed sense of shared purpose [41]. Regardless of the direction of the change, the transition to parenthood requires partners to reorganize their roles and redistribute time, attention, and emotional resources. In particular, new parents tend to devote a substantial portion of their cognitive and emotional energy to the child [26]. This shift may reduce the attention directed toward the partner, potentially leading to fatigue, communication difficulties, or reduced intimacy [23, 25], but it may also promote mutual support and collaboration within the couple [10].

Motivated by these observations, we propose a first modeling approach in which the presence of a child is represented through the introduction of two additional parameters: $N \geq 0$ represents the overall level of needs associated with the child, while $\epsilon \in [0, 1]$ denotes the fraction of caregiving responsibilities assumed by partner 1, with $(1 - \epsilon)$

representing the fraction assumed by partner 2. In this framework, $N = 0$ corresponds to the absence of caregiving demands (i.e., the absence of the child), the case $\epsilon = 1$ indicates that partner 1 assumes the entire caregiving load, whereas $\epsilon = 0$ corresponds to partner 2 bearing all responsibilities; intermediate values of $\epsilon$ represent different allocations of caregiving tasks between the partners. This modeling choice reflects the idea that the distribution of caregiving responsibilities can significantly influence both individual and relational outcomes, as documented in the literature (see, e.g, [17]).

Within the framework of our model, these parameters are incorporated into the reaction to love term. This modeling choice reflects the idea that the child does not directly modify the partners' perceptions of each other, but rather competes for their emotional attention. Depending on individual characteristics and initial conditions, this redistribution of emotional resources may lead either to a weakening or to a reorganization, and in some cases a strengthening, of the couple's emotional dynamics.

Although the literature reports some gender-related differences in the transition to parenthood (see, e.g., [3], [34], [9]),in this work we adopt a simplified representation of reality, considering individuals different solely on the basis of their attachment style [42]. This assumption allows us to reduce the dimensionality of the model while preserving its generality with respect to the type of couple considered and retaining the key psychological mechanisms of interest. Denoting by $N_1 = \epsilon N$ and $N_2 = (1 - \epsilon)N$ the caregiving loads assigned to partner 1 and partner 2, respectively, we model the impact of parenthood by modifying the reaction to love function $R_i^L(x_j)$. The underlying idea is that caregiving demands reduce the emotional resources available for responding to the partner's involvement. Since the functional form of $R_i^L$ depends on the attachment style, it is necessary to distinguish between secure and insecure individuals.

For secure individuals (Equation (1.8)), the presence of the child is assumed to affect the asymptotic levels of the reaction to love, rather than its qualitative shape. In particular, increasing caregiving demands are expected to limit the maximum positive (and negative) response that an individual can exhibit toward the partner, while preserving the monotonic nature of the reaction function. This effect is modeled by rescaling the asymptotic values as follows:

$$R_i^{\pm} \to \frac{R_i^{\pm}}{1 + h_i N_i} \tag{1.12}$$

Here, the parameters $h_i$, $i = 1, 2$, quantify how sensitive each individual's emotional reactivity is to the caregiving load, and therefore regulate how strongly the asymptotic values

decrease as functions of $N$ and $\epsilon$. Figures 1.7 and 1.8, show how variations in $\epsilon$ and $N$ may differently affect the emotional responses of the two partners.

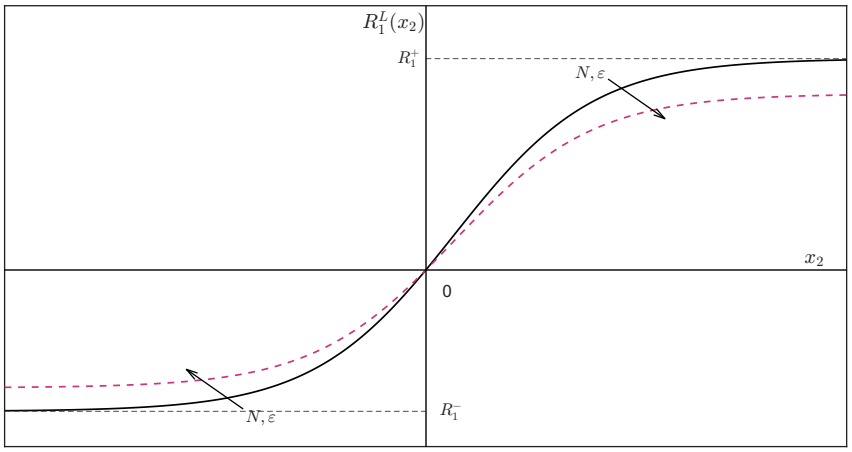


Figure 1.7: Reaction to love of a secure partner 1. The solid line represents the baseline case, while the pink dashed line illustrates the effect of increasing values of $N$ or $\epsilon$.

If instead we consider an insecure individual, the reaction to love must be modified differently. For the sake of clarity, we assume that partner 1 is insecure; the case in which partner 2 is insecure is obtained analogously by replacing $N_1$ with $N_2$. As discussed previously, insecure individuals tend to experience discomfort when emotional closeness becomes intense, and their reaction to love is described by a non-monotonic function of the partner's involvement (see equation (1.9)). In this case, the presence of a child is expected to amplify feelings of emotional overload, due to increased responsibilities and perceived demands [6]. From a modeling perspective, this suggests that parenthood should not only attenuate the overall intensity of the reaction, but should also affect the level of partner involvement at which the insecure individual reaches the maximum of emotional response. For this reason, we intervene on the parameter $k$, which determines the location of the peak of the reaction function, rather than on $\beta$, which controls the intrinsic reactivity to love and is interpreted as a stable individual trait. More precisely, while the asymptotic value $R_1^-$ is modified as in the equation (1.12), the parameter $k$ is rescaled according to:

$$k_1 \to k_1(1 + N_1 h_1), \tag{1.13}$$

where $h_1$ plays the same role as in the secure case, regulating the sensitivity of the reaction function to the caregiving load. We can see in Figure 1.9 the effects of $N$ and $\epsilon$ on the reaction function.

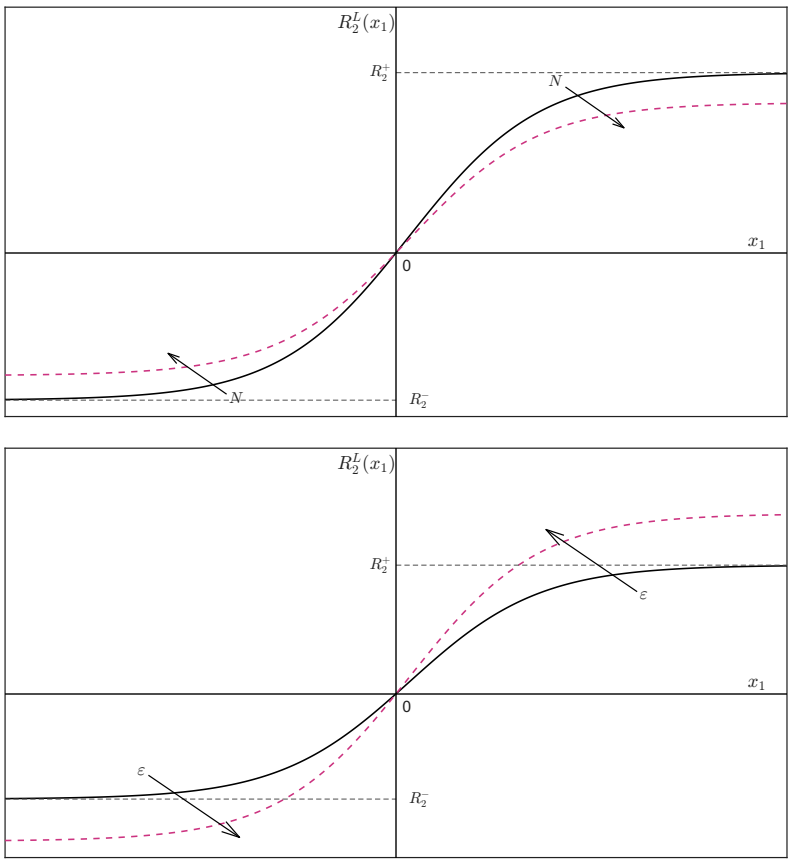


Figure 1.8: Reaction function $R_2^L(x_1)$ of a secure partner 2. The solid line represents the baseline case, while the pink dashed line illustrates the effect of increasing values of $N$ or $\epsilon$. Top panel: $\varepsilon = 0.5$ and increasing $N$. Bottom panel: $N = 1$ and increasing $\varepsilon$.

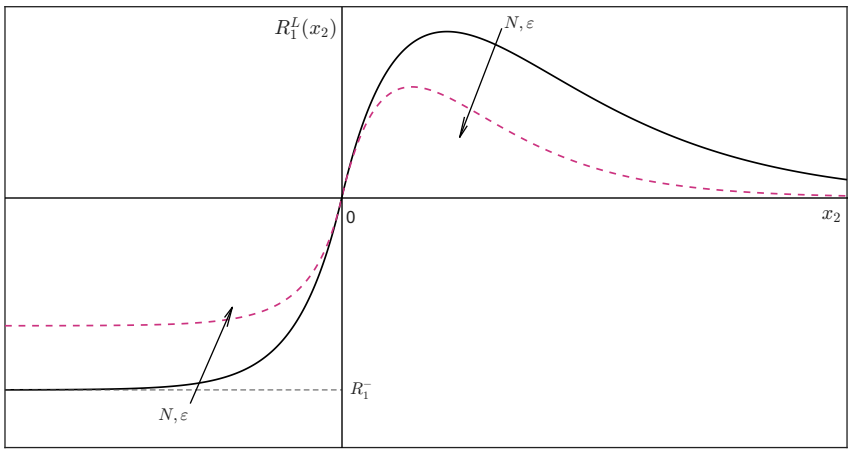


Figure 1.9: Reaction to love of an insecure partner 1. The solid line denotes the baseline case, while the pink dashed line shows the effect of increasing $N$ or $\epsilon$.

The modeling framework is now complete, and the resulting system can be expressed as (1.11), with parameters suitably adjusted according to individual characteristics.

Before proceeding, it is worth making a final remark on the role of the parameters. Quantifying psychological traits such as emotional reactivity or sensitivity to love is inherently nontrivial. Although some studies have proposed quantitative approaches to these aspects by identifying categories of individuals with high or low responsiveness to emotional involvement [22, 32], a precise estimation of such parameters would require extensive longitudinal data, typically obtained through prolonged observation or detailed questionnaires administered over weeks or months. In this work, we do not address the problem of parameter identification from empirical data. Instead, the focus is on the qualitative behaviour of the model. By exploring different parameter regimes, we aim to investigate whether the resulting dynamics are consistent with patterns and phenomena reported in the psychological literature, rather than to reproduce the behaviour of specific real couples.

# 2 | Couples of secure individuals

The model developed in the previous chapter allows for a wide range of individual traits and interaction mechanisms. As a first step in the analysis, we consider the case of couples composed of secure and non-synergic individuals in the absence of a child, which serves as a baseline scenario for understanding the fundamental dynamical properties of the system. We then investigate how the introduction of a child modifies the dynamics. In particular, we begin with robust couples and examine their response to caregiving demands, before turning to fragile couples, for which a bifurcation analysis is performed to assess whether the transition to parenthood may induce qualitative changes in the dynamics, potentially promoting robustness. Finally, we compare the overall level of couple satisfaction before and after the introduction of the child, highlighting the role of caregiving demands in shaping long-term outcomes.

The dynamical model for a couple composed of two secure and non-synergic individuals takes the following form:

$$\begin{cases} \dot{x}_1 = -\alpha_1 x_1 + \gamma_1 A_2 + \dfrac{e^{x_2} - e^{-x_2}}{\dfrac{e^{x_2}}{\dfrac{R_1^+}{1+\epsilon N h_1}} - \dfrac{e^{-x_2}}{\dfrac{R_1^-}{1+\epsilon N h_1}}} \\ \dot{x}_2 = -\alpha_2 x_2 + \gamma_2 A_1 + \dfrac{e^{x_1} - e^{-x_1}}{\dfrac{e^{x_1}}{\dfrac{R_2^+}{1+(1-\epsilon) N h_2}} - \dfrac{e^{-x_1}}{\dfrac{R_2^-}{1+(1-\epsilon) N h_2}}} \end{cases} \tag{2.1}$$

where the values of all parameters are case–specific and will be specified as needed throughout the analysis.

For a general introduction to bifurcation theory, we refer to [30, 47]. All numerical bifurcation analyses presented in this work were performed using MATCONT, a MATLAB software package for the numerical continuation and bifurcation analysis of dynamical systems [12].

## 2.1. Couples without children

We begin the analysis by considering couples in the absence of a child, corresponding to the case $N = 0$. This setting represents the simplest dynamical configuration of the model and, therefore, provides a natural starting point for understanding the qualitative behaviour of the system. In the childless case, the dynamics are governed exclusively by the mutual interaction between the two partners, without additional caregiving demands.

To provide a concrete reference for the numerical investigations, we first introduce a baseline set of parameter values. Unless otherwise stated, this parameter set is used throughout the present section. Variations around this reference configuration are introduced when exploring different dynamical regimes. The chosen values are meant to illustrate the qualitative behaviour of the system and do not correspond to any specific real couple. For the baseline configuration, the system exhibits robust dynamics.

| **Parameter** | **Value** |
|---|---|
| $\alpha_1$ | 0.1 |
| $\alpha_2$ | 0.3 |
| $\gamma_1$ | 0.5 |
| $\gamma_2$ | 1 |
| $A_1$ | 1 |
| $A_2$ | 0.5 |
| $R_1^+$ | 1 |
| $R_1^-$ | $-1$ |
| $R_2^+$ | 2 |
| $R_2^-$ | $-1$ |

Table 2.1: Baseline parameter values used in the simulations for robust couples.

As discussed in the previous chapter, couples composed of secure and non-synergic individuals may exhibit either robust or fragile dynamics, depending on the parameters [38]. Robust couples are characterized by the presence of a globally stable equilibrium point, toward which the system converges independently of the initial conditions. Fragile couples, instead, display two stable equilibria separated by a saddle point, giving rise to bistable dynamics.

From a geometrical point of view, equilibrium points can be identified as the intersections of the two *nullclines* defined by $\dot{x}_1 = 0$ and $\dot{x}_2 = 0$, as illustrated in Figure 2.1. These nullclines are given explicitly by:

$$x_1 = \frac{R_1^L(x_2) + \gamma_1 A_2}{\alpha_1} \qquad x_2 = \frac{R_2^L(x_1) + \gamma_2 A_1}{\alpha_2} \tag{2.2}$$

In the robust regime, the nullclines intersect at a single point, and the phase–plane dynamics converge toward this equilibrium from any initial condition. When this intersection lies in the first quadrant (Figure 2.1a), the system reaches a stable positive equilibrium of mutual emotional involvement, corresponding to a persistent positive relationship between the partners. In general, robustness represents a desirable dynamical regime, since robust couples are able to withstand perturbations and return to the same equilibrium state.

As shown in Figure 2.1, by varying model parameters, the qualitative structure of the nullclines may change, leading to the appearance of additional intersection points. In particular, variations in the appeal parameters $A_1$ and $A_2$ result in vertical or horizontal shifts of the nullclines, respectively. As a consequence, two additional equilibria may emerge, giving rise to a fragile configuration in which two stable equilibria coexist and are separated by a saddle point (Figure 2.1b).

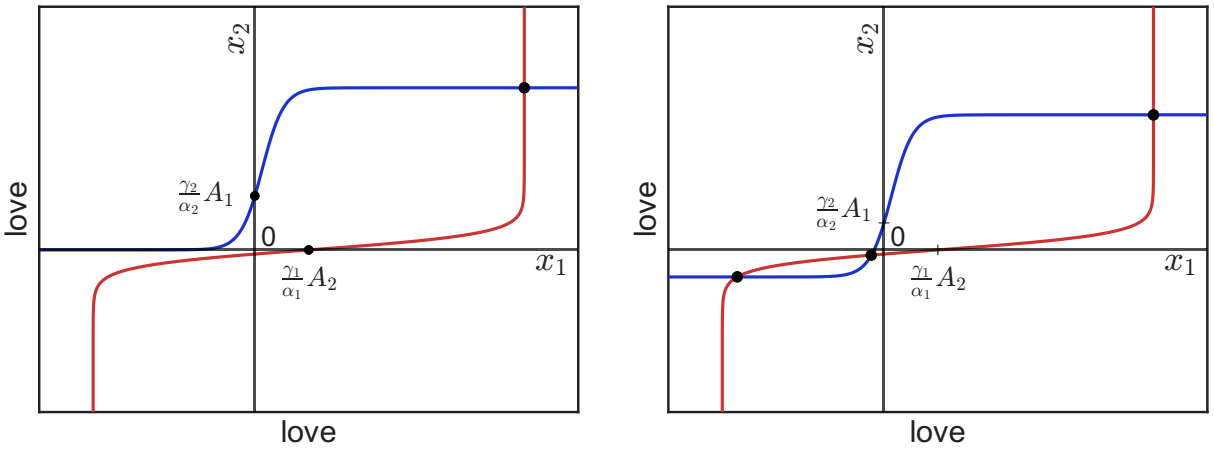


(a) Robust couples (b) Fragile couples

Figure 2.1: Nullclines of the system for childless couples ($N = 0$). The red curve corresponds to $\dot{x}_1 = 0$, while the blue curve corresponds to $\dot{x}_2 = 0$.

This transition from robust to fragile dynamics, and vice versa, corresponds to a *saddle-node bifurcation*. Typically, reducing the appeal of one or both partners favours the onset of alternative stable states (ASS), allowing the system to switch between states of mutual attraction and hostility in response to sufficiently strong perturbations. Conversely, increasing the appeal parameters causes one of the stable equilibria to collide with the

saddle point and disappear, restoring a single globally stable equilibrium and recovering robust dynamics.

The region of the appeal parameter space $(A_1, A_2)$ associated with the presence of alternative stable states (ASS) can be identified through numerical bifurcation analysis and continuation techniques [37]. This region delimits the parameter values for which childless couples exhibit fragile behaviour, as opposed to robust dynamics.

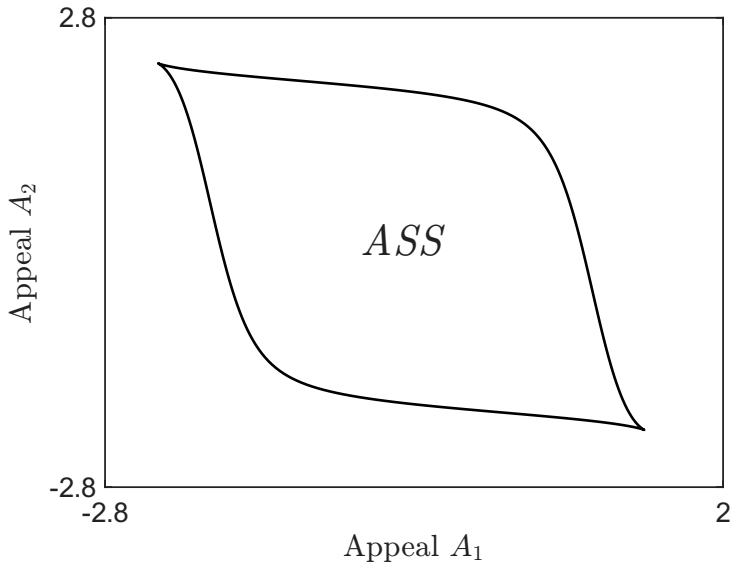


Figure 2.2: Region of alternative stable states (ASS) in the $(A_1, A_2)$ parameter space for $N = 0$.

The boundary of this region is characterized by saddle–node bifurcations of equilibria. In particular, along the upper boundary the saddle–node bifurcation, it involves the unstable saddle point and the equilibrium associated with negative emotional involvement, whereas along the lower boundary the bifurcation occurs between the saddle point and the equilibrium corresponding to positive emotional involvement. As a consequence, outside the ASS region the system admits a unique stable equilibrium, and the long–term sign of the partners' feelings is uniquely determined.

This analysis highlights the significant role played by appeal in shaping the qualitative dynamics of a couple. As shown in Figure 2.2, variations in the appeal parameters alone are sufficient to induce transitions between robust and fragile regimes. However, appeal does not fully determine the emotional dynamics of a relationship: an equally important role is played by the way individuals respond to their partner's emotional involvement. For this reason, an analogous analysis can be carried out in the parameter space $(R_1^+, R_2^+)$, which characterizes the intensity of the reaction to love. This allows us to investigate

how individual responsiveness to emotional engagement affects the emergence of robust or fragile dynamics, independently of appeal. In this analysis, we focus on the positive reaction to love and neglect the negative one, assuming that negative reactions do not significantly influence the long–term perception of the partner in the present setting.

The region of the $(R_1^+, R_2^+)$ space associated with the presence of alternative stable states is shown in Figure 2.3. As can be observed, starting from a bistable configuration, namely when the appeal parameters $(A_1, A_2)$ lie within the ASS region, it is possible to recover robust dynamics through a saddle-node bifurcation by reducing the values of the reaction parameters.

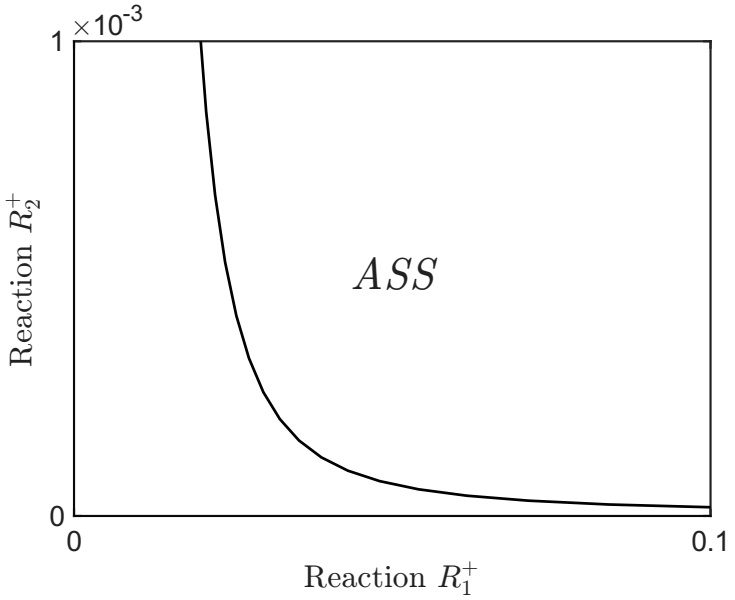


Figure 2.3: Region of alternative stable states (ASS) in the $(R_1^+, R_2^+)$ parameter space for $N = 0$. The parameter $A_1 = 0.2$, while all other parameters are reported in Table 2.1.

This effect can be interpreted both geometrically and from a modeling perspective. From a geometrical point of view, decreasing the asymptotic value of the reaction function leads to a flattening of the corresponding nullcline, thereby reducing the likelihood of multiple intersections. As a result, the system is driven back toward a configuration with a single equilibrium point. From the modeling perspective, a lower maximum reaction to love corresponds to a reduced level of emotional involvement. In this configuration, individuals are less prone to extreme emotional responses, making abrupt transitions to strongly negative emotional states less likely. Consequently, although reduced reactivity may correspond to lower overall involvement, it also "stabilizes" the dynamics by preventing the emergence of fragile behaviour.

Overall, the analysis of childless couples shows that robust and fragile dynamics emerge from the interplay between appeal and responsiveness to love. Both components can independently induce qualitative transitions in the system through saddle–node bifurcations. This characterization of the childless case provides a clear baseline for assessing how the introduction of parenthood modifies the emotional dynamics of initially robust couples.

## 2.2. Robust couples: the effect of the transition to parenthood

Having characterized the dynamics of couples in the absence of a child, we now investigate how this behaviour is affected by the introduction of parenthood. In particular, we focus on couples that are robust in the childless case and analyze how the presence of a child modifies their long–term emotional dynamics. We also compare the levels of emotional involvement in the cases with and without a child.

The introduction of a child is modeled through the parameters $N$ and $\epsilon$, which represent the overall caregiving demands and their distribution between the two partners, respectively. As discussed in the previous chapter, these parameters affect the reaction to love by reducing the emotional resources available for responding to the partner's involvement [26]. In this section, we aim to assess whether robust dynamics are preserved under the additional load associated with parenthood, or whether the presence of a child may induce qualitative changes in the system, potentially leading to fragile behaviour.

To this end, we start from parameter configurations that yield a robust regime in the absence of a child (see Table 2.1) and progressively increase the caregiving demands.

As a first step, we can make a geometrical observation. Fixing the parameter $\epsilon$, for instance at $\epsilon = 0.5$, and progressively increasing the caregiving demand $N$, the nullclines of the system undergo a gradual flattening, as illustrated in Figure 2.4. As a consequence, the intersection point of the nullclines shifts downward for both partners, indicating a reduction in the equilibrium levels of emotional involvement.

From a geometrical perspective, the flattening of both nullclines has an important dynamical implication. Compared to the childless case, the reduced slopes prevent the appearance of additional intersection points, making the emergence of bistability impossible. In other words, for sufficiently large values of $N$, the system cannot enter a fragile configuration, and the dynamics remain characterized by a single globally stable equilibrium.

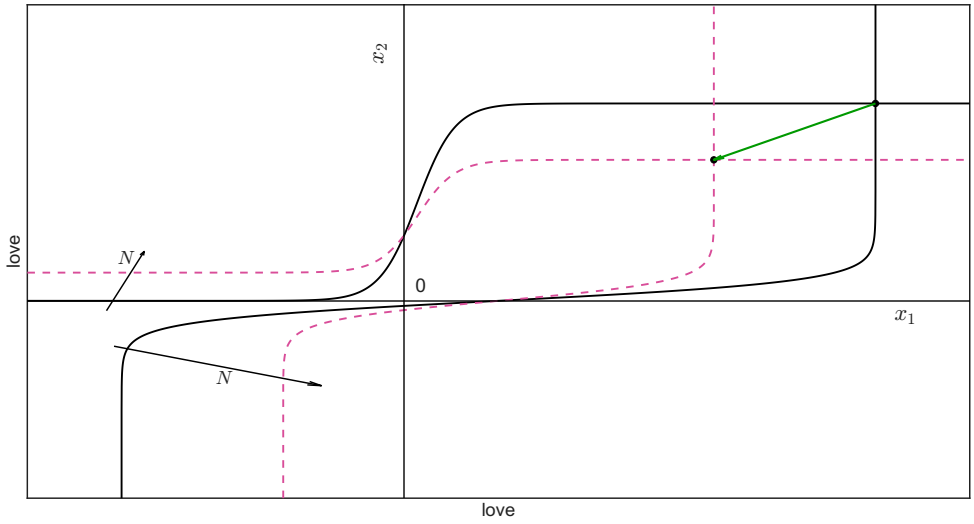


Figure 2.4: Effect of increasing $N$ on the nullclines for $\epsilon = 0.5$. The solid curve corresponds to $N = 0$, while the pink dashed curve corresponds to $N = 1.5$.

These observations suggest a clear qualitative effect of parenthood on robust couples. On one hand, increasing caregiving demands leads to lower equilibrium levels of mutual involvement, reflecting a reduction in the emotional resources that partners can devote to one another. This can be interpreted as a decrease in couple satisfaction, likely associated with the redistribution of time, attention, and energy toward the child, as documented in the literature (see, e.g., [5, 26]). On the other hand, the presence of a child, by inhibiting the transition to a fragile regime, prevents the system from exhibiting bistability and abrupt switches between positive and negative emotional states. From the perspective of the model, this implies that although the partners may experience lower levels of mutual involvement, the relationship becomes more robust, as it moves farther from the threshold of fragility.

We now consider a complementary scenario in which the overall caregiving demand is kept fixed, while the distribution of care between the two partners is varied. In particular, we fix $N$, for instance at $N = 1$, and investigate whether it is possible to induce a transition from a robust to a fragile configuration by varying the parameter $\epsilon$ from 0 to 1.In this analysis, we also allow the sensitivity parameters $h_1$ and $h_2$ to vary, in order to account for different individual responses to caregiving demands. As illustrated in Figure 2.5, when $N$ is fixed and $\epsilon$ is varied, the two nullclines are affected in different ways. As $\epsilon$ increases from 0 to 1, the nullcline $\dot{x}_2 = 0$ progressively widens, reaching its maximum width when partner 2 has no caregiving load, corresponding to the childless configuration for that partner. Conversely, the nullcline $\dot{x}_1 = 0$ becomes progressively flatter as $\epsilon$ approaches 1, reflecting the increasing caregiving load borne by partner 1. Despite these deformations,

the qualitative structure of the nullclines does not change in a way that allows for the creation of additional intersection points. In particular, if the system admits a single equilibrium in the childless case ($N = 0$), no new equilibria emerge when varying $\epsilon$ at fixed $N$.

This result indicates that, for robust couples, the division of caregiving responsibilities alone is not sufficient to induce fragile behaviour. In other words, once robustness is established in the absence of a child, it is preserved regardless of how caregiving demands are distributed between the partners.

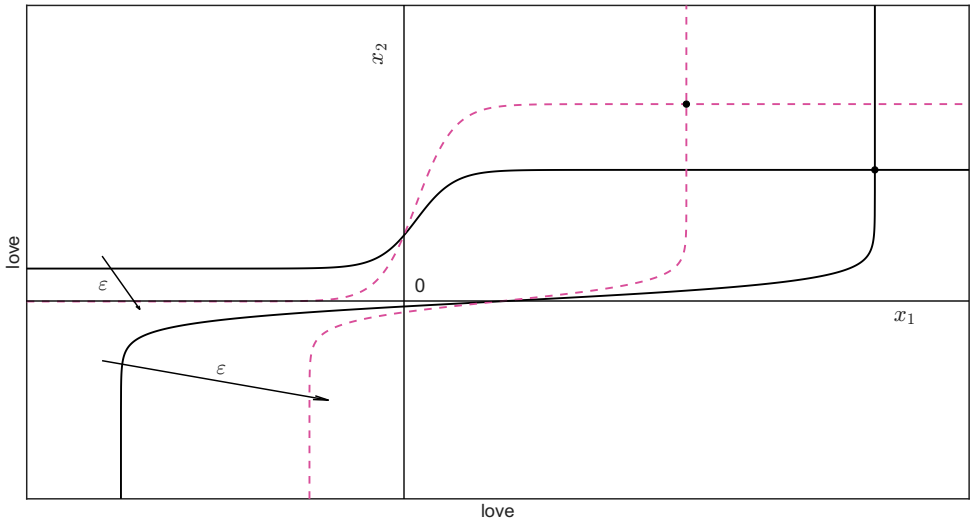


Figure 2.5: Effect of increasing $\epsilon$ on the nullclines for $N = 1$. The solid curve corresponds to $\epsilon = 0$, while the pink dashed curve corresponds to $\epsilon = 1$.

Robustness is certainly a desirable dynamical property for a couple; however, robustness alone is not sufficient to guarantee a high level of mutual satisfaction. For this reason, we now complement the stability analysis with an investigation of the equilibrium levels of emotional involvement. To this end, we consider a couple characterized by parameter set reported in Table 2.1. We first analyze how the equilibrium values of the partners' involvement depend on the caregiving demand $N$, with $\epsilon = 0.5$ fixed (Figure 2.6), and subsequently on the caregiving division parameter $\epsilon$, with $N = 1.5$ fixed (Figure 2.7). Increasing the caregiving demand $N$ leads to a monotonic decrease in the equilibrium involvement of both partners. This reflects the fact that, as caregiving demands grow, a larger fraction of emotional and energetic resources is diverted away from the couple toward the child, as documented in the literature (see, e.g., [13, 26]). When varying the caregiving division parameter $\epsilon$, a different effect is observed. As $\epsilon$ increases, the

equilibrium involvement of partner 1 decreases, consistently with the fact that partner 1 progressively bears a larger share of the caregiving load and therefore becomes less responsive to the partner's emotional involvement. At the same time, the involvement of partner 2 increases, as this partner is relieved from caregiving responsibilities and can devote more emotional resources to the relationship. At first glance, one might expect the involvement of partner 2 to decrease as well, since the reaction to love depends on the partner's emotional state. However, this does not occur. The reason is that the reduction in partner 1's involvement is not sufficient to offset the increase in partner 2's effective emotional responsiveness due to the absence of caregiving demands. In other words, the direct effect of caregiving redistribution on partner 2 dominates the indirect effect mediated through the partner's involvement, leading to an overall increase in $x_2$.

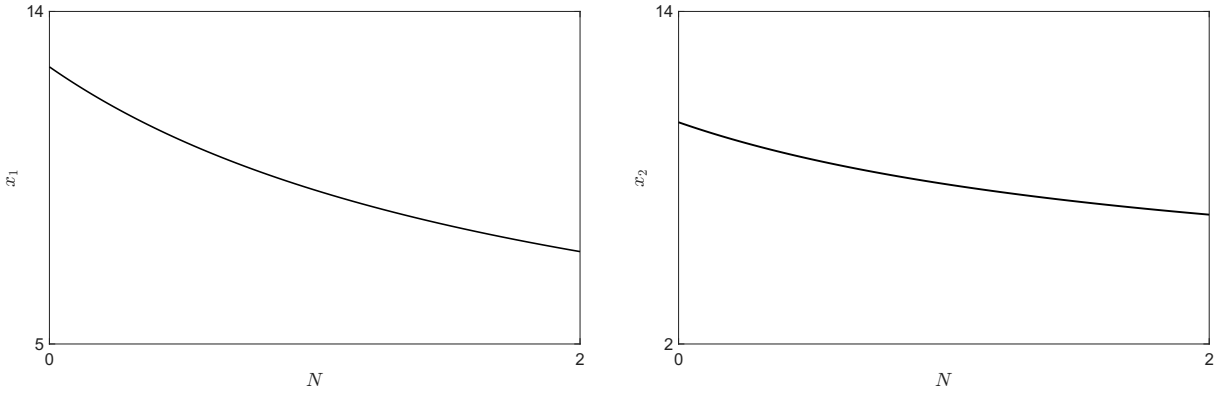


Figure 2.6: Evolution of $x_1$ and $x_2$ with respect to $N$ ($\epsilon = 0.5$).

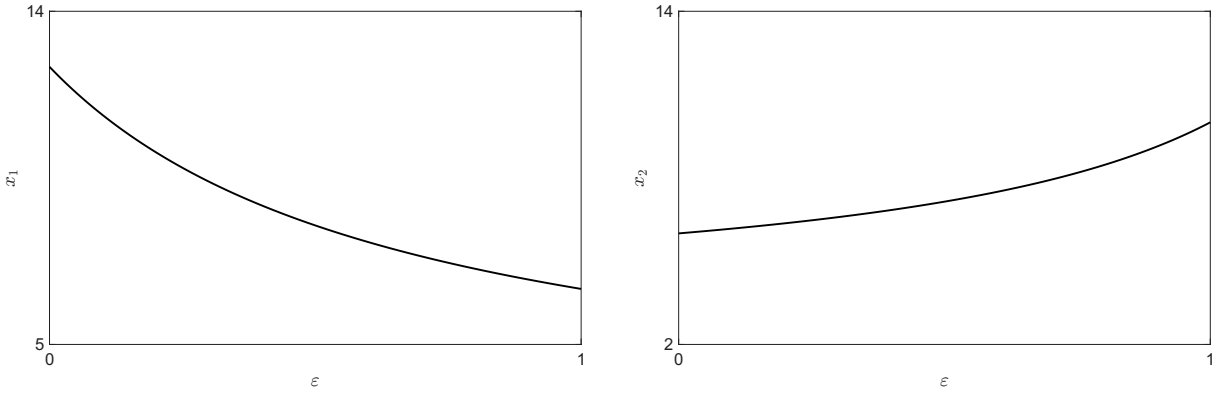


Figure 2.7: Evolution of $x_1$ and $x_2$ with respect to $\epsilon$ ($N = 1$).

We then examine the combined effect of these two parameters by studying the equilibrium involvement in the $(\epsilon, N)$ parameter space. In particular, we analyze the equilibrium involvement of partner 1 and partner 2 separately (Figure 2.8a and Figure 2.8b), and then

consider the overall emotional involvement of the couple at equilibirum, quantified by the sum $(x_1 + x_2)$ (Figure 2.8c), in order to assess not only how caregiving demands affect each partner individually, but also how they impact the couple as a whole. From this analysis, we observe that, independently of the overall caregiving demand $N$, the preferred distribution of caregiving responsibilities from the perspective of partner 1 corresponds to $\epsilon = 0$, that is, assigning the entire caregiving load to partner 2. Conversely, partner 2 prefers configurations close to $\epsilon = 1$, where the caregiving burden is entirely borne by partner 1. This outcome is consistent with both the structure of the model and the previous analyses: the larger the caregiving load experienced by a partner, the more their emotional reactivity to the other is reduced, leading each individual to favour configurations in which they bear as little caregiving responsibility as possible in order to maximizes their involvement. One might therefore expect that, when considering the couple as a whole, a compromise solution would emerge, favouring an equal subdivision of caregiving responsibilities in order to balance individual losses and maximize total emotional involvement. However, the model reveals a different outcome. As shown in Figure 2.8c, the total emotional involvement of the couple is generally maximized for asymmetric caregiving configurations, while equal sharing of caregiving tends to minimize $x_1 + x_2$, except in the regime of very small caregiving demands.

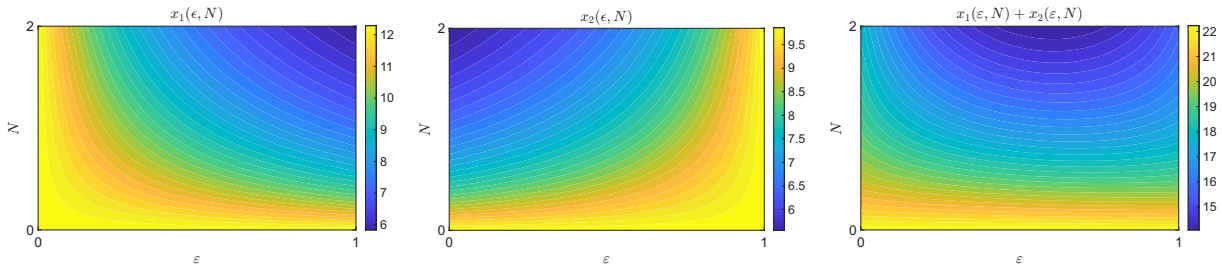


Figure 2.8: Evolution of individual and collective emotional involvement in the $(\epsilon, N)$ parameter space: (a) involvement $x_1$; (b) involvement $x_2$; (c) total involvement $(x_1 + x_2)$.

Finally, we compare the equilibrium levels of involvement with those obtained in the childless case, quantifying the percentage decrease in emotional involvement induced by the transition to parenthood. To this end, the surfaces in Figure 2.9 are computed by evaluating, for all pairs $(\epsilon, N)$:

$$\Delta x_i = \frac{x_i(\epsilon, N) - x_i(\epsilon, 0)}{x_i(\epsilon, 0)} \cdot 100, \tag{2.3}$$

where $i = 1, 2$, and $x_i(\epsilon, N)$ denotes the equilibrium involvement in the presence of a child, while $x_i(\epsilon, 0)$ corresponds to the childless case. In Figure 2.9c, the same computation is performed by replacing $x_i$ with the total emotional involvement $(x_1 + x_2)$. This analysis allows us to quantify how much emotional involvement deteriorates due to parenthood, and how this deterioration depends on both the caregiving demand $N$ and its distribution $\epsilon$. In all panels, the black curve represents the locus of points in the $(\epsilon, N)$ parameter space where both partners experience the same percentage decrease in involvement. From an equity perspective, one might regard this curve as identifying the fairest caregiving configurations, since the emotional cost of parenthood is equally shared. However, Figure 2.9c reveals a nontrivial outcome. For fixed values of $N$, the point on the equal–decrease curve often lies close to the configuration that maximizes the percentage loss of total emotional involvement. In other words, caregiving allocations that equally distribute the emotional deterioration between partners tend to correspond to near–minimal levels of overall couple involvement. This result indicates that, even when fairness is explicitly taken into account, symmetric caregiving distributions do not necessarily lead to better collective outcomes. On the contrary, for fixed caregiving demands, asymmetric distributions of responsibilities generally result in a smaller percentage decrease in the total emotional involvement of the couple.

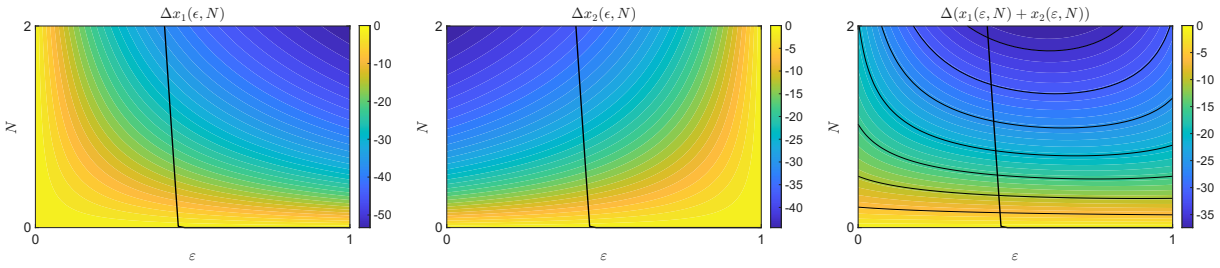


Figure 2.9: Comparison between the cases with and without a child in the $(\epsilon, N)$ parameter space: (a) variation in involvement $\Delta x_1$; (b) variation in involvement $\Delta x_2$; (c) variation in total involvement $\Delta(x_1 + x_2)$.

We conclude with a final remark. As extensively documented in the literature (see, e.g., [10, 29, 33, 39]), the transition to parenthood does not produce uniform outcomes across couples, and its effects may vary substantially depending on individual and relational characteristics. Motivated by these observations, we now introduce alternative parameter configurations that give rise to different dynamical behaviours. In particular, Table 2.2 reports a parameter set for which both partners increase their involvement as $\epsilon$ approaches 1.

| Parameter | Value |
|---|---|
| $\alpha_1$ | 0.3 |
| $\alpha_2$ | 0.6 |
| $\gamma_1$ | 0.5 |
| $\gamma_2$ | 1 |
| $A_1$ | 0.01 |
| $A_2$ | 0.2 |
| $R_1^+$ | 0.6 |
| $R_1^-$ | $-0.1$ |
| $R_2^+$ | 0.7 |
| $R_2^-$ | $-1$ |

Table 2.2: Baseline parameter values used in the simulations for robust couples exhibiting a different behaviour.

The reason for including this remark at this stage is that the above parameter set corresponds to a robust couple. As shown in Figure 2.10, when $\epsilon = 0.5$ is fixed and $N$ increases, the involvement of both partners decreases. On the other hand, Figure 2.11 shows that, for fixed $N = 0.2$, increasing $\epsilon$ leads to a configuration in which the involvement of both partners increases. In other words, love is enhanced when the caregiving load is primarily taken by partner 1. This effect can be interpreted as a consequence of the strong imbalance in appeal terms: shifting responsibility toward the less appealing partner mitigates the asymmetric feedback and promotes a mutually reinforcing involvement.

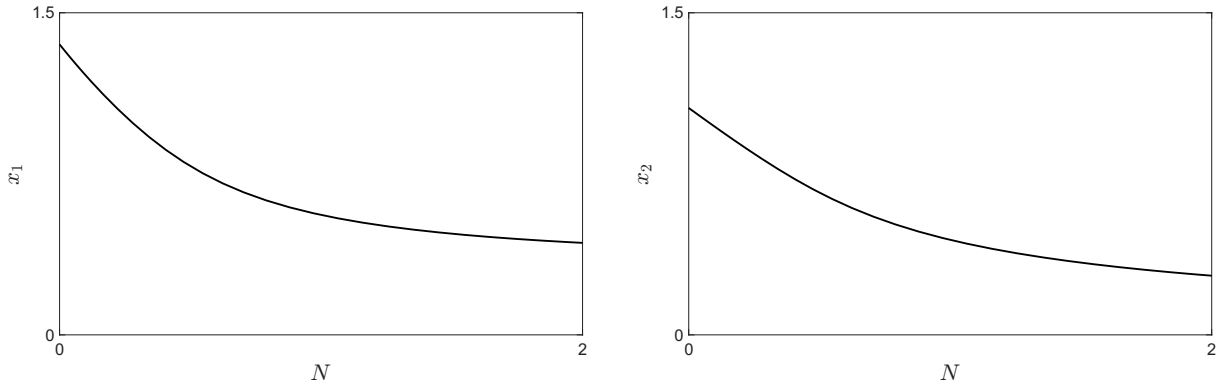


Figure 2.10: Evolution of $x_1$ and $x_2$ with respect to $N$ ($\epsilon = 0.5$).

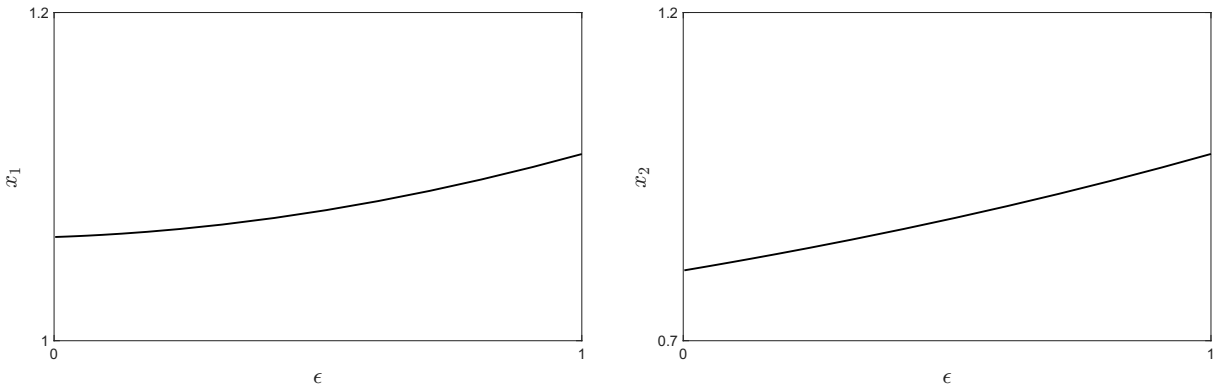


Figure 2.11: Evolution of $x_1$ and $x_2$ with respect to $\epsilon$ ($N = 0.2$).

We then turn to the $(\epsilon, N)$ parameter space. Figure 2.12a shows that, for sufficiently large values of $N$, the involvement of partner 1 displays a U-shaped dependence on $\epsilon$. This behavior indicates that extreme caregiving allocations are favored over balanced ones, leading to a more asymmetric division of responsibilities. A complementary picture emerges for partner 2. As shown in Figure 2.12b, the most favourable configuration corresponds to $\epsilon = 1$, independently of the value of $N$. This suggests that partner 2 consistently benefits from a caregiving allocation in which partner 1 bears the primary responsibility. This interpretation is further supported by Figure 2.12c which reports the total level of involvement. Total love is maximized at $\epsilon = 1$ for all values of $N$, while it exhibits a U-shaped dependence on $\epsilon$ with a minimum shifted toward $\epsilon = 0$. Overall, these results indicate that asymmetric caregiving allocations not only favor individual involvement but also enhance the collective outcome of the couple.

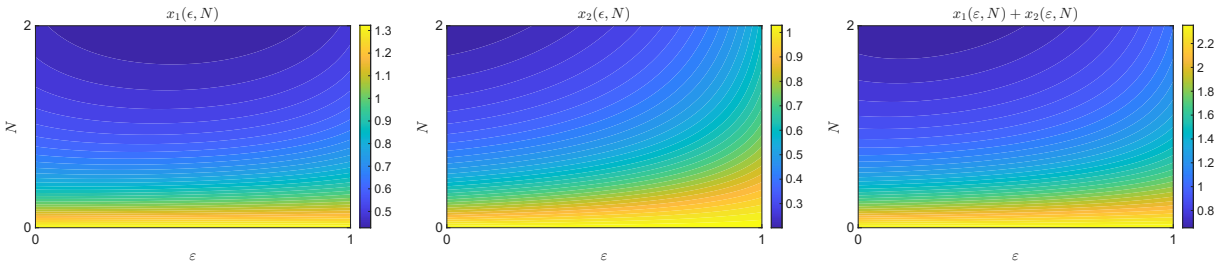


(a) (b) (c)

Figure 2.12: Evolution of individual and collective emotional involvement in the $(\epsilon, N)$ parameter space: (a) involvement $x_1$; (b) involvement $x_2$; (c) total involvement $(x_1 + x_2)$.

We conclude the analysis of involvement in this case by comparing the equilibrium levels of involvement in the $(\epsilon, N)$ parameter space with the childless scenario, using Equation (2.3). The black curve shown in the figures identifies the region of the parameter space for

which both partners experience the same percentage decrease in equilibrium involvement. In this configuration, the curve originates near $\epsilon = 0$ and progressively shifts toward larger values of $\epsilon$ as $N$ increases. This behavior suggests that, for higher caregiving demands, an increasingly asymmetric allocation is required in order for both partners to undergo an equal relative reduction in involvement, with partner 1 bearing a larger share of responsibilities. The implications of this result are clarified by the total involvement at equilibrium, shown in Figure 2.13c. For sufficiently large values of $N$, the configuration corresponding to equal percentage loss does not lie close to the maximum reduction of total love, in contrast with the previous case. This indicates that, for this couple, choosing an allocation that equalizes the relative loss between partners remains a favorable strategy even under high caregiving demands.

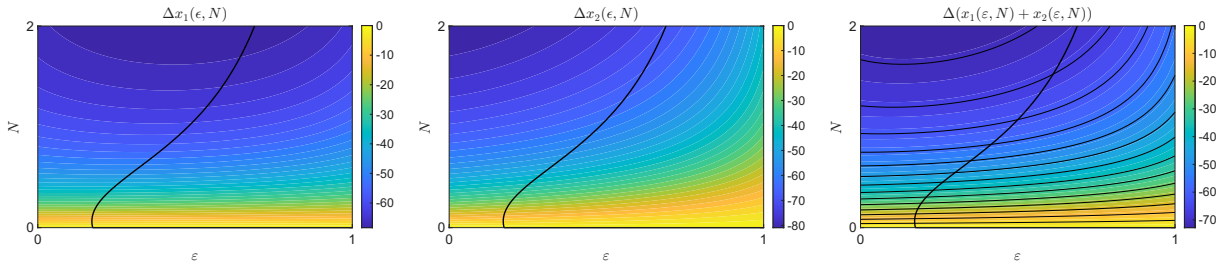


Figure 2.13: Comparison between the cases with and without a child in the $(\epsilon, N)$ parameter space: (a) variation in involvement $\Delta x_1$; (b) variation in involvement $\Delta x_2$; (c) variation in total involvement $\Delta(x_1 + x_2)$.

We have shown that for couples that are robust in the absence of a child, the transition to parenthood does not alter the qualitative stability of the dynamics. Increasing caregiving demands systematically reduce equilibrium levels of emotional involvement while inhibiting the emergence of bistability, thereby preserving a single stable equilibrium. The analysis highlights a meaningful trade-off in the allocation of caregiving responsibilities. Couples may choose configurations that ensure an equal percentage reduction in involvement, leading to greater equity between partners, or favor asymmetric allocations that preserve higher total involvement at the expense of one partner, who bears a larger emotional cost. Within the framework of the model, parenthood therefore does not impose a unique optimal outcome. Couples may either prioritize equity between partners, accepting a larger overall reduction in emotional involvement, or maximize total emotional involvement by concentrating the caregiving burden, and the associated emotional cost, on a single partner.

This concludes the analysis of secure-secure robust couples and naturally motivates the

investigation of configurations that are secure but fragile, where caregiving demands may instead induce qualitative changes in the equilibrium structure.

## 2.3. Fragile couples: the effect of the transition to parenthood

In this section, we consider fragile couples, focusing on the effects of the transition to parenthood on this type of dynamics, and investigate whether the presence of a child may promote a shift toward a robust configuration or, instead, preserve or reinforce fragility. We analyze how caregiving demands influence the regions of alternative stable states associated both with appeal parameters and with reactions to love, in order to assess whether parenthood modifies the parameters for which bistability occurs. Finally, following the same approach adopted for robust couples in Section 2.2, we study how the equilibrium levels of emotional involvement of both partners vary in the $(\epsilon, N)$ parameter space.

The numerical analysis is performed using the baseline parameter set reported in Table 2.3. Unless otherwise stated, these values are kept fixed throughout this section, and any variation will be explicitly indicated. We begin by considering the effect of caregiving demands $N$ on fragile couples under symmetric caregiving conditions, $\epsilon = 0.5$. Progressively increasing $N$, we observe that for sufficiently large values of $N$, the system always shifts to a robust configuration. As in the case of robust couples, this transition is associated with a flattening of the nullclines, which prevents the persistence of bistability. At the same time, the equilibrium levels of emotional involvement of both partners decrease, as shown in Figure 2.14.

| Parameter | Value |
|---|---|
| $\alpha_1$ | 0.1 |
| $\alpha_2$ | 0.3 |
| $\gamma_1$ | 0.5 |
| $\gamma_2$ | 1 |
| $A_1$ | 0.5 |
| $A_2$ | 0.5 |
| $R_1^+$ | 1 |
| $R_1^-$ | $-1$ |
| $R_2^+$ | 2 |
| $R_2^-$ | $-1$ |

Table 2.3: Baseline parameter values used in the simulations for fragile couples.

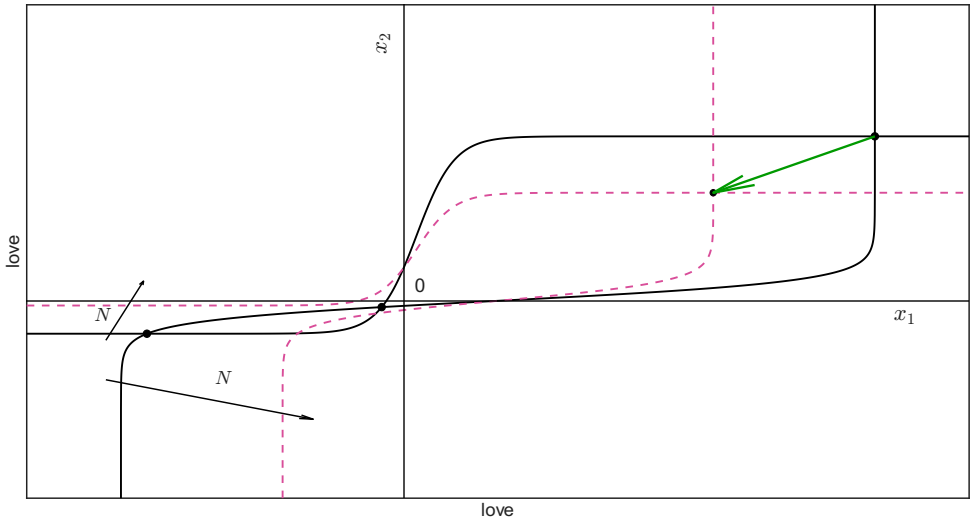


Figure 2.14: Effect of increasing $N$ on the nullclines for $\epsilon = 0.5$. The solid curve corresponds to $N = 0$, while the pink dashed curve corresponds to $N = 1.5$.

We then investigate the effect of caregiving division $\epsilon$ by fixing $N \neq 0$ and varying $\epsilon$. In this case, the outcome depends on the magnitude of the caregiving demand: for sufficiently small values of $N$, the division of caregiving responsibilities becomes relevant, allowing the couple either to recover robustness or to remain in a fragile configuration, as illustrated in Figure 2.15.

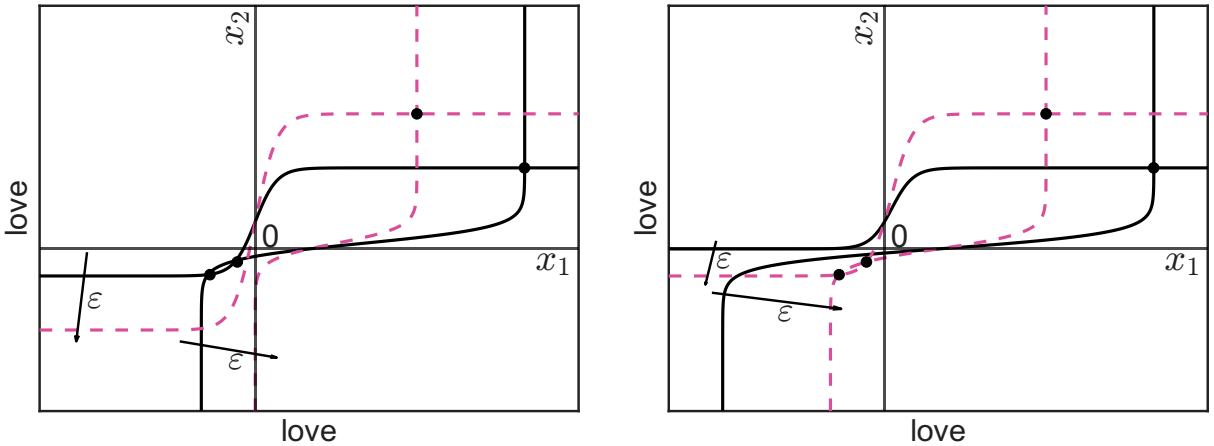


(a) Transition from a fragile to a robust configuration.

(b) Transition from a robust to a fragile configuration.

Figure 2.15: Effect of increasing $\epsilon$ on the nullclines for $N = 1$. The solid curve corresponds to $\epsilon = 0$, while the pink dashed curve corresponds to $\epsilon = 1$. The right panel is obtained by modifying the parameters in Table 2.3 to $R_1^- = -0.5$ and $R_2^- = -2$.

To characterize the transition from fragile to robust couples, we perform a numerical con-

tinuation of equilibria in the $(\epsilon, N)$ parameter space, identifying the locus of saddle–node bifurcations, as illustrated in Figure 2.16a. As expected, the resulting bifurcation diagram shows that increasing caregiving demands generally favours robustness. However, for small values of $N$, robustness can only be recovered if the caregiving load is predominantly assigned to partner 2.

Which partner should bear the larger share of caregiving depends on the appeal asymmetry within the couple. To clarify this point, we analyze how the bifurcation structure changes when the appeal parameters are modified.

First, we reduce the appeal of partner 1 as perceived by partner 2, setting $A_1 = 0.1$ (Figure 2.16c). In this case, increasing $N$ still leads to robustness, but for fixed $N$ the caregiving load must be shifted toward partner 1 in order to exit the region of alternative stable states. Conversely, when considering an intermediate value $A_2 = 0.2$ (Figure 2.16b), robustness is favoured by a more balanced distribution of caregiving responsibilities.

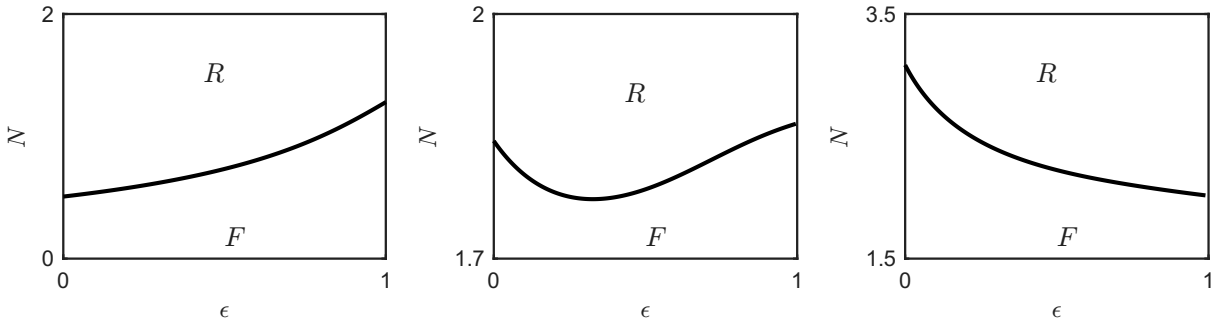


(a) $A_1 = 0.5$ (b) $A_1 = 0.2$ (c) $A_1 = 0.1$

Figure 2.16: Comparison of saddle-node bifurcation on the parameter space $(\epsilon, N)$ for different values of $A_1$.

These results indicate that appeal plays a crucial role in shaping the effect of caregiving division on fragile couples. When one partner is significantly more appealing to the other, robustness is recovered by assigning a larger share of caregiving to the less appealing partner. This can be understood by comparing the reaction to appeal terms in the model: while $\gamma_1 A_2 = 0.25$ remains fixed, $\gamma_2 A_1$ varies with $A_1$, altering the balance between the partners' emotional responses. When the two reaction to appeal terms are comparable, a more symmetric division of caregiving demands becomes preferable. A comparison of the three cases is reported in Figure 2.17. As shown, larger values of $A_1$ systematically reduce the region of alternative stable states, making the transition to robustness easier. This confirms that higher appeal is always favourable from a dynamical perspective, as it facilitates the exit from fragile regimes.

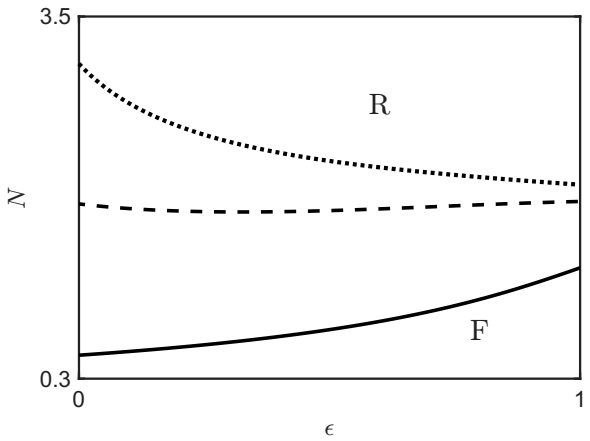


Figure 2.17: Saddle-node bifurcation curves in the $(\epsilon, N)$ parameter space for different values of $A_1$. The solid line corresponds to $A_1 = 0.5$, the dashed line to $A_1 = 0.2$, the dotted line to $A_1 = 0.1$.

Starting from the intermediate case $A_1 = 0.2$, we also investigate whether the appeal $A_2$ plays an analogous role. As expected, varying $A_2$ leads to a symmetric conclusion: when partner 2 is less appealing to partner 1, robustness can be recovered by assigning a larger share of caregiving responsibilities to partner 2. Conversely, as the appeal $A_2$ increases, robustness is favoured by shifting the caregiving load toward partner 1. These effects are illustrated in Figure 2.18. This analysis confirms that asymmetries in appeal play a key role in shaping the preferred distribution of caregiving responsibilities. In all cases, higher appeal values systematically reduce the parameter region associated with fragile dynamics, thereby facilitating the transition to robustness.

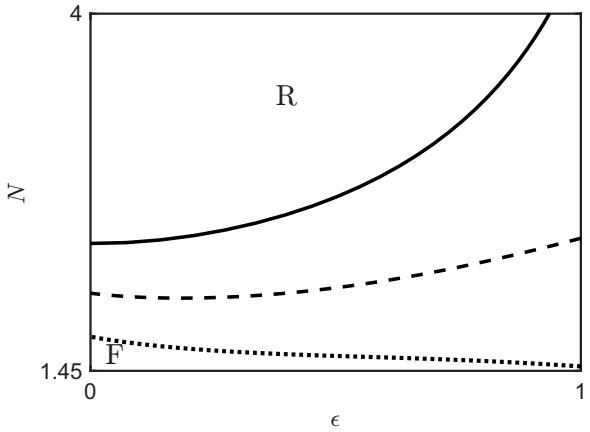


Figure 2.18: Saddle-node bifurcation curves in the $(\epsilon, N)$ parameter space for different values of $A_2$. The solid line corresponds to $A_2 = 0.2$, the dashed line to $A_2 = 0.4$, the dotted line to $A_2 = 0.6$.

To conclude the analysis of the role of appeal in the presence of a child, we now examine how caregiving demands and their distribution affect the region of alternative stable states. Specifically, we compare the ASS region obtained in the childless case (Figure 2.2) with the corresponding regions computed for different values of $N$ and $\epsilon$, namely $N = 0.5, 1$ and $\epsilon = 0, 0.5, 1$. Figure 2.19a shows the region of alternative stable states computed for $N = 0.5$ and different values of $\epsilon$. The shape and orientation of the ASS region depend strongly on how caregiving responsibilities are distributed between the two partners. Indeed, for $\epsilon = 0$, the ASS region appears vertically elongated, indicating that, with respect to the childless case (Figure 2.2), partner 1 needs to vary their appeal over a smaller range in order to exit the bistable regime. This behaviour can be interpreted by noting that, when partner 2 carries the entire caregiving load, a substantial portion of their emotional resources is redirected toward childcare, which reduces their sensitivity to the appeal of the partner. In contrast, partner 1 remains more responsive to the partner's appeal, leading to an asymmetric deformation of the ASS region. A symmetric reasoning applies to the case $\epsilon = 1$, for which the ASS region becomes horizontally elongated. Here, partner 1 bears the full caregiving burden, and the corresponding reduction in sensitivity to appeal is reflected in the horizontal stretching of the bistable region. When caregiving responsibilities are equally shared ($\epsilon = 0.5$), the ASS region becomes approximately concentric with respect to that observed in the childless case. As expected, the region is overall smaller, reflecting the fact that the introduction of a child facilitates robustness by reducing the parameter range associated with bistability. In this symmetric configuration, both partners devote a significant fraction of their emotional resources to childcare, which results in a reduced sensitivity to each other's appeal.

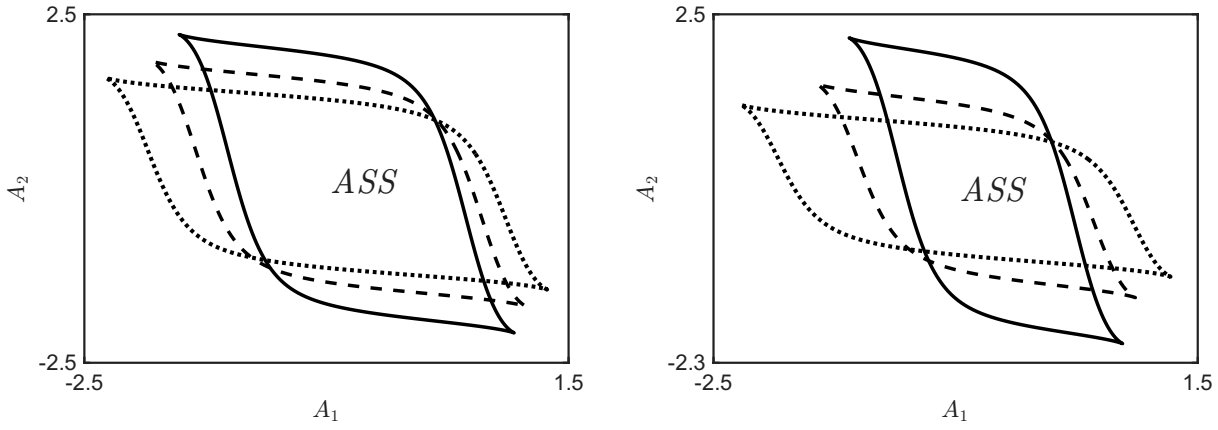


Figure 2.19: Alternative stable states regions in $(A_1, A_2)$ parameter space for $N = 0.5$ (a) and $N = 1$ (b): solid line $\epsilon = 0$, dashed line $\epsilon = 0.5$, dotted line $\epsilon = 1$.

The same qualitative effects are observed for larger values of the caregiving demand $N$, as illustrated in Figure 2.19b, where the deformation and contraction of the ASS region become more pronounced. This confirms that increasing caregiving demands further promote robustness by progressively suppressing bistability in the system.

A summary of the main effects of caregiving demand and its distribution on the region of alternative stable states is provided in Table 2.4.

We now investigate how variations in the reaction to love modulate the transition from fragile to robust dynamics. In particular, we analyze how changes in emotional reactivity affect the structure of the bifurcation diagrams in the $(\epsilon, N)$ parameter space and, consequently, the preferred distribution of caregiving responsibilities.

Using the baseline parameter set reported in Table 2.3, and fixing the appeal parameter to $A_1 = 0.2$, we study the effect of varying the positive reaction-to-love parameters $R_1^+$ and $R_2^+$ by computing the corresponding bifurcation diagrams in the $(\epsilon, N)$ parameter space and identifying the regions associated with the transition from fragile to robust configurations.

As shown in Figure 2.20, increasing the value of $R_1^+$ significantly alters the geometry of the transition region. For low values of $R_1^+$, robustness is recovered when the caregiving load is predominantly assigned to partner 2. As $R_1^+$ increases, the system undergoes a qualitative change: robustness is first promoted by a more balanced distribution of caregiving responsibilities and, for sufficiently large values of $R_1^+$, by assigning most of the caregiving load to partner 1.

This behaviour indicates that modifications in the emotional reactivity of partner 1 can shift the preferred caregiving configuration required to recover robustness. From a modeling perspective, increasing $R_1^+$ corresponds to enhancing the capacity of partner 1 to respond positively to the partner's emotional involvement. In this regime, assigning a larger share of caregiving responsibilities to partner 1 becomes dynamically favourable, as this partner remains emotionally responsive despite the increased caregiving load.
Finally, we observe that higher levels of emotional reactivity tend to make the transition to robustness more demanding in terms of caregiving parameters. In particular, for large values of $R_1^+$, the region of robustness in the $(\epsilon, N)$ parameter space becomes narrower, suggesting that while caregiving demands act as a stabilizing mechanism, excessive emotional reactivity may counteract this effect by sustaining fragile dynamics over a wider parameter range.

| | $\epsilon = 0$ | $\epsilon = 0.5$ | $\epsilon = 1$ |
|---|---|---|---|
| $N = 0$ | 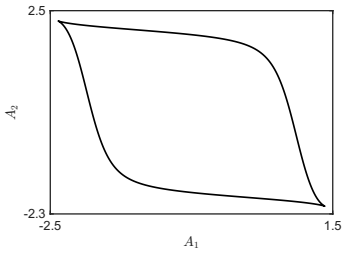 | 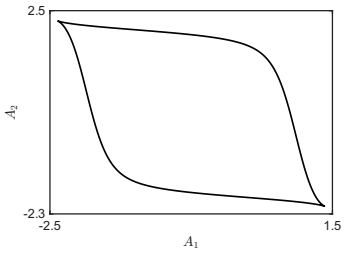 | 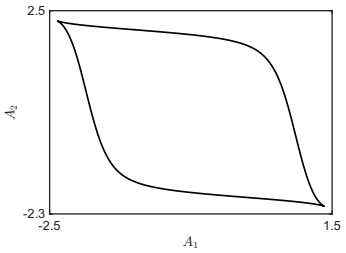 |
| $N = 0.5$ | 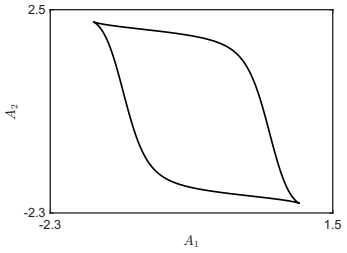 | 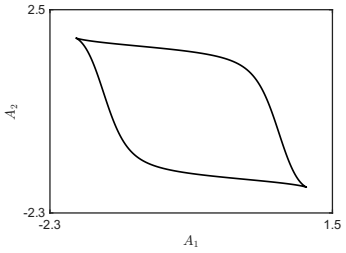 | 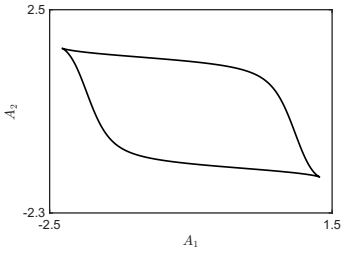 |
| $N = 1$ | 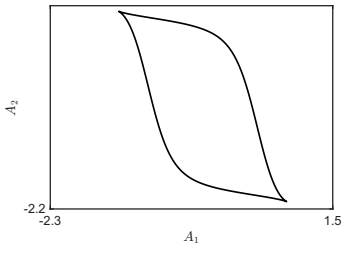 | 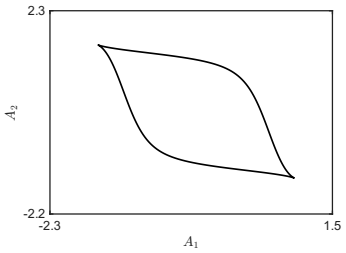 | 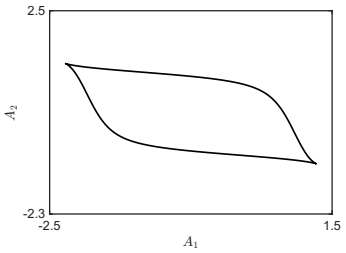 |

Table 2.4: Different alternative stable states regions on $(\epsilon, N)$ grid. Columns: $\epsilon \in \{0, 0.5, 1\}$. Rows: $N \in \{0, 0.5, 1\}$.

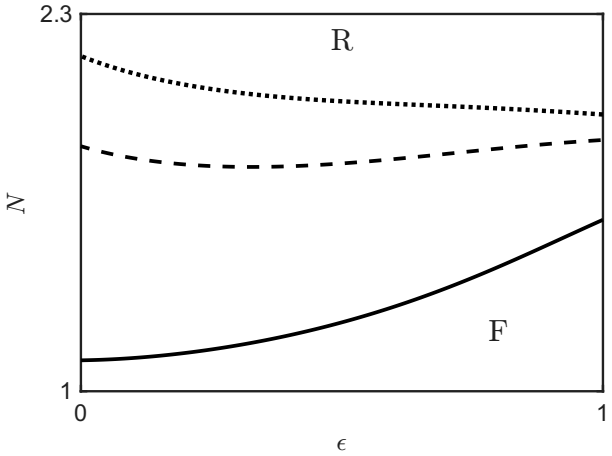


Figure 2.20: Saddle-node bifurcation curves in the $(\epsilon, N)$ parameter space for different values of $R_1^+$: solid line $R_1^+ = 0.2$, dashed line $R_1^+ = 1$ and dotted line $R_1^+ = 3$.

Using the same parameter configuration, we perform an analogous analysis for the reaction parameter $R_2^+$, in order to assess whether it plays a role comparable to that of $R_1^+$. As shown in Figure 2.21, variations in $R_2^+$ also significantly affect the structure of the bifurcation diagrams and, consequently, the transition from fragile to robust dynamics. Marking a notable difference with respect to the case of $R_1^+$, even for large values of $R_2^+$, it is not required to bear the entire caregiving load in order to recover robustness: a minimum of the bifurcation curve persists at intermediate values of $\epsilon$. This indicates that, unlike the previous case, robustness can be achieved without fully concentrating caregiving responsibilities on partner 2.

This behaviour can be explained by considering the interplay between emotional reactivity and caregiving in the model. Increasing $R_2^+$ enhances partner 2's responsiveness to the partner's emotional involvement, which tends to favour fragile dynamics. However, the stabilizing effect induced by caregiving does not need to be fully concentrated on the same partner in order to counterbalance this increased reactivity. A partial reduction of partner 2's effective responsiveness is already sufficient to prevent the emergence of bistability. Finally, this analysis confirms a general trend already observed in previous sections: lower values of the positive reaction to love facilitate the transition to robustness. High levels of emotional reactivity tend to preserve fragile dynamics over a wider parameter range, making the recovery of robustness more demanding in terms of caregiving parameters.

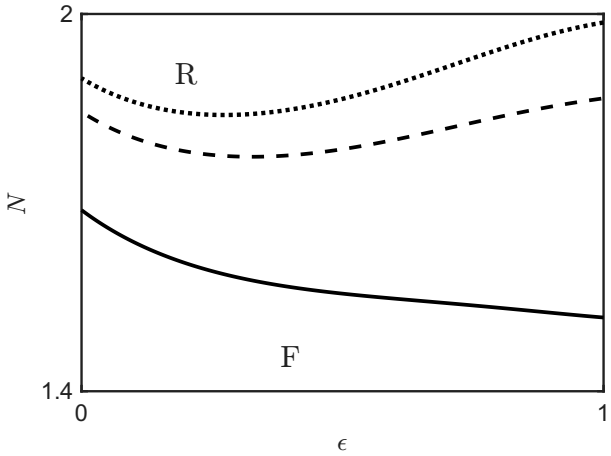


Figure 2.21: Saddle-node bifurcation curves in the $(\epsilon, N)$ parameter space for different values of $R_2^+$: solid line $R_2^+ = 0.3$, dashed line $R_2^+ = 2$ and dotted line $R_1^+ = 20$.

To conclude the analysis of the role played by positive reactions to love in presence of a child, we investigate how caregiving affects the region of alternative stable states, comparing them to Figure 2.3. As in the case of the appeals parameter space, we compute the new ASS region for $N = 0.5, 1$ and $\epsilon = 0, 0.5, 1$.

Figure 2.22 shows how the region of alternative stable states depends on the caregiving division when $N$ is fixed at $N = 0.5$ and the reaction to love is considered. When $\epsilon = 0$, that is, when the entire caregiving burden is borne by partner 2, the system becomes robust for relatively small reductions of the positive reaction of partner 1. Conversely, for $\epsilon = 1$, where partner 1 bears the full caregiving load, robustness can be recovered by smaller changes in the positive reaction of partner 2. As expected, the case $\epsilon = 0.5$ corresponds to an intermediate situation.

This behaviour can be explained by considering how caregiving demands affect emotional responsiveness in the model. The partner who bears most of the caregiving burden experiences an effective attenuation of emotional reactivity due to the presence of the child and is therefore already partially stabilized by caregiving demands. In contrast, the partner who is less involved in childcare remains more emotionally reactive and consequently plays a dominant role in determining the transition out of the bistable regime. As a result, robustness can be recovered through relatively small adjustments in the reaction to love parameters of the non-caregiving partner.

This indicates that the partner who is less engaged in childcare retains a greater influence on the emotional balance of the couple. Having more emotional resources available for the relationship, this partner effectively acts as a regulator of the couple's dynamics, while

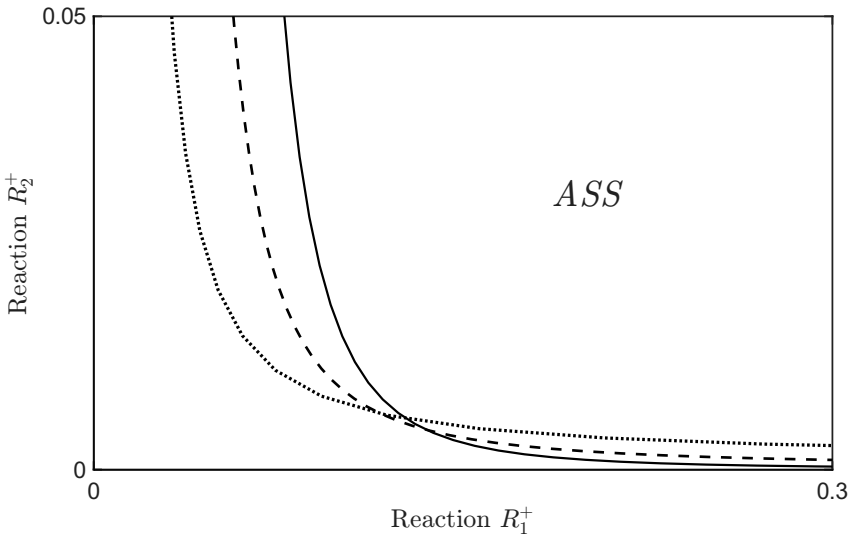


Figure 2.22: Effect on the ASS of reactions region ($N = 0.5$): solid line $\epsilon = 0$, dashed line $\epsilon = 0.5$, dotted line $\epsilon = 1$.

the caregiving partner, being more emotionally absorbed by parental responsibilities, has a reduced impact on the overall stability of the relationship.

As in the $(A_1, A_2)$ parameter space, increasing the caregiving demand leads to a contraction of the ASS region, as illustrated in Figure 2.23. The qualitative behaviour is the same as that observed in Figure 2.22, but the effect is more pronounced due to the higher caregiving load.

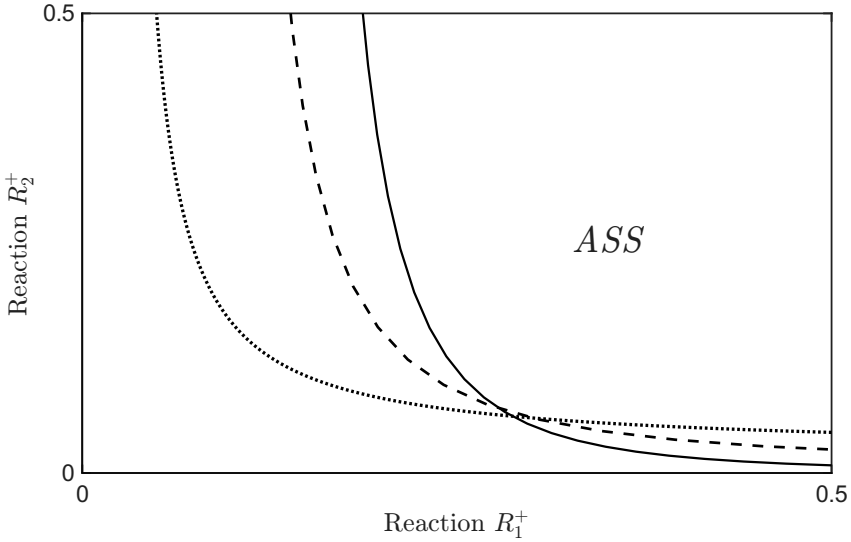


Figure 2.23: Effect on the ASS of reactions region ($N = 1$): solid line $\epsilon = 0$, dashed line $\epsilon = 0.5$, dotted line $\epsilon = 1$.

To conclude the analysis of fragile couples, we examine how the equilibrium levels of emotional involvement vary with respect to the caregiving demand $N$ and the caregiving division parameter $\epsilon$, following the same approach adopted in Section 2.2. The reference parameter configuration is given in Table 2.3 with the appeal parameter fixed at $A_1 = 0.2$. Figure 2.24 shows that, similarly to the case of robust couples, when caregiving responsibilities are equally shared ($\epsilon = 0.5$), increasing $N$ leads to a decrease in the equilibrium involvement of both partners. This reflects the progressive reduction of emotional resources available for the couple as caregiving demands increase.

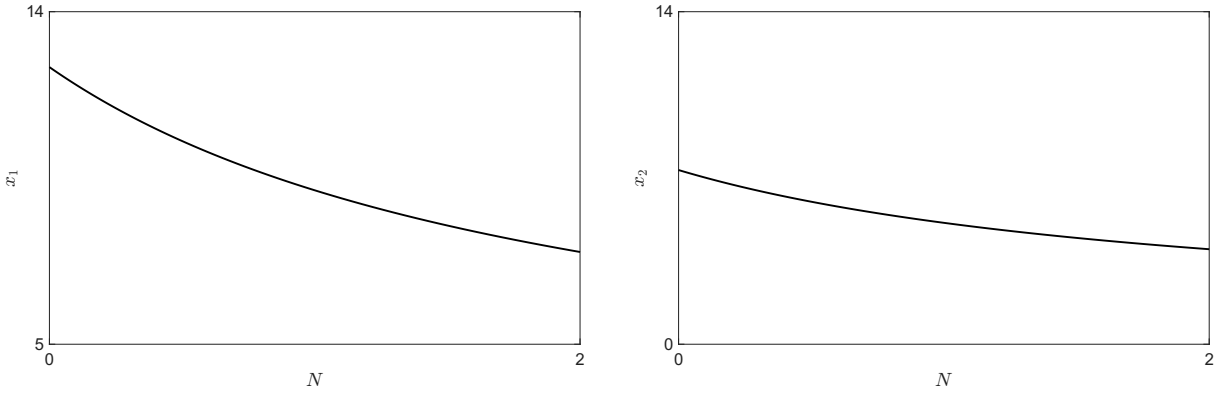


Figure 2.24: Evolution of $x_1$ and $x_2$ with respect to $N$ ($\epsilon = 0.5$).

For $N = 1.5$, varying the caregiving division parameter $\epsilon$ from 0 to 1, we observe that partner 1 becomes progressively less involved as they take on an increasing share of the caregiving responsibilities, while partner 2 exhibits a corresponding increase in emotional involvement (Figure 2.25).

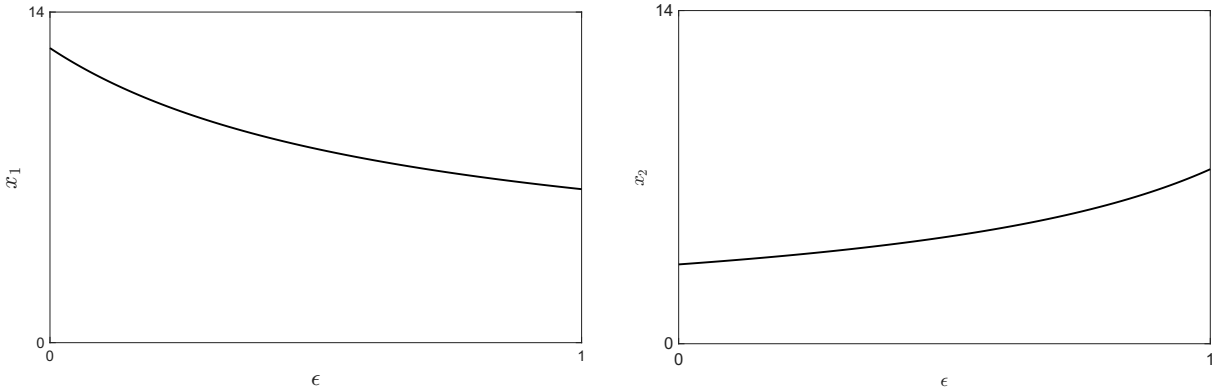


Figure 2.25: Evolution of $x_1$ and $x_2$ with respect to $\epsilon$ ($N = 1.5$).

We finally analyze the equilibrium level of involvements in the $(\epsilon, N)$ parameter space, following the same approach adopted for robust couples. In these diagrams, the white curve

represents the locus of saddle–node bifurcations separating fragile (below) and robust (above) couples, while the black curve has the same interpretation as in the robust case. Since robustness is a desirable dynamical property, we restrict our attention to configurations lying above the saddle–node curve, which guarantee robustness while minimizing the negative effect of increasing caregiving demands. Under this assumption, each partner's preferred caregiving division can be inferred by examining how their equilibrium involvement varies along this curve. In particular, partner 1 tends to prefer configurations close to $\epsilon = 0$, as this choice maximizes their individual level of involvement (Figure 2.26a), while partner 2 strongly strongly favours configurations close to $\epsilon = 1$ for the same reason (Figure 2.26b). However, a different picture emerges when considering the couple as a whole. By examining the total emotional involvement, quantified by the sum $(x_1 + x_2)$, we observe that configurations with $\epsilon = 0$ are generally preferable, as they maximize the overall level of involvement within the couple (Figure 2.26c), whereas intermediate values of $\epsilon$ are associated with lower total involvement.

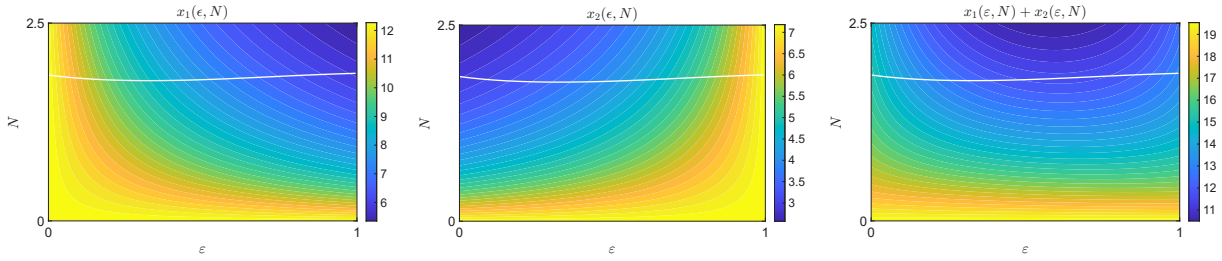


(a) (b) (c)

Figure 2.26: Evolution of individual and collective emotional involvement in the $(\epsilon, N)$ parameter space: (a) involvement $x_1$; (b) involvement $x_2$; (c) total involvement $(x_1 + x_2)$.

To further assess the impact of parenthood, we compare the equilibrium involvement in the $(\epsilon, N)$ parameter space with the corresponding value obtained for the same couple in the absence of a child, using Equation (2.3). This allows us to compute the percentage decrease in emotional involvement induced by caregiving demands. The additional black curve showed in these plots represents the locus of points where both partners experience the same percentage decrease in involvement. From a fairness perspective, couples may wish to position themselves along this curve in order to share the emotional cost of parenthood equally. Ideally, one might expect the optimal configuration to correspond to the intersection between the saddle–node curve (ensuring robustness) and the equal–decrease curve (ensuring balance), as shown in Figure 2.27a and Figure 2.27b. However, Figure 2.27c shows that, for sufficiently large values of $N$, this intersection lies close to the minimum of the total emotional involvement of the couple at fixed $N$. This indicates a

trade–off between robustness, fairness, and overall couple satisfaction.

These results show that, under the assumption that a couple can influence both the total caregiving demand $N$ and its distribution $\epsilon$, different combinations of these parameters may be preferred depending on the desired outcome, whether it be individual satisfaction, fairness between partners, or maximization of the overall emotional involvement of the couple.

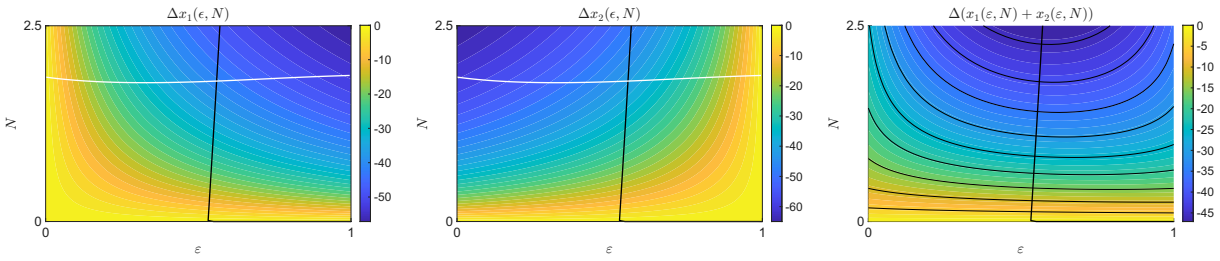


(a) (b) (c)

Figure 2.27: Comparison between the cases with and without a child in the $(\epsilon, N)$ parameter space: (a) variation in involvement $\Delta x_1$; (b) variation in involvement $\Delta x_2$; (c) variation in total involvement $\Delta(x_1 + x_2)$.

In this section, we have investigated how the transition to parenthood affects couples that are fragile in the absence of a child. By combining bifurcation analysis with a detailed study of equilibrium involvement levels, we have shown that caregiving demands generally promote robustness by reducing the regions of alternative stable states. However, the way in which robustness is recovered depends crucially on the distribution of caregiving responsibilities and on individual traits such as appeal and emotional reactivity.

Our results indicate that, for fragile couples, parenthood does not lead to a unique optimal outcome. Different caregiving configurations may favour robustness, individual satisfaction, fairness between partners, or overall couple involvement, but these objectives do not necessarily coincide. As a consequence, the transition to parenthood introduces a nontrivial trade–off between robustness and emotional outcomes, whose resolution depends on the specific characteristics of the partners and on how caregiving demands are managed.

Overall, parenthood emerges as a "stabilizing factor" for initially fragile couples, but this effect is always accompanied by a decrease in emotional involvement as caregiving demands grow. The balance between "stability" and involvement is therefore strongly influenced by differences in partners' appeal and emotional reactivity, as well as by how caregiving responsibilities are distributed between them.

# 3 | Couples of insecure and secure individuals

Having analyzed couples composed of two secure individuals, we now investigate whether and how the dynamics change when one partner, specifically partner 1, exhibits an insecure attachment style. This case represents a natural extension of the previous analysis and allows us to assess the impact of attachment asymmetry on both the qualitative structure of the dynamics and the resulting emotional outcomes.

Following the framework introduced in Chapter 2, we first study the behaviour of insecure–secure couples in the absence of a child, and then examine how their dynamics are affected by the transition to parenthood. In particular, we begin by analyzing robust configurations and subsequently turn to fragile couples, for which a bifurcation analysis is performed. In both cases, we also investigate the equilibrium levels of emotional involvement and compare them with those obtained in the childless scenario, in order to evaluate the influence of caregiving demands on couple satisfaction.

We recall here the explicit form of the model used throughout this chapter, describing a couple composed of one insecure (partner 1) and one secure (partner 2) individual:

$$\begin{cases} \dot{x}_1 = -\alpha_1 x_1 + \gamma_1 A_2 + \begin{cases} \beta_1 x_2 e^{-k_1(1+\epsilon N h_1)x_2} & \text{if } x_2 \geq 0 \\ \dfrac{e^{x_2}-e^{-x_2}}{\frac{e^{x_2}}{R_1^+} - \frac{e^{-x_2}}{R_1^-(1+\epsilon N h_1)^{-1}}} & \text{if } x_2 < 0 \end{cases} \\ \dot{x}_2 = -\alpha_2 x_2 + \gamma_2 A_1 + \dfrac{e^{x_1}-e^{-x_1}}{\frac{e^{x_1}}{\frac{R_2^+}{1+(1-\epsilon)N h_2}} - \frac{e^{-x_1}}{\frac{R_2^-}{1+(1-\epsilon)N h_2}}} \end{cases} \tag{3.1}$$

Here, the reaction to love parameters of the insecure individual satisfy the relation

$$R_1^+ = \frac{1}{\frac{1}{R_1^-} + \frac{2}{\beta_1}}$$

ensuring continuity of the derivative at $x_2 = 0$.

For a general introduction to bifurcation theory, we again refer to [30, 47]. All numerical bifurcation analyses presented in this chapter are performed using MATCONT [12].

## 3.1. Couples without children

We start by considering the absence of a child, corresponding to $N = 0$, in order to isolate the intrinsic dynamics of a insecure–secure couple and provide a reference scenario for assessing the effects of parenthood, considering only the mutual interaction between the two partners.

The parameter set used in this section is reported in Table 3.1. For this choice of parameters, the system exhibits robust dynamics in the childless case.

| Parameter | Value |
|---|---|
| $\alpha_1$ | 1 |
| $\alpha_2$ | 0.3 |
| $\gamma_1$ | 1 |
| $\gamma_2$ | 1 |
| $A_1$ | 1 |
| $A_2$ | 0.5 |
| $\beta$ | 15 |
| $k$ | 1 |
| $R_1^-$ | $-2$ |
| $R_2^+$ | 2 |
| $R_2^-$ | $-1$ |

Table 3.1: Parameter values for model 3.1.

In this configuration, the system admits only equilibrium solutions, since insecurity alone is not sufficient to generate more complex dynamics; the presence of synergism is also required [21, 38]. Therefore, we restrict our attention to equilibrium dynamics, focusing on transitions between robust and fragile configurations.

As in the previous chapter, the qualitative behaviour of the system can be conveniently interpreted from a geometrical perspective by analyzing the nullclines defined by $\dot{x}_1 = 0$ and $\dot{x}_2 = 0$ (see Figure 3.1). These are given explicitly by:

$$x_1 = \frac{R_1^L(x_2) + \gamma_1 A_2}{\alpha_1}, \qquad x_2 = \frac{R_2^L(x_1) + \gamma_2 A_1}{\alpha_2} \tag{3.2}$$

When the nullclines intersect at a single point, the system exhibits robust dynamics (Figure 3.1a), with all trajectories converging to the unique stable equilibrium. In contrast, fragile configurations are characterized by three intersection points (Figure 3.1b), corresponding to two stable equilibria separated by a saddle-point whose stable manifold (not shown in the figure) defines the boundary between their basins of attraction. As in the case of secure couples, robustness represents a desirable dynamical regime, as it ensures resilience with respect to perturbations.

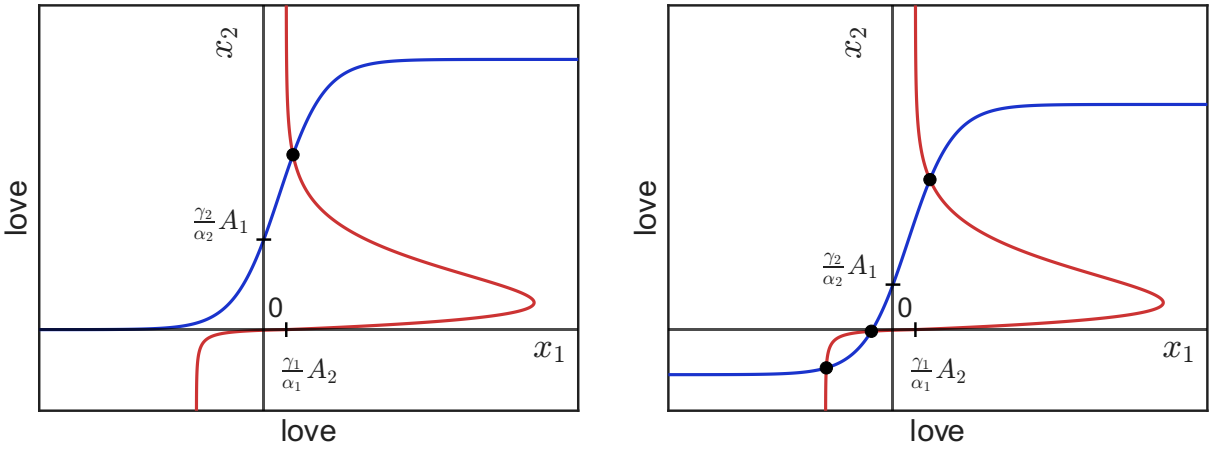


(a) Robust couples

(b) Fragile couples

Figure 3.1: Nullclines of the system for childless couples ($N = 0$). The red curve corresponds to $\dot{x}_1 = 0$, while the blue curve corresponds to $\dot{x}_2 = 0$.

As in the case of secure couples, variations in the appeal parameters $A_1$ and $A_2$ induce horizontal and vertical shifts of the nullclines, respectively. These shifts may lead to a saddle–node bifurcation, which governs the transition between fragile and robust configurations. Accordingly, it is possible to identify regions of the appeal parameter space $(A_1, A_2)$ where alternative stable states (ASS) are present. This is achieved through a bifurcation analysis and numerical continuation of equilibria in the $(A_1, A_2)$ parameter space [37]. The resulting region characterizes the combinations of appeal values for which childless insecure–secure couples exhibit fragile dynamics (see Figure 3.2).

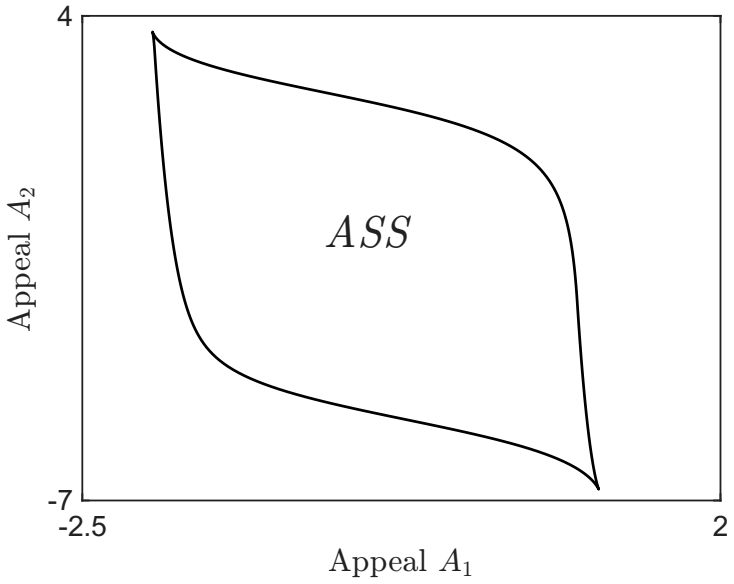


Figure 3.2: Region of alternative stable state (ASS) in the space of appeals for $N = 0$.

The boundary of the ASS region (fragile couples) is characterized by saddle–node bifurcations. In particular, along the upper boundary a saddle–node bifurcation involves the saddle point and one of the stable equilibria, whereas along the lower boundary the saddle collides with the other stable equilibrium. As a consequence, crossing either boundary leads to the disappearance of bistability and to the recovery of a robust configuration.

Following the same reasoning developed for secure couples, we observe that appeal plays a relevant role in shaping the dynamics, but it does not fully determine the qualitative behaviour of the system. An equally important contribution comes from the way individuals respond to their partner's emotional involvement.

For this reason, we now investigate how the positive reaction to love parameter of partner 2, $R_2^+$, influences the structure of the region of alternative stable states, in combination with the parameter $\beta$, which characterizes the reaction to love of the insecure partner. In the present setting, the insecure individual does not possess a positive asymptotic reaction to love parameter $R_1^+$, as their response is non-monotonic and does not saturate at a positive plateau. Consequently, $\beta$ represents the most relevant parameter controlling the intensity of the insecure partner's reaction to positive involvement, as it directly affects both the height of the reaction peak and the steepness of the response near the origin, which are crucial features for the occurrence of saddle–node bifurcations. From a modeling prospective, $\beta$ therefore constitutes the natural counterpart of $R_1^+$ in the secure–secure case, as it governs the strength of the positive feedback induced by the partner's emotional involvement.

Figure 3.3 shows the region of alternative stable state in the $(\beta, R_2^+)$ parameter space.

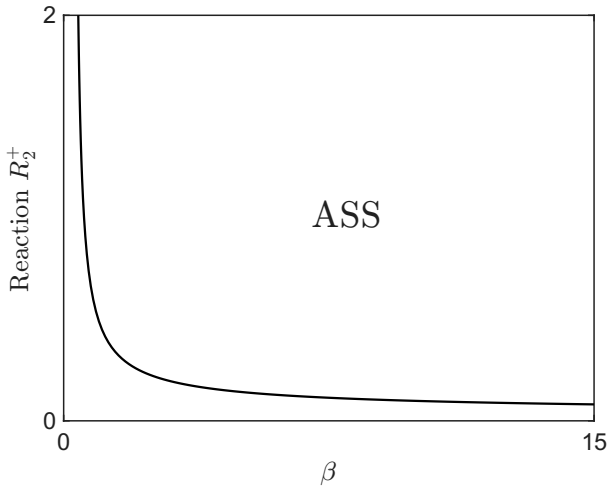


Figure 3.3: Region of alternative stable states (ASS) in the parameter space $(\beta, R_2^+)$ for $N = 0$, with $A_1 = 0.3$ and the remaining parameters as in Table 3.1.

This behaviour can be interpreted from a geometrical perspective: decreasing either parameter flattens the corresponding nullcline, thereby reducing the number of possible intersections and suppressing bistability. From a modeling point of view, consistently with what observed for secure couples, a weaker reaction to the partner's emotional involvement makes it harder for the system to transition toward states of mutual hostility. At the same time, however, reduced emotional responsiveness also results in lower equilibrium levels of mutual involvement, reflecting a diminished intensity of the relationship.

Overall, the analysis of childless insecure–secure couples highlights the distinct roles played by appeal and emotional responsiveness in shaping the system's dynamics. Higher appeal values consistently promote both increased emotional involvement and robustness, facilitating convergence toward a single stable equilibrium. In contrast, the intensity of the reaction to love introduces a trade-off between stability and emotional involvement. Strong emotional responses favour higher levels of mutual involvement but allow for the emergence of fragile configurations characterized by bistability, whereas weaker reactions promote robustness by suppressing fragile dynamics, at the cost of reduced equilibrium involvement.

This interplay between appeal, emotional responsiveness, and robustness provides the reference framework for the following sections, where caregiving demands associated with parenthood are introduced and their impact on both stability and emotional satisfaction are systematically investigated.

## 3.2. Robust couples: the effect of the transition to parenthood

We focus first on couples that are robust in the absence of a child and examine whether this property is preserved once caregiving demands are taken into account. As in the secure–secure case, we address two main questions: whether parenthood, represented by the parameters $N$ and $\epsilon$, can induce qualitative changes in the dynamics, potentially leading to fragile behaviour, and how the equilibrium levels of involvement are reshaped by the presence of a child.

We start the analysis by considering the parameter set reported in Table 3.1 and introducing caregiving demands into the system. As a first step, we perform a geometrical analysis by fixing the caregiving division parameter at $\epsilon = 0.5$ progressively increasing the caregiving demand $N$. As illustrated in Figure 3.4, the nullcline associated with the insecure partner also undergoes a gradual flattening as $N$ increases. This deformation leads to a downward shift of the equilibrium point for both partners and, importantly, prevents the emergence of additional intersections between the nullclines. As a consequence, increasing caregiving demands alone cannot induce a transition from a robust to a fragile configuration.

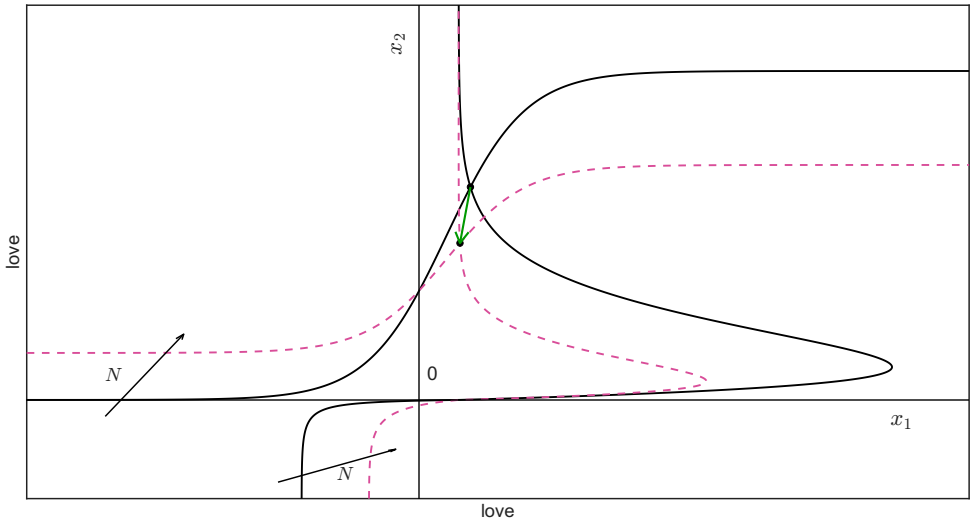


Figure 3.4: Effect of increasing $N$ on the nullclines with $\epsilon = 0.5$. The solid curve corresponds to $N = 0$, while the pink dashed curve corresponds to $N = 1.5$.

From a modeling perspective, this result mirrors what was observed in the secure–secure case. The introduction of a child acts as a stabilizing mechanism: robust couples become less sensitive to perturbations and are less likely to transition toward states of

mutual hostility. At the same time, this stabilizing effect comes at the cost of reduced equilibrium levels of emotional involvement for both partners, at least for the chosen parameter configuration. More generally, these results suggest that, independently of the specific attachment styles involved, increasing caregiving demands systematically reduces the emotional resources that partners can devote to one another. In the model, this reflects the intuitive idea that time, attention, and energy allocated to childcare are necessarily subtracted from the couple relationship, as documented in the literature [3, 5, 26].

Similarly, we fix the caregiving demand $N$ and vary the parameter $\epsilon$ from 0 to 1 in order to investigate whether a redistribution of caregiving responsibilities alone can induce a transition from a robust to a fragile configuration. As shown in Figure 3.5, the qualitative behaviour is analogous to that observed for secure–secure couples. As $\epsilon$ increases, the nullcline $\dot{x}_2 = 0$, associated with the secure partner, progressively widens, approaching its childless shape when the caregiving load is entirely shifted away from partner 2. Conversely, the nullcline $\dot{x}_1 = 0$, associated with the insecure partner, becomes progressively flatter as the caregiving burden assumed by partner 1 increases. Despite these deformations, no additional intersections between the nullclines appear. Therefore, as in the case of secure couples, for sufficiently high caregiving load, the redistribution of caregiving responsibilities alone is not sufficient to induce fragile behaviour. Robust dynamics are preserved for all values of $\epsilon$.

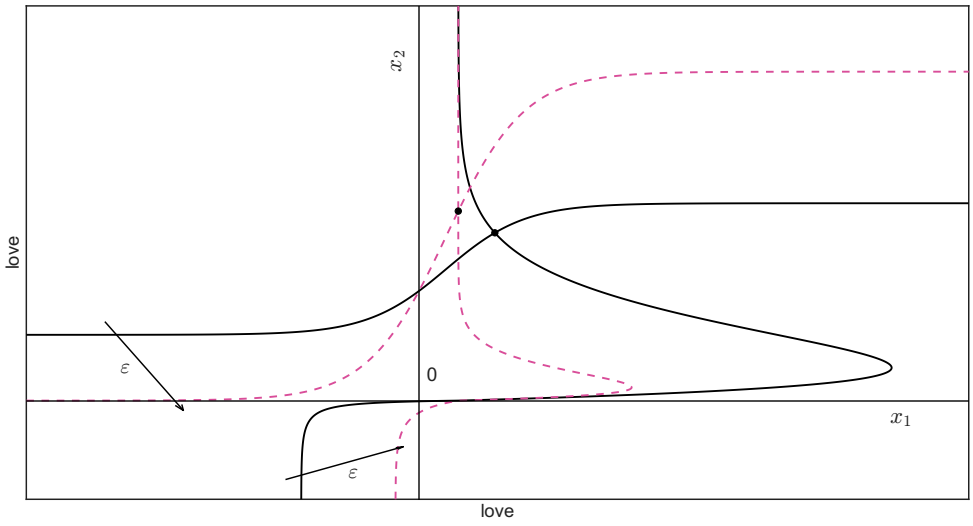


Figure 3.5: Effect of increasing $\epsilon$ on the nullclines with $N = 1.5$. The solid curve corresponds to $\epsilon = 0$, while the pink dashed curve corresponds to $\epsilon = 1$.

We complete the analysis of robust insecure–secure couples by investigating the equilibrium levels of emotional involvement for a couple characterized by the parameter set

reported in Table 3.1.

Figure 3.6, shows how the equilibrium values of the partners' involvement, $x_1$ and $x_2$, vary as the caregiving demand $N$ increases, with the caregiving division fixed at $\epsilon = 0.5$. As expected, the level of involvement of both partners decreases with increasing $N$, reflecting the fact that caregiving responsibilities associated with a newborn necessarily subtract time, attention, and energy from the couple relationship [3, 5, 26].

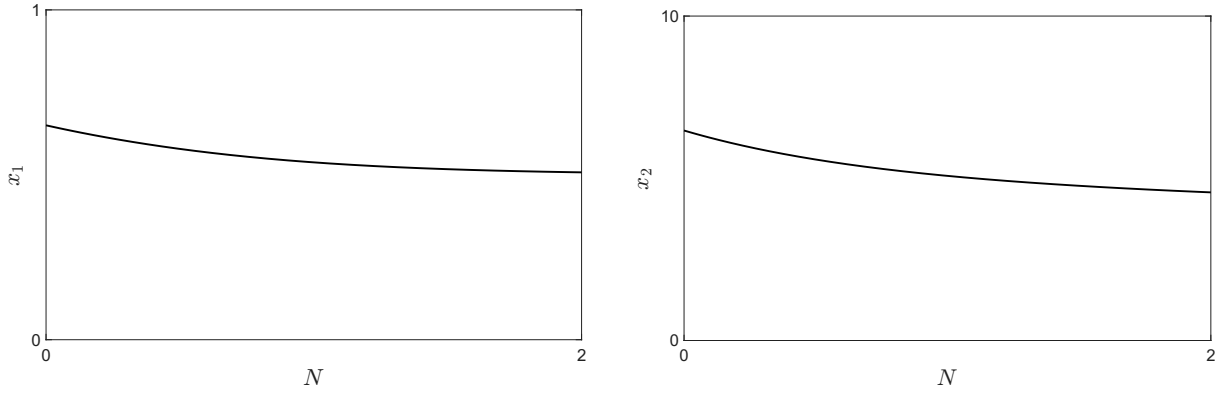


Figure 3.6: Evolution of $x_1$ and $x_2$ with respect to $N$, for $\epsilon = 0.5$.

In Figure 3.7, we fix the caregiving demand at $N = 1.5$ and analyze the effect of varying the caregiving division parameter $\epsilon$ from 0 to 1. As $\epsilon$ increases, the equilibrium involvement of partner 1 decreases, consistently with the fact that partner 1 progressively bears a larger share of the caregiving burden. Notably, this decrease saturates beyond an intermediate value of $\epsilon$, leading to a plateau for larger caregiving loads. This behaviour may be interpreted by noting that the insecure partner becomes overwhelmed once a certain level of responsibility is reached, so that further increases in caregiving demands do not produce additional reductions in emotional involvement. In this regime, the total perceived burden is effectively indistinguishable from the partner's perspective.

The response of partner 2 is instead non-monotonic. The equilibrium involvement $x_2$ remains relatively high for values of $\epsilon$ close to 0 and close to 1, while it attains a minimum for intermediate values of $\epsilon$. This U-shaped dependence can be interpreted within the model as follows: when caregiving is concentrated on one partner (i.e., $\epsilon$ close to 0 or 1), at least one individual is largely relieved from caregiving demands and can sustain higher emotional involvement, either directly (when partner 2 carries little or no caregiving load) or indirectly through a higher $x_1$, which supports $x_2$ via the reaction to love term. In contrast, when caregiving is shared, both partners experience an attenuation of emotional responsiveness, so the reduction in involvement affects both sides of the interaction, leading to a lower equilibrium level for $x_2$. Overall, these results are consistent with findings in

the psychological literature (see, e.g, [17, 29, 42]): which suggest that insecure individuals tend to experience greater difficulty in coping with caregiving responsibilities, particularly when such demands are sustained.

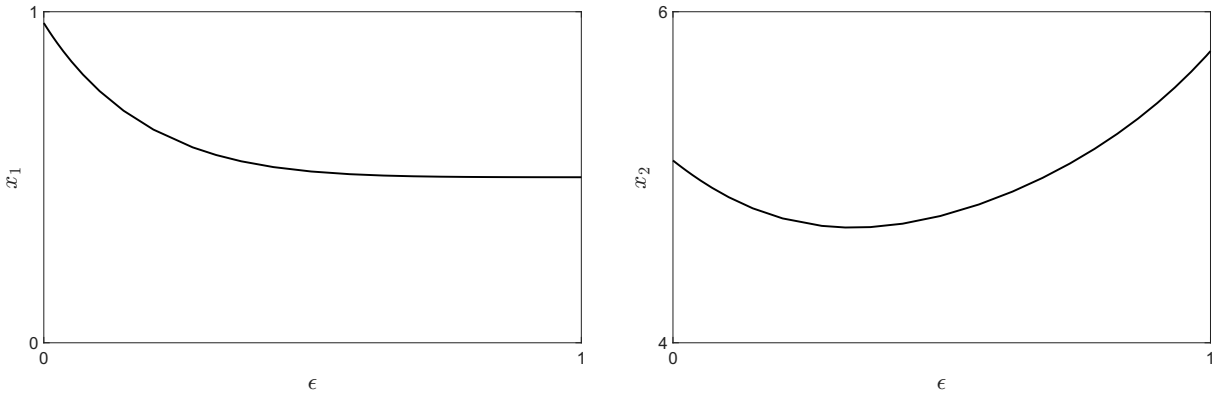


Figure 3.7: Evolution of $x_1$ and $x_2$ with respect to $\epsilon$, for $N = 1.5$.

We then investigate how the equilibrium levels of involvement depend on the combined effect of the caregiving demand $N$ and its distribution $\epsilon$, by analyzing their variation in the $(\epsilon, N)$ parameter space. Figure 3.8a shows that, for sufficiently high caregiving demands, the involvement of partner 1 is maximized when partner 2 bears most of the caregiving load. From a geometrical perspective, this behaviour is related to the shape of the nullcline associated with the insecure partner. When partner 2 is less emotionally involved, the nullcline $\dot{x}_1 = 0$ becomes flatter and shifts downward. As a consequence, the equilibrium point moves closer to the peak of the insecure partner's reaction to love function, leading to higher equilibrium involvement for partner 1. From a modeling point of view, this can be interpreted by noting that the avoidant partner feels less overwhelmed when the other partner devotes more time and energy to childcare rather than to the couple interaction, thereby sustaining higher emotional involvement, in line with findings reported in the literature (see, e.g., [17]). Figure 3.8b shows that partner 2 achieves the highest levels of involvement for low caregiving demands. However, for sufficiently large values of $N$, the dependence of $x_2$ on $\epsilon$ becomes non-monotonic, recovering the U-shaped pattern already observed in Figure 3.7. This indicates that, when caregiving demands are high, intermediate divisions of responsibilities lead to lower involvement for partner 2 compared to more asymmetric allocations. Finally, Figure 3.8c reports the overall emotional involvement of the couple, quantified by the sum $(x_1 + x_2)$. Also in this case, for sufficiently large values of $N$, the total involvement exhibits a minimum at intermediate values of $\epsilon$, while smaller caregiving demands consistently correspond to higher levels of overall couple involvement.

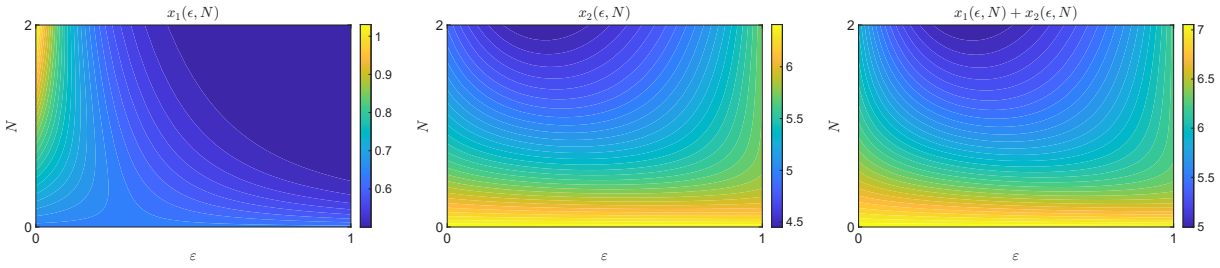


(a) (b) (c)

Figure 3.8: Evolution of individual and collective emotional involvement in the $(\epsilon, N)$ parameter space: (a) involvement $x_1$; (b) involvement $x_2$; (c) total involvement $(x_1 + x_2)$.

Referring to Equation (2.3), we compare, on the $(\epsilon, N)$ parameter space, the equilibrium levels of involvement with respect to the childless case. A particularly interesting result is shown in Figure 3.9a, where, for sufficiently large values of $N$ (i.e., the entire caregiving burden is borne by partner 2), the involvement of partner 1 increases by up to 50% relative to the childless case. This effect is a direct consequence of the insecure attachment style of partner 1 and can be interpreted following the same geometrical reasoning discussed above: concentrating caregiving on partner 2 modifies the nullcline structure in such a way that the equilibrium point moves closer to the peak of the insecure partner's reaction to love function. Figure 3.9b shows the corresponding percentage variation for partner 2. Except for very low caregiving demands, the largest deterioration of involvement occurs for intermediate values of $\epsilon$, confirming that shared caregiving responsibilities tend to penalize emotional involvement more than asymmetric allocations when $N$ is sufficiently large. The black curve in both figures represents the locus of points where the two partners experience the same percentage change in involvement. Notably, this curve is shifted toward configurations in which the insecure partner bears a larger share of the caregiving load, suggesting that, if an equal relative deterioration is desired, partner 1 should assume more caregiving responsibilities than partner 2. However, Figure 3.9c shows that this same curve lies close to the minimum of the total emotional involvement of the couple. This indicates that configurations ensuring an equal distribution of emotional deterioration between partners do not, in general, maximize the overall level of love within the couple. These results appear to be consistent with findings in the literature (e.g., [17, 29, 42]), according to which insecurely attached individuals generally experience greater difficulties in managing childcare responsibilities. Such demands may activate avoidance tendencies, as these individuals can feel a reduced sense of autonomy and control over their time and daily activities.

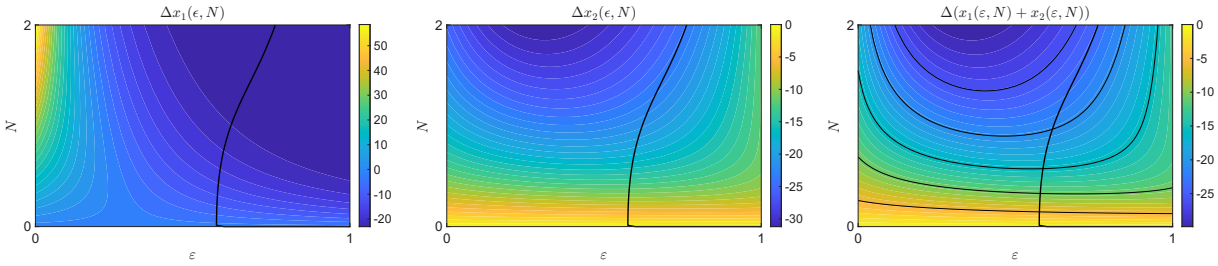


(a) (b) (c)

Figure 3.9: Comparison between the cases with and without a child in the $(\epsilon, N)$ parameter space: (a) variation in involvement $\Delta x_1$; (b) variation in involvement $\Delta x_2$; (c) variation in total involvement $\Delta(x_1 + x_2)$.

Following the approach adopted in Section 2.2, we repeat the above analysis using different parameter sets, in order to illustrate how variations in individual characteristics may modulate the impact of caregiving demands on couple involvement. As a first case, we consider the parameter configuration reported in Table 3.2.

| Parameter | Value |
|---|---|
| $\alpha_1$ | 1 |
| $\alpha_2$ | 0.3 |
| $\gamma_1$ | 1 |
| $\gamma_2$ | 1 |
| $A_1$ | 0.7 |
| $A_2$ | 0.6 |
| $\beta$ | 30 |
| $k$ | 1 |
| $R_1^-$ | $-2$ |
| $R_2^+$ | 1 |
| $R_2^-$ | $-1$ |

Table 3.2: Parameter values for model 3.1.

Figure 3.10 shows the dependence of the equilibrium involvement on the caregiving demand $N$ with $\epsilon = 0.5$. As observed throughout the analysis, increasing $N$ leads to a reduction in emotional involvement for both partners, reflecting the progressive reallocation of emotional resources toward caregiving activities .

Figure 3.11, instead, illustrates the dependence on the caregiving division parameter $\epsilon$ with caregiving demand fixed at $N = 0.3$. In this case, the involvement of partner 1

decreases monotonically as $\epsilon$ increases, consistently with the fact that partner 1 bears an increasing share of the caregiving burden. In contrast, partner 2 exhibits a maximum at intermediate values of $\epsilon$, shifted toward smaller values of $\epsilon$. This indicate that, for this parameter configuration, partner 2 reaches the highest level of emotional involvement when caregiving is partially shared but still predominantly assigned to partner 2. Overall, these results suggest that, at least for this value of $N$, both partners achieve higher levels of emotional involvement when partner 2 assumes most of the caregiving responsibilities, while a fully symmetric division is not optimal in terms of relational involvement.

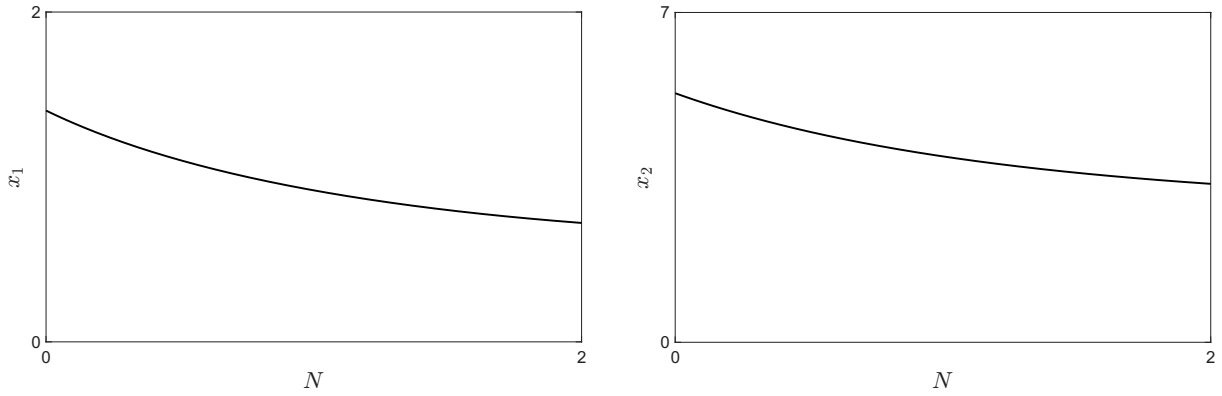


Figure 3.10: Evolution of $x_1$ and $x_2$ with respect to $N$, for $\epsilon = 0.5$.

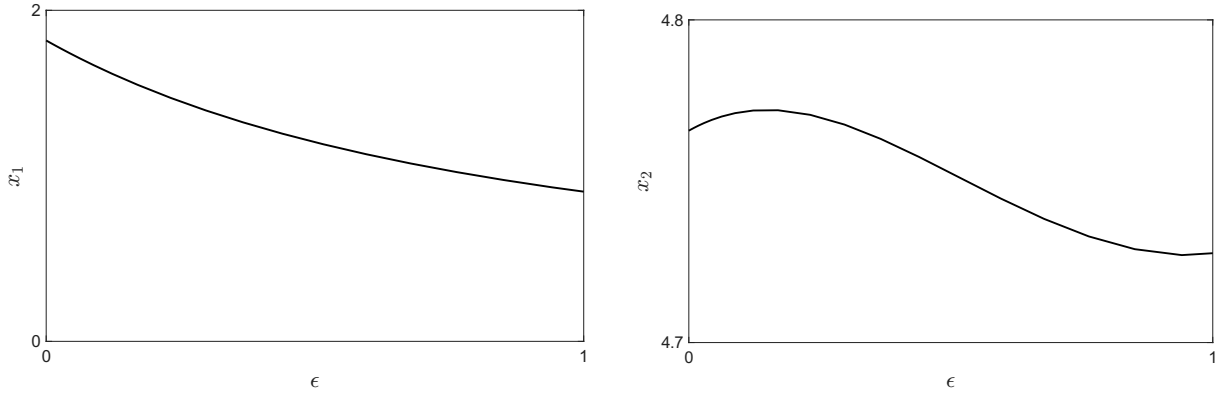


Figure 3.11: Evolution of $x_1$ and $x_2$ with respect to $\epsilon$, for $N = 0.3$.

We then turn to the $(\epsilon, N)$ parameter space to analyze how different caregiving demands and divisions of responsibility affect the equilibrium levels of involvement (Figure 3.12). Figure 3.12a shows that, for partner 1, the most favourable configuration corresponds to situations in which partner 2 assumes most or all of the caregiving burden. This preference becomes particularly pronounced for high values of the caregiving demand $N$, in agreement with the behaviour previously observed in Figure 3.8a. The situation is more articulated

for partner 2. As shown in Figure 3.12b, the highest levels of involvement are achieved for low values of $N$. As $N$ increases, the dependence on $\epsilon$ becomes non-monotonic: a local maximum of involvement first appears for values of $\epsilon$ close to zero, followed by a minimum at intermediate values of $\epsilon$, and finally a recovery of involvement as $\epsilon$ approaches one. This behaviour reflects the complex interplay between caregiving load and emotional responsiveness in this parameter configuration. Finally, Figure 3.12c, reports the total emotional involvement of the couple. Here, the highest overall levels of involvement are consistently attained for $\epsilon = 0$, corresponding to configurations in which partner 2 bears the caregiving burden. In contrast, intermediate values of $\epsilon$ and values close to $\epsilon = 1$ are associated with lower total involvement. Overall, this analysis confirms that, for this parameter set, asymmetric caregiving arrangements, particularly those in which partner 2 assumes most of the caregiving responsibilities, are not only preferred by the insecure partner, but also maximize the total emotional involvement of the couple.

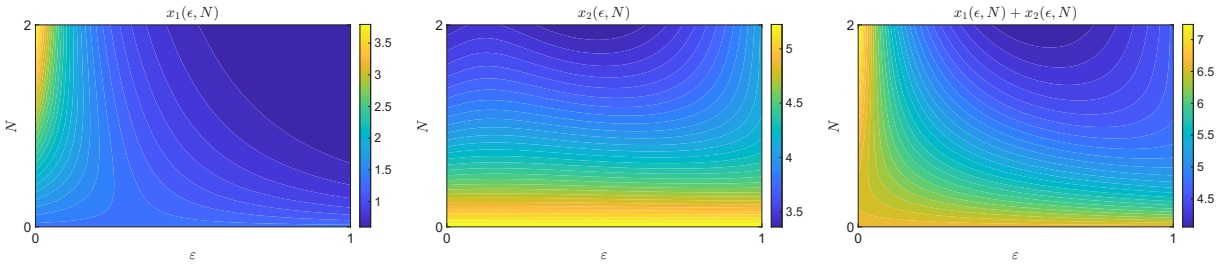


(a) (b) (c)

Figure 3.12: Evolution of individual and collective emotional involvement in the $(\epsilon, N)$ parameter space: (a) involvement $x_1$; (b) involvement $x_2$; (c) total involvement $(x_1 + x_2)$.

To conclude the analysis for this couple, we compare the equilibrium involvement in the $(\epsilon, N)$ parameter space with the corresponding childless case (Figure 3.13), using Equation (2.3). The black curve represents the locus of parameter values for which both partners experience the same percentage loss of emotional involvement. In this configuration, the black curve lies at intermediate values of $\epsilon$, slightly shifted toward partner 2. For this couple, such configurations do not correspond to the worst-case scenario in terms of emotional loss, nor to the optimal one. Instead, they represent a meaningful compromise between fairness, understood as an equal relative deterioration for both partners, and the preservation of emotional involvement.

Overall, this result highlights that, for certain parameter configurations, equitable caregiving arrangements can constitute a reasonable trade-off, balancing relational fairness and emotional costs, without severely penalizing either partner or the couple as a whole.

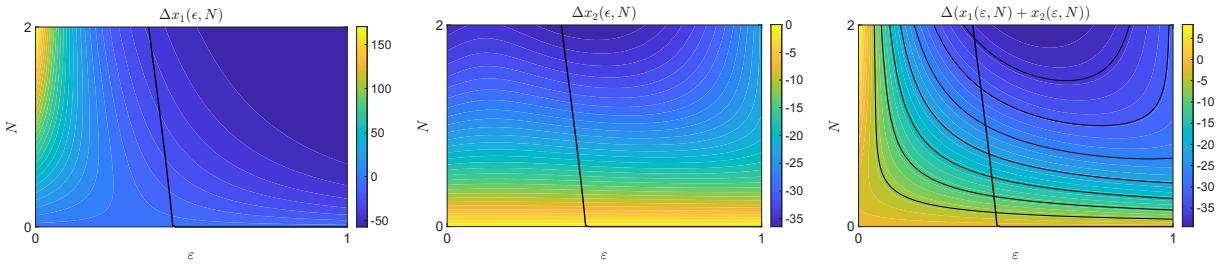


(a) (b) (c)

Figure 3.13: Comparison between the cases with and without a child in the $(\epsilon, N)$ parameter space: (a) variation in involvement $\Delta x_1$; (b) variation in involvement $\Delta x_2$; (c) variation in total involvement $\Delta(x_1 + x_2)$.

Then we introduce another parameter configuration, reported in Table 3.3, which provides an additional illustrative case. This example further emphasizes the wide variety of possible dynamical behaviours, showing that the effects of parenthood depend not only on attachment style, but also on individual characteristics encoded in the model parameters.

| Parameter | Value |
|---|---|
| $\alpha_1$ | 1.3 |
| $\alpha_2$ | 0.7 |
| $\gamma_1$ | 1 |
| $\gamma_2$ | 1 |
| $A_1$ | 0.1 |
| $A_2$ | 0.5 |
| $\beta$ | 7 |
| $k$ | 0.3 |
| $R_1^-$ | $-1$ |
| $R_2^+$ | 0.5 |
| $R_2^-$ | $-0.1$ |

Table 3.3: Parameter values for model 3.1.

As in the previous analyses, we begin by observing that, for increasing caregiving demands $N$ with $\epsilon = 0.5$, the equilibrium levels of involvement of both partners systematically decrease (Figure 3.14).

More interesting insights emerge when we examine the dependence on the caregiving division parameter $\epsilon$ for a fixed value $N = 0.3$ (Figure 3.15). In this case, we observe

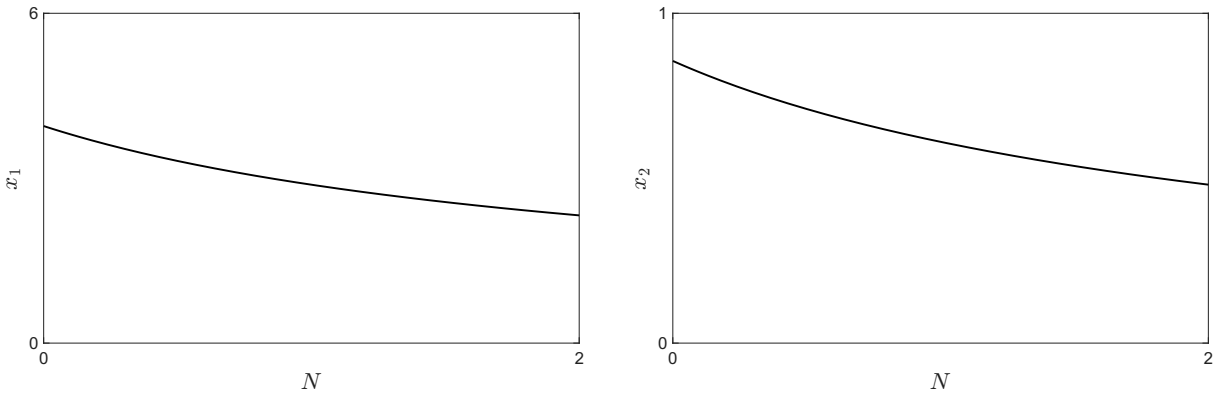


Figure 3.14: Evolution of $x_1$ and $x_2$ with respect to $N$, for $\epsilon = 0.5$.

an unexpected outcome: the emotional involvement of both partners increases when the caregiving burden is predominantly assigned to partner 1, the insecure individual. At first glance, this seems to contradict the typical interpretation of insecure attachment, according to which caregiving responsibilities tend to overwhelm avoidant individuals and reduce their emotional involvement. However, this behavior can be clarified by considering the parameter values. In particular, the parameter $k = 0.3$, which regulates the position of the peak in the insecure individual's reaction to love function and thus captures the degree of insecurity, is relatively small. This implies that partner 1's insecurity is weakly expressed: emotional responsiveness declines only at relatively high levels of the partner's involvement. Consequently, assigning caregiving responsibilities to partner 1 does not immediately trigger withdrawal. A possible connection with the literature is that lower levels of marital satisfaction are generally associated with highly insecure partners [17, 29], whereas in the present configuration the degree of insecurity is relatively low.

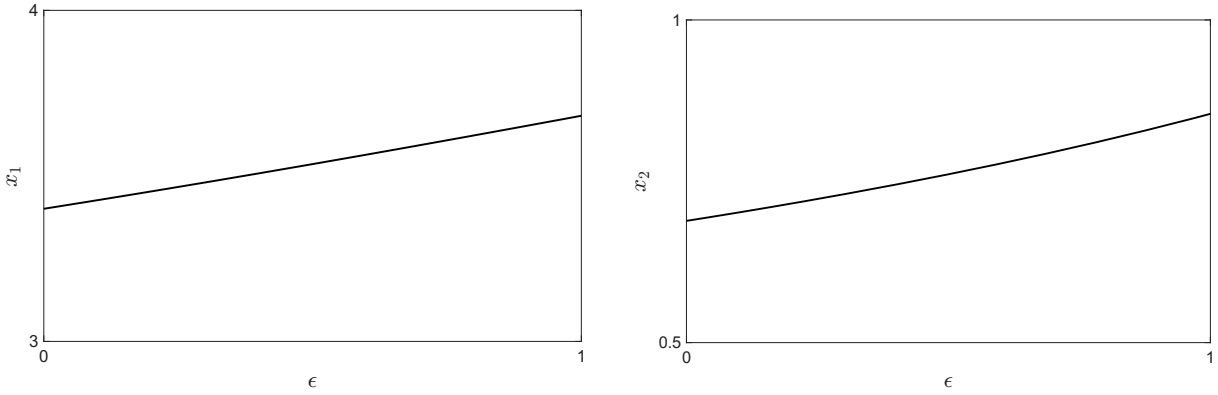


Figure 3.15: Evolution of $x_1$ and $x_2$ with respect to $\epsilon$, for $N = 0.3$.

We then examine the behaviour in the $(\epsilon, N)$ parameter space, shown in Figure 3.16. This analysis confirms that the effect described above persists across the entire range of

caregiving demands considered, at least up to $N = 2$. In particular, for all values of $N$, the highest involvement levels are attained when caregiving is predominantly assigned to partner 1. This conclusion is reinforced by Figure 3.16c, which reports the total emotional involvement of the couple. The sum $(x_1 + x_2)$ is maximized for all values of $N$ when $\epsilon = 1$, indicating that, for this parameter configuration, concentrating caregiving responsibilities on the insecure partner yields the most favourable outcome in terms of overall involvement.

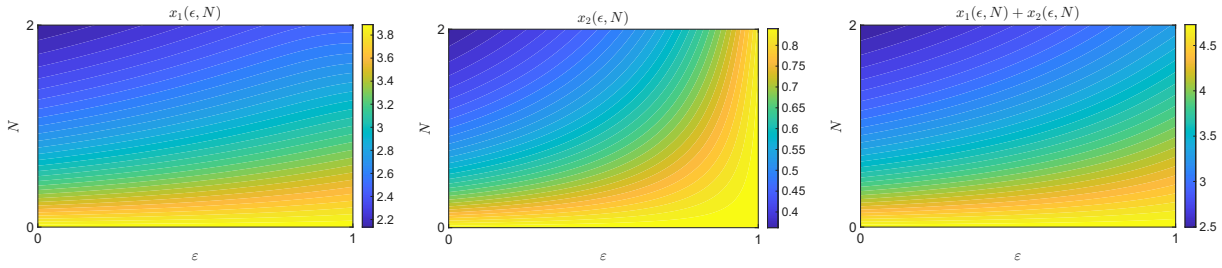


Figure 3.16: Evolution of individual and collective emotional involvement in the $(\epsilon, N)$ parameter space: (a) involvement $x_1$; (b) involvement $x_2$; (c) total involvement $(x_1 + x_2)$.

Moreover, using Equation (2.3), we compare the equilibrium involvement in the $(\epsilon, N)$ parameter space with the corresponding childless configuration (Figure 3.17). The black curve identifies the parameter values for which both partners experience the same percentage loss of emotional involvement. In this configuration, the curve lies at intermediate values of $\epsilon$ and gradually shifts toward partner 1 as $N$ increases. As shown in Figure 3.17c, this equitable configuration does not coincide with extreme losses of total emotional involvement; rather, it represents a reasonable compromise between fairness and relational well-being. In this case, assigning caregiving responsibilities in a way that equalizes the relative emotional cost for both partners can be both convenient and balanced, without severely penalizing the overall level of involvement of the couple.

Overall, the analysis shows that robust insecure–secure couples preserve their robustness under the introduction of caregiving demands. As in the secure–secure case, increasing childcare requirements systematically prevents the emergence of fragile dynamics, ensuring the persistence of a globally stable equilibrium. In this sense, parenthood further reinforces robustness, moving the system deeper into the robust region of the parameter space.

At the same time, other features of the dynamics are deeply affected by caregiving demands and their distribution. Increasing $N$ invariably reduces the equilibrium levels of emotional involvement, reflecting the unavoidable reallocation of time and energy toward childcare. However, the heterogeneity in attachment styles within the couple gives

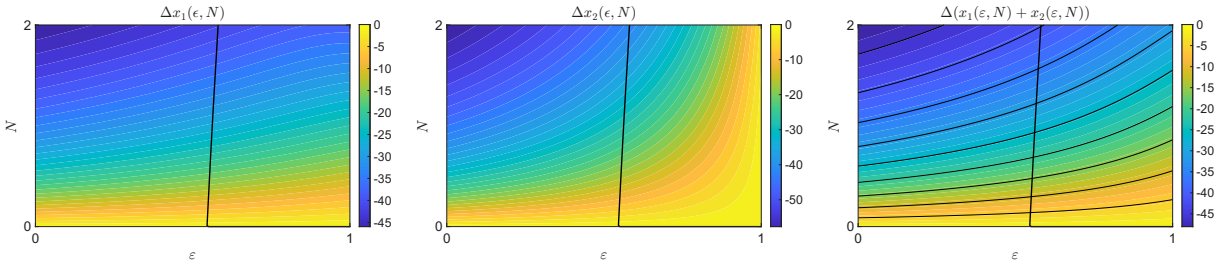


(a) (b) (c)

Figure 3.17: Comparison between the cases with and without a child in the $(\epsilon, N)$ parameter space: (a) variation in involvement $\Delta x_1$; (b) variation in involvement $\Delta x_2$; (c) variation in total involvement $\Delta(x_1 + x_2)$.

rise to nontrivial effects when caregiving responsibilities are redistributed. In particular, asymmetric allocations of caregiving tend to sustain higher levels of individual and total involvement than equal subdivisions, especially for large caregiving demands.

Finally, the comparison with the childless case highlights a tension between equity and overall emotional well-being. Configurations that equalize the relative emotional deterioration of the two partners do not, in general, maximize the total involvement within the couple. This suggests that, even within a robust regime, different caregiving strategies may correspond to qualitatively different trade-offs between fairness and collective satisfaction.

Importantly, the additional parameter configurations explored in this section show that these trade-offs are not universal, but depend sensitively on individual characteristics. While the stabilizing role of caregiving demands is robust across all cases considered, the quantitative outcomes in terms of involvement may differ substantially. This reinforces the idea that parenthood does not impose a single relational trajectory, but rather opens a range of possible outcomes shaped by the specific traits of the partners and by the caregiving strategies they adopt.

## 3.3. Fragile couples: the effect of the transition to parenthood

We now turn to couples that are fragile in the absence of a child, in order to investigate how parenthood affects the qualitative behaviour of the system and whether it may promote robustness. In particular, we analyze how the caregiving demand and division parameters, $N$ and $\epsilon$ respectively, modify the regions of alternative stable states (ASS),

both in the appeal parameter space and in the reaction to love parameter space. Finally, following the same approach adopted in Section 3.2, we examine the equilibrium levels of emotional involvement in the $(\epsilon, N)$ parameter space and compare them with the childless configuration.

The numerical analysis is performed using the parameter set reported in Table 3.4; any deviation from this reference configuration will be explicitly indicated.

As a first step, we examine the effect of increasing caregiving demand $N$ while keeping the caregiving division fixed at $\epsilon = 0.5$, as illustrated in Figure 3.18. In this setting, we recover a well-established result: increasing caregiving demands promote a transition from a fragile to a robust configuration while simultaneously reducing the equilibrium levels of emotional involvement, a behaviour that can be directly traced back to the progressive flattening of the nullclines induced by larger values of $N$, and that is also consistent with findings reported in the literature (see, e.g., [3, 26]).

| Parameter | Value |
|---|---|
| $\alpha_1$ | 1 |
| $\alpha_2$ | 0.3 |
| $\gamma_1$ | 1 |
| $\gamma_2$ | 1 |
| $A_1$ | 0.5 |
| $A_2$ | 0.5 |
| $\beta$ | 15 |
| $k$ | 1 |
| $R_1^-$ | $-2$ |
| $R_2^+$ | 2 |
| $R_2^-$ | $-1$ |

Table 3.4: Parameter values for model 3.1.

We then fix the caregiving demand at $N = 0.45$ and investigate how varying the caregiving division parameter $\epsilon$ from 0 to 1 influences the qualitative behaviour of the system, as shown in Figure 3.19. As already observed in Section 2.3, whether a transition to a robust configuration occurs or not depends crucially on the magnitude of the caregiving demand: for sufficiently small values of $N$, varying $\epsilon$ alone may induce a saddle–node bifurcation, allowing the system to transition from a fragile to a robust regime; conversely, when $N$ is large enough, the system is already robust, and no saddle–node bifurcation can be obtained by modifying $\epsilon$ alone, at least for the parameter set considered here.

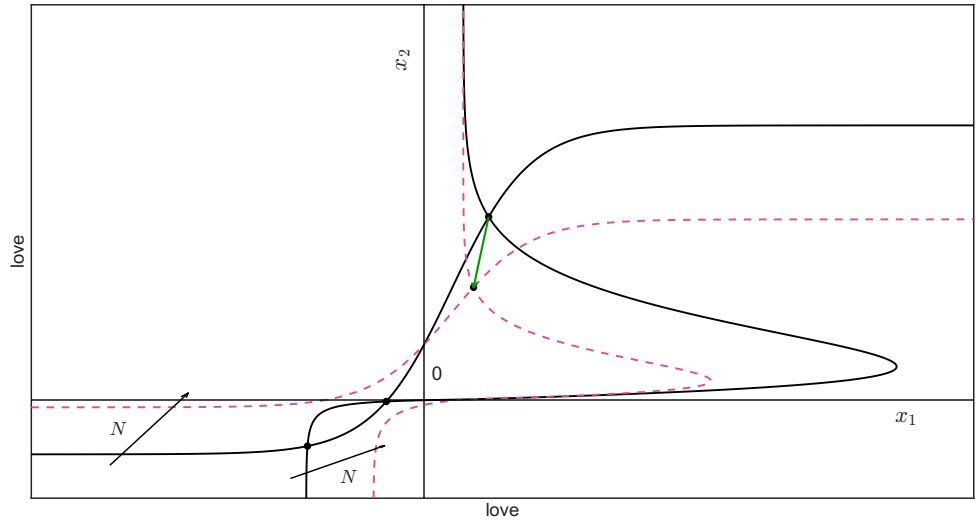


Figure 3.18: Effect of increasing $N$ on the nullclines with $\epsilon = 0.5$. The solid curve corresponds to $N = 0$, while the pink dashed curve corresponds to $N = 1.5$.

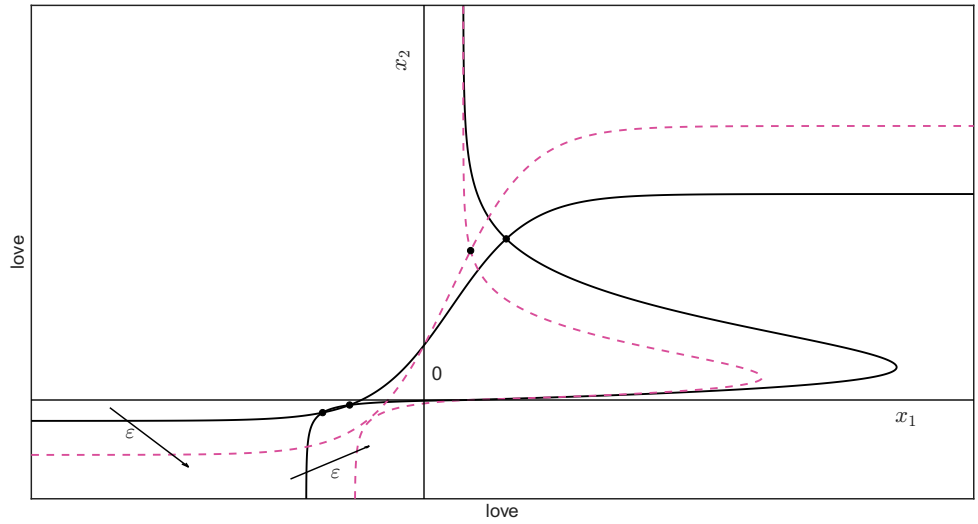


Figure 3.19: Effect of increasing $\epsilon$ on the nullclines with $N = 0.45$. The solid curve corresponds to $\epsilon = 0$, while the pink dashed curve corresponds to $\epsilon = 1$.

Having established that the transition from fragile to robust dynamics depends on the combined effect of the caregiving parameters $N$ and $\epsilon$, we perform a numerical continuation of equilibria in the $(\epsilon, N)$ parameter space in order to identify the locus of saddle-node bifurcations. The resulting bifurcation curve is shown in Figure 3.20a. We observe that, for relatively small caregiving demands, robustness can be recovered by assigning most of the caregiving load to partner 2. Conversely, for sufficiently large values of $N$, the system becomes robust independently of how caregiving responsibilities are distributed, confirming that high caregiving demands alone are sufficient to suppress fragile dynamics.

As already observed for secure couples, the preferred allocation of caregiving responsibilities may depend on the appeal parameters. For this reason, we perform an analogous bifurcation analysis by varying the appeal of partner 1.

First, we consider a drastic reduction of partner 1's appeal, setting $A_1 = 0.1$, as shown in Figure 3.20c. In this case, robustness can be recovered only if the caregiving burden is shifted to partner 1. This indicates that, when partner 1 is weakly appealing, concentrating caregiving responsibilities on this partner is necessary to stabilize the dynamics. When a more intermediate value is chosen, namely $A_1 = 0.3$, the bifurcation structure changes accordingly, as illustrated in Figure 3.20b. In this configuration, robustness is achieved for a more balanced allocation of caregiving responsibilities, suggesting that neither extreme nor strongly asymmetric divisions are optimal in this case.

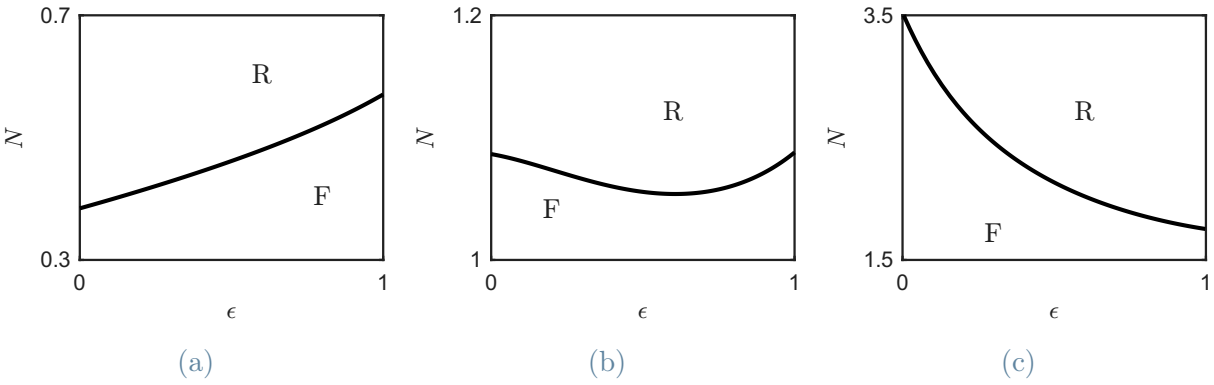


(a) (b) (c)

Figure 3.20: Comparison of saddle-node bifurcation on the $(\epsilon, N)$ parameter space for different values of $A_1$: (a) $A_1 = 0.5$; (b) $A_1 = 0.3$; (c) $A_1 = 0.1$.

Unlike the secure–secure setting, however, it is not possible to interpret these results solely in terms of the relative magnitude of the appeal terms. In secure–insecure couples, the asymmetry in attachment style plays a crucial role alongside appeal, and the interaction between these two sources of asymmetry determines which caregiving configurations are most effective in restoring robustness. As a result, the preferred division of caregiving responsibilities emerges from a combined effect of emotional appeal and attachment-related responsiveness, rather than from appeal alone.

A comparison of the three cases is reported in Figure 3.21. It is worth emphasizing that, also in this setting, higher appeal values systematically facilitate the recovery of robustness, enlarging the range of caregiving configurations for which the system exhibits a single stable equilibrium.

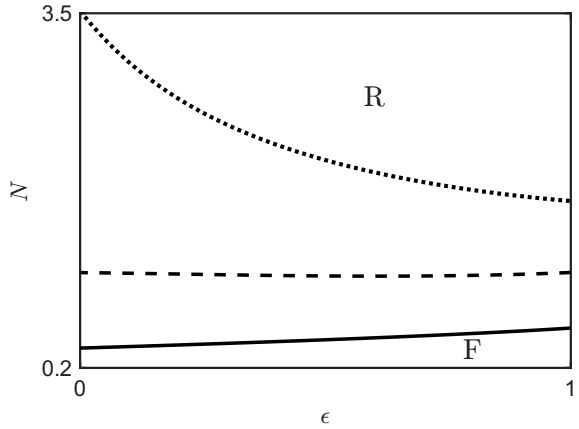


Figure 3.21: Different saddle-node bifurcation on the $(\epsilon, N)$ parameter space depending on different values of $A_1$. The solid line corresponds to $A_1 = 0.5$, the dashed line to $A_1 = 0.3$, the dotted line to $A_1 = 0.1$.

Fixing $A_1 = 0.3$, we investigate whether the appeal of partner 2, $A_2$, plays an analogous role in shaping the division of caregiving responsibilities required to recover robustness. Since the qualitative behaviour closely parallels that of secure–secure couples, it is natural to expect that the appeal of the secure partner plays a central role in determining the preferred caregiving configuration. This expectation is confirmed by the numerical results shown in Figure 3.22. Varying $A_2$ shows that changes in appeal systematically shift the caregiving division needed to restore robustness: increasing $A_2$ (solid line) facilitates robustness when a larger share of caregiving is assigned to partner 1, whereas decreasing $A_2$ (dashed line) requires partner 2 to assume most responsibilities. As for $A_1$, higher appeal levels reduce the region in which fragility persists.

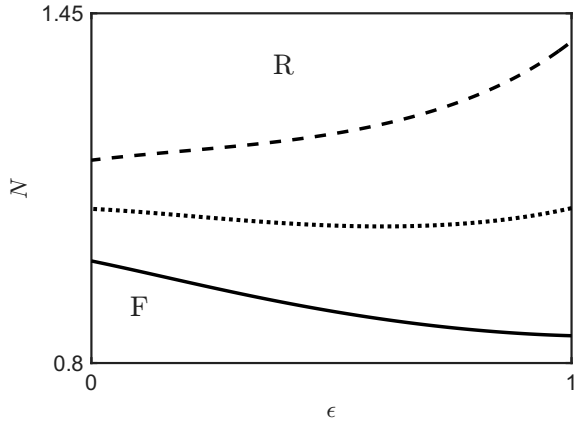


Figure 3.22: Different saddle-node bifurcation on the $(\epsilon, N)$ parameter space depending on different values of $A_2$. The solid line corresponds to $A_2 = 0.6$, the dashed line to $A_2 = 0.4$, the dotted line to $A_2 = 0.3$.

Finally, we investigate how the introduction of a child modifies the region of alternative stable states in the appeal parameter space by comparing different combinations of $N$ and $\epsilon$ with the childless case reported in Figure 3.2. We first fix the caregiving demand at $N = 0.5$ and analyze how the ASS region changes for $\epsilon = 0, 0.5, 1$, as shown in Figure 3.23a. As in the secure-secure case, when $\epsilon = 0$ the ASS region becomes vertically elongated, indicating that partner 1's appeal can vary over a smaller range before exiting the bistable region. This behaviour can be interpreted by noting that, when partner 2 bears the entire caregiving burden, attention and emotional resources are primarily directed toward the child, making partner 2 less sensitive to variations in the partner's appeal, while partner 1 remains comparatively more responsive to the appeal of partner 2. When $\epsilon = 1$, the ASS region becomes horizontally elongated, and an analogous interpretation applies, with the roles of the two partners effectively reversed. For $\epsilon = 0.5$ an intermediate configuration is obtained, in which the ASS region appears almost concentric with respect to the childless case shown in Figure 3.2, reflecting a more symmetric attenuation of sensitivity to appeal. Increasing the caregiving demand further to $N = 1$, as illustrated in Figure 3.23b, leads to the same qualitative behaviour, but with more pronounced deformations of the ASS region. In particular, the region of bistability shrinks significantly, indicating that higher caregiving demands systematically facilitate the recovery of robustness.

Overall, this analysis confirms that caregiving demands strongly influence the transition from fragile to robust dynamics: increasing $N$ consistently reduces the extent of the ASS region in the appeal space, making fragile configurations progressively less likely, independently of the specific allocation of caregiving responsibilities. We summarize all the possible combinations in Table 3.5.

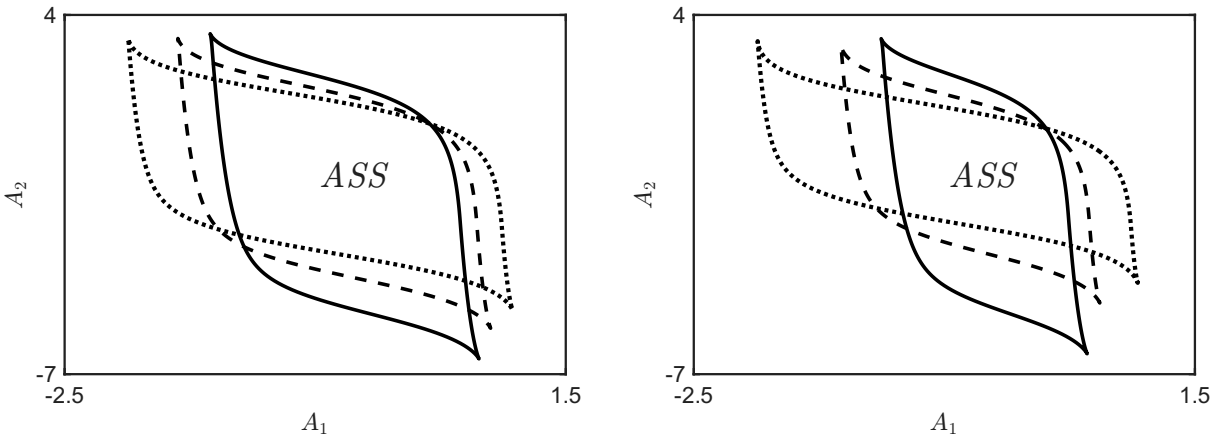


(a) (b)

Figure 3.23: Alternative stable states regions in $(A_1, A_2)$ parameter space for $N = 0.5$ (a) and $N = 1$ (b). In solid line $\epsilon = 0$, in dashed line $\epsilon = 0.5$, in dotted line $\epsilon = 1$

| | $\epsilon = 0$ | $\epsilon = 0.5$ | $\epsilon = 1$ |
|---|---|---|---|
| $N = 0$ | 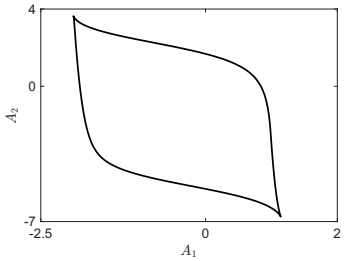 | 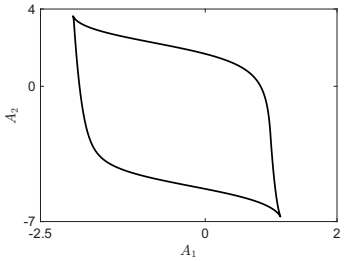 | 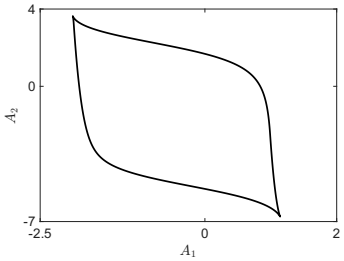 |
| $N = 0.5$ | 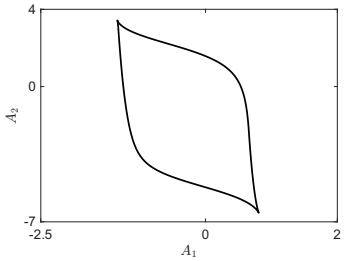 | 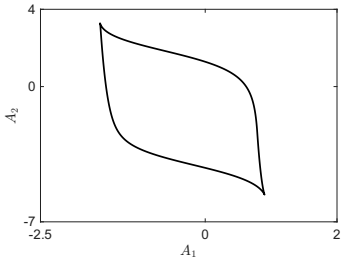 | 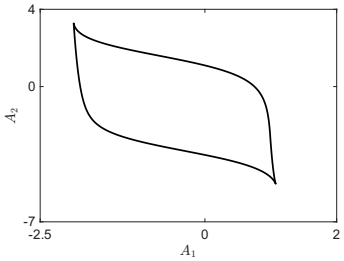 |
| $N = 1$ | 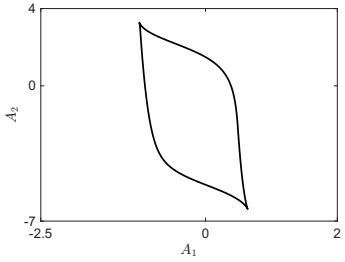 | 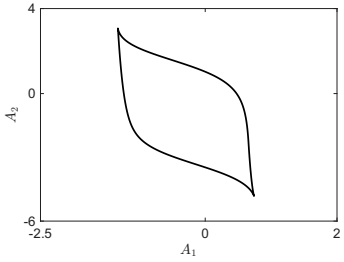 | 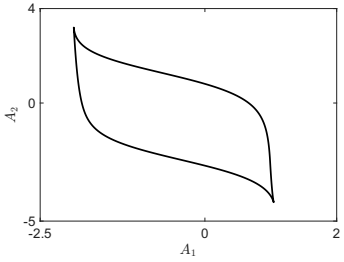 |

Table 3.5: Different alternative stable states regions on $(\epsilon, N)$ grid. Columns: $\epsilon \in \{0, 0.5, 1\}$. Rows: $N \in \{0, 0.5, 1\}$.

We now investigate how variations in the reactions to love affect the transition between fragile and robust configurations. In particular, we analyze how the bifurcation structure in the $(\epsilon, N)$ parameter space changes for different values of the parameters $\beta$ and $R_2^+$. The analysis is performed using the parameter set reported in Table 3.4, with the appeal of partner 1 fixed at $A_1 = 0.3$.

As shown in Figure 3.24, increasing $\beta$ preserves the existence of a minimum in the bifurcation curve, but progressively shifts it toward larger values of $\epsilon$, that is, toward configurations in which partner 1 bears a larger share of the caregiving load. Conversely, decreasing $\beta$ leads to a recovery of robustness when most of the caregiving responsibilities are assigned to partner 2. This behaviour indicates that modifying the emotional reactivity of partner 1 can affect the preferred distribution of caregiving required to restore robustness. In particular, increasing $\beta$ makes it advantageous for partner 1 to assume a larger caregiving burden, while lower values of $\beta$ favour configurations in which caregiving is concentrated on partner 2. This mechanism is consistent with what observed in secure–secure couples, but its interpretation must account for the non-monotonic structure of the insecure individual's reaction to love. For insecure partners, emotional responsiveness is characterized by a peak followed by a decrease when the partner's involvement becomes too intense. Increasing $\beta$ makes the system more sensitive to operating near this peak region. In this setting, assigning a larger share of caregiving responsibilities to the insecure partner has a stabilizing effect, because caregiving attenuates the reaction to love. Therefore, increasing the emotional reactivity of the insecure partner makes it advantageous to allocate more caregiving to that partner in order to recover robustness. At the same time, consistently with what observed in secure couples, we also find that lower values of $\beta$ reduce the extent of the fragile region, whereas higher values enlarge it.

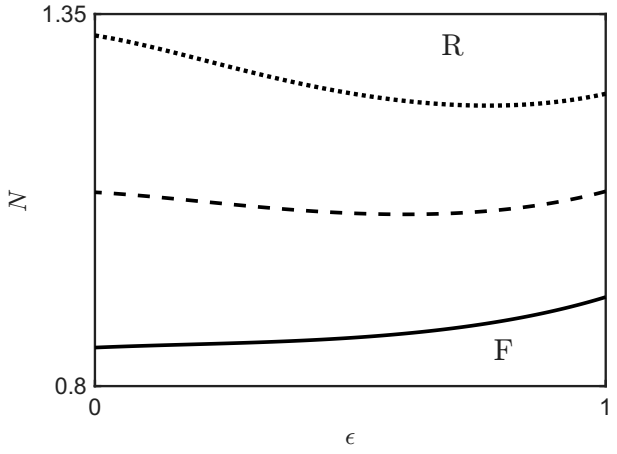


Figure 3.24: Different saddle-node bifurcation on the $(\epsilon, N)$ parameter space depending on different values of $\beta$. Solid line $\beta = 8$, dashed line $\beta = 15$, dotted line $\beta = 30$.

Using the same parameter configuration, we now vary the positive reaction to love parameter of the secure partner, $R_2^+$, in order to assess whether it plays a role analogous to that of $\beta$. The corresponding bifurcation diagrams in the $(\epsilon, N)$ parameter space are shown in Figure 3.25 for different values of $R_2^+$. The results reveal a behaviour closely analogous to that observed for $\beta$. In particular, increasing $R_2^+$ shifts the preferred caregiving allocation toward configurations in which partner 2 assumes most of the caregiving burden in order to recover robustness. Conversely, for lower values of $R_2^+$, robustness is more easily restored when caregiving responsibilities are concentrated on partner 1. This confirms that the partner who is more emotionally reactive is also the one for whom caregiving plays a stronger stabilizing role. Assigning caregiving responsibilities to the more reactive partner attenuates their response to emotional involvement and prevents the system from operating in parameter regimes that favour bistability. Moreover, this analysis reinforces a general conclusion already observed throughout the previous sections: lower levels of emotional reactivity facilitate robust dynamics, shrinking the region of alternative stable states and making transitions toward mutual hostility increasingly unlikely.

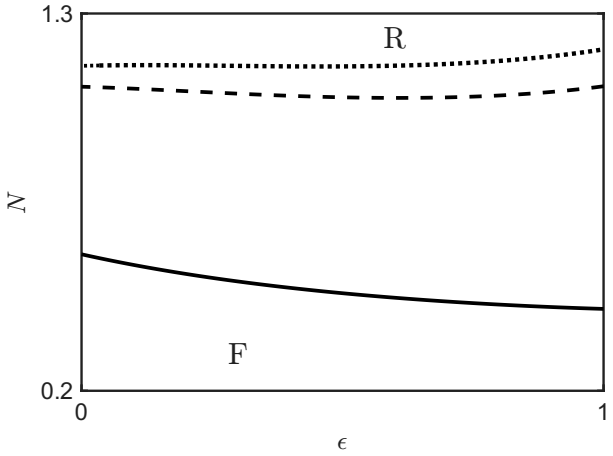


Figure 3.25: Different saddle-node bifurcation in the $(\epsilon, N)$ parameter space depending on different values of $R_2^+$. Solid line $R_2^+ = 0.3$, dashed line $R_2^+ = 2$, dotted line $R_2^+ = 3.5$.

To conclude the analysis of the role played by reactions to love in the presence of a child, we examine how caregiving demands and their distribution affect the region of alternative stable states in the $(\beta, R_2^+)$ parameter space. In particular, we compare the resulting ASS regions with the childless case reported in Figure 3.3, in order to assess how parenthood modifies the qualitative structure of the dynamics. Figure 3.26a illustrates the ASS region obtained for a fixed caregiving demand $N = 0.5$ and different values of the caregiving division parameter $\epsilon = 0, 0.5, 1$. Compared to the childless case (Figure 3.3), the presence of caregiving demands reduces the extent of the bistable region, indicating

that parenthood facilitates the recovery of robust dynamics. In particular, when $\epsilon = 0$, robustness can be recovered with a relatively small reduction of the parameter $\beta$. This effect can be interpreted by noting that partner 2 bears the entire caregiving load, which already attenuates their emotional responsiveness; consequently, only a limited decrease in the reactivity of partner 1 is required to suppress bistability. When $\epsilon = 1$, an analogous behaviour is observed with the roles of the two partners reversed, confirming that the stabilizing effect depends not only on the total caregiving demand but also on how it is distributed within the couple. For $\epsilon = 0.5$, the ASS region exhibits an intermediate structure, reflecting the symmetric sharing of caregiving responsibilities and the resulting balanced attenuation of emotional reactions. Figure 3.26b presents the same analysis for a higher caregiving demand ($N = 1$). While the qualitative features remain unchanged, there is a contraction of the ASS region as $N$ increases. This confirms that increasing caregiving demands consistently promote robustness, regardless of the specific allocation of responsibilities, by progressively eliminating the parameter combinations associated with fragile dynamics.

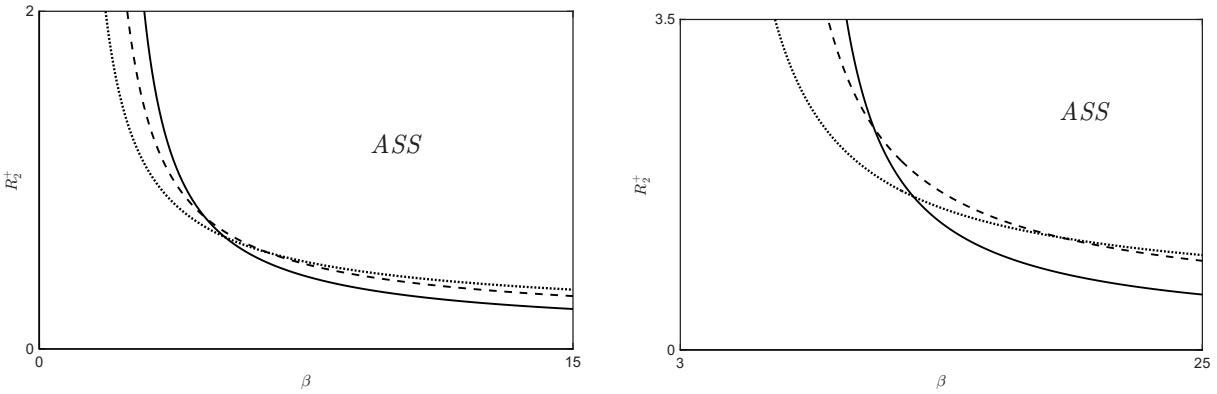


(a) (b)

Figure 3.26: Alternative stable states regions in $(\beta, R_2^+)$ parameter space for $N = 0.5$ (a) and $N = 1$ (b). Solid line $\epsilon = 0$, dashed line $\epsilon = 0.5$, dotted line $\epsilon = 1$.

Overall, these results highlight that caregiving demands reinforce structural robustness also through their impact on emotional reactivity. By attenuating reactions to love, parenthood reduces the likelihood of bistability in insecure–secure couples, although, as discussed in the previous sections, this stabilization is accompanied by a decrease in equilibrium levels of emotional involvement.

For this reason, we now investigate how the equilibrium levels of involvement of both partners, $x_1$ and $x_2$, are quantitatively affected by caregiving demands. We first analyze their dependence on an increasing caregiving demand $N$, keeping the caregiving division

fixed at $\epsilon = 0.5$. We then fix $N = 1.5$ and study how the equilibrium involvement varies as the caregiving division parameter $\epsilon$ is shifted from 0 to 1. All numerical results in this analysis are obtained using the parameter set reported in Table 3.4, with the appeal parameter fixed at $A_1 = 0.3$.

Figure 3.27 shows the effect of increasing caregiving demands on the equilibrium levels of involvement. As consistently observed throughout the analysis, increasing $N$ requires a redistribution of time, attention, and emotional resources toward the child, which inevitably leads to a reduction in the emotional involvement of both partners, as documented in literature [5, 26].

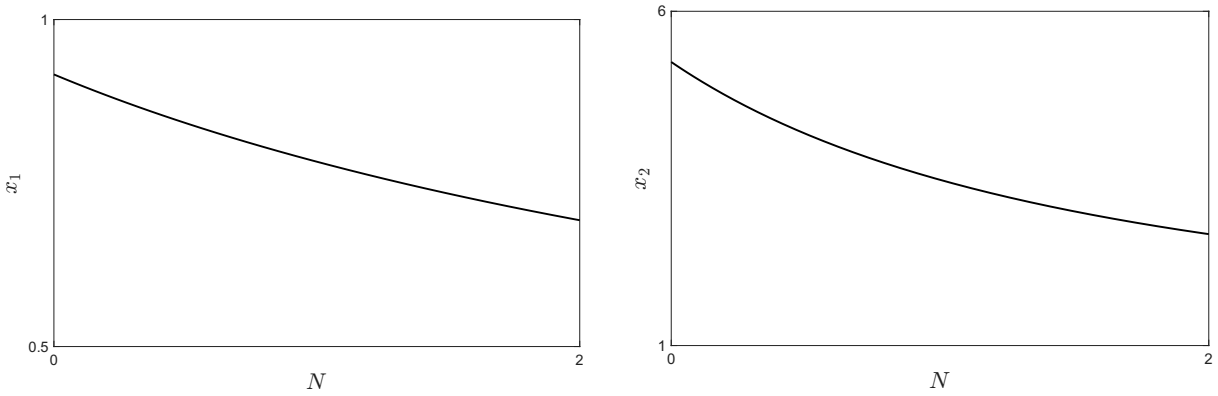


Figure 3.27: Evolution of $x_1$ and $x_2$ with respect to $N$, for $\epsilon = 0.5$.

For $N = 1.5$ and varying $\epsilon$, as shown in Figure 3.28, the equilibrium involvement of partner 1 decreases sharply as $\epsilon$ increases. This effect is amplified by the insecure attachment style: assigning a larger share of the caregiving burden to the insecure partner shifts the peak of the reaction to love function toward lower values of the partner's involvement, effectively anticipating the point at which emotional responsiveness starts to decline. As a result, when caregiving is predominantly borne by the insecure individual, partner 1 becomes emotionally overwhelmed at lower levels of involvement, leading to a pronounced reduction in equilibrium feelings, in line with empirical findings on parenting and attachment styles [17, 29, 42]. The response of partner 2 is instead non-monotonic and exhibits a clear U-shaped dependence on $\epsilon$. Emotional involvement remains relatively high when caregiving responsibilities are concentrated on either partner, while it reaches a minimum for intermediate values of $\epsilon$, corresponding to a more balanced division of caregiving. Within the framework of the model, this behaviour reflects the fact that when caregiving is shared, both partners experience a simultaneous attenuation of emotional responsiveness, which weakens the reciprocal reinforcement between their feelings. Conversely, when caregiving is asymmetric, at least one partner retains sufficient emotional

resources to sustain higher involvement, either directly or through the reaction to love coupling. Overall, this result suggests that, for insecure–secure couples under high caregiving demands, an equal subdivision of responsibilities may be particularly detrimental to emotional involvement. While such a division may appear fair from an external perspective, the model indicates that it can lead to lower equilibrium levels of involvement for both partners, compared to more asymmetric caregiving arrangements.

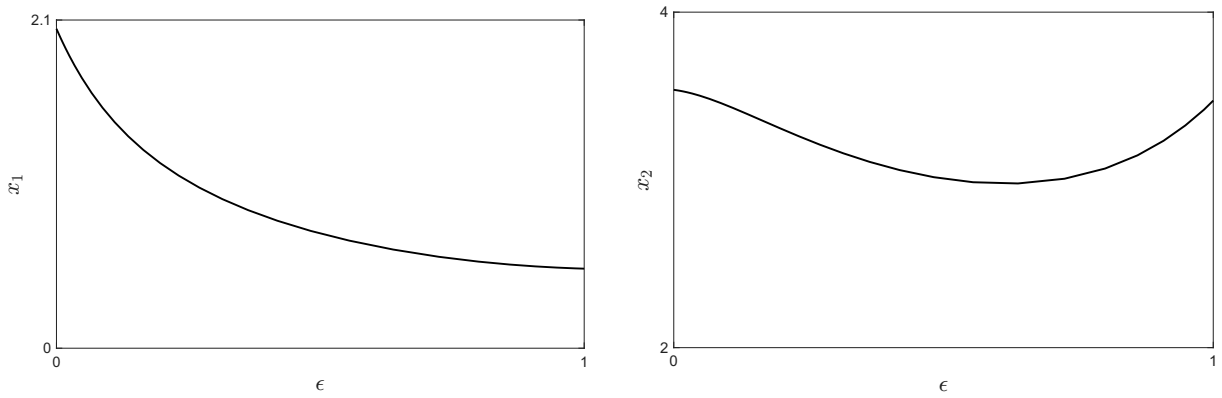


Figure 3.28: Evolution of $x_1$ and $x_2$ with respect to $\epsilon$, for $N = 1.5$.

To conclude the analysis of the trade-off induced by caregiving demands, between robustness, which is a desirable dynamical property, and the reduction of mutual emotional involvement, which is less desirable, we examine the equilibrium levels of involvement of both partners in the $(\epsilon, N)$ parameter space. As in Chapter 2, the white curve represents the locus of saddle–node bifurcations, separating regions of robust dynamics (above the curve) from fragile configurations (below it).

Figure 3.29a shows that partner 1 generally benefits from configurations in which the caregiving burden is entirely borne by the other partner. In particular, when robustness is required, i.e., for parameter values lying above the saddle–node bifurcation curve, the most favourable situation for partner 1 corresponds to $\epsilon = 0$, meaning that partner 2 takes full responsibility for childcare. This result is consistent with the insecure attachment of partner 1, for whom caregiving demands rapidly reduce emotional involvement [17, 29, 42]. Turning to Figure 3.29b, we observe that the highest levels of involvement for partner 2 are attained for low values of the caregiving demand $N$. However, such values correspond to fragile configurations and therefore do not guarantee robustness. When $N$ is increased to ensure robustness, partner 2 exhibits a non-monotonic response: emotional involvement reaches a minimum for intermediate values of $\epsilon$. This behaviour suggests that, contrary to what the bifurcation analysis alone indicates, a more asymmetric division of caregiving responsibilities may be preferable from the perspective of emotional

involvement. This conclusion is further supported by Figure 3.29c, which reports the total emotional involvement of the couple, quantified by $(x_1 + x_2)$. Here, intermediate values of $\epsilon$, typically associated with a more equal distribution of caregiving, correspond to lower levels of overall involvement. Conversely, the total emotional involvement is maximized when caregiving is fully assigned to one partner, particularly for $\epsilon = 0$.

These results highlight an important trade-off between structural robustness and emotional outcomes. While the bifurcation analysis suggests that a more balanced division of caregiving may facilitate the recovery of robustness for moderate values of $N$, such a strategy does not necessarily maximize the overall emotional involvement of the couple. As a consequence, the caregiving arrangement that ensures robustness may differ from the one that optimizes relational satisfaction, revealing a nontrivial trade-off faced by couples undergoing the transition to parenthood.

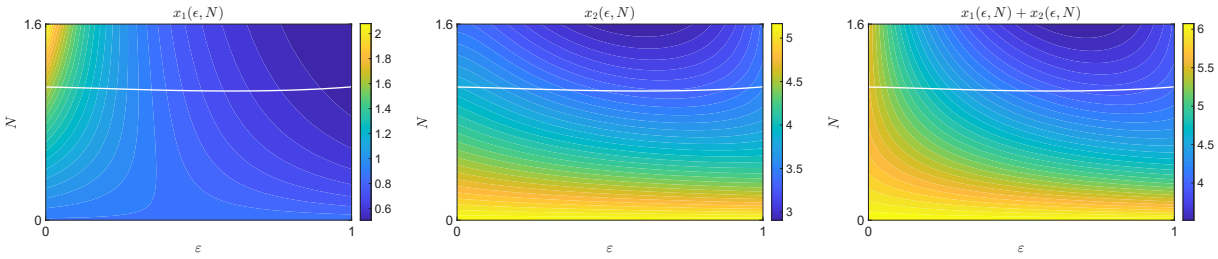


(a) (b) (c)

Figure 3.29: Evolution of individual and collective emotional involvement in the $(\epsilon, N)$ parameter space: (a) involvement $x_1$; (b) involvement $x_2$; (c) total involvement $(x_1 + x_2)$.

Having established that, at least when caregiving responsibilities are shared, increasing $N$ inevitably leads to a deterioration of mutual emotional involvement, we finally compare the equilibrium involvement in the $(\epsilon, N)$ parameter space with the corresponding childless configuration, using the relative variation defined in Equation (2.3). As in Chapter 2 and in Section 3.2, the black curve represents the locus of parameter values $(\epsilon, N)$ for which both partners experience the same percentage decrease in emotional involvement. From a purely equity-based perspective, this curve may be interpreted as representing the fairest allocation of the deterioration induced by parenthood. We begin by examining Figure 3.30a. From an equity viewpoint, the most balanced choice would correspond to the intersection between the black curve and the white saddle–node bifurcation curve, which ensures both robustness and equal deterioration. However, this configuration is clearly unfavourable for partner 1, who experiences a low level of involvement, as seen in Figure 3.29a. A similar conclusion can be drawn from Figure 3.30b. Also in this case, the intersection between the equity line and the robustness boundary corresponds to a

point at which the percentage decrease in involvement is close to its maximum for partner 2. In contrast, smaller losses are observed for more asymmetric caregiving distributions, associated with extreme values of $\epsilon$. This observation is further reinforced by Figure 3.30c. The region where both partners experience the same relative deterioration lies systematically close to the worst-case scenario in terms of total emotional loss. In other words, configurations that appear equitable at the individual level are often suboptimal when the couple is considered as a whole.

Overall, these results indicate that an equal percentage decrease in emotional involvement, while seemingly fair, does not necessarily represent an optimal strategy for the couple. In particular, when the objective is to maximize the total level of emotional involvement while preserving robustness, more asymmetric caregiving arrangements may be preferable, even if they imply an uneven distribution of the emotional costs associated with parenthood.

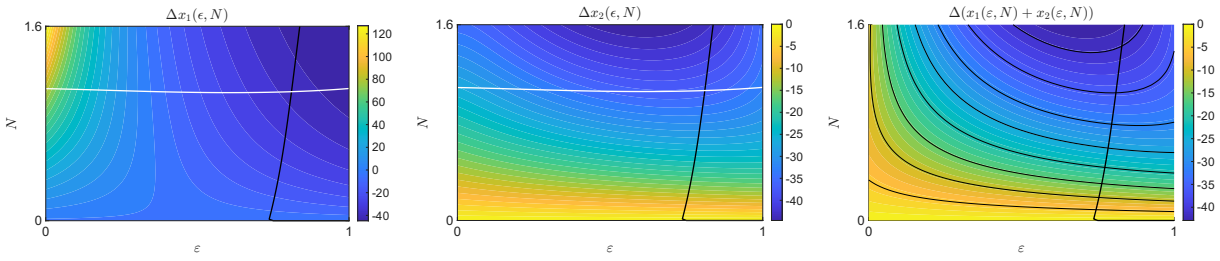


(a) (b) (c)

Figure 3.30: Comparison between the cases with and without a child in the $(\epsilon, N)$ parameter space: (a) variation in involvement $\Delta x_1$; (b) variation in involvement $\Delta x_2$; (c) variation in total involvement $\Delta(x_1 + x_2)$.

The analysis carried out in this section shows that the introduction of parenthood has a profound and multifaceted impact on the dynamics of couples composed of one secure and one insecure individual. Caregiving demands reinforce structural robustness: increasing $N$ consistently promotes the transition from fragile to robust dynamics by suppressing bistability, in line with what observed for secure–secure couples. However, this reinforcement of structural robustness is systematically accompanied by a reduction in equilibrium levels of emotional involvement, highlighting a fundamental trade-off between robustness and relational satisfaction.

The presence of different attachment styles significantly shapes how this trade-off unfolds. While appeals and reactions to love both influence the recovery of robustness, their effects are strongly modulated by the insecure partner's non-monotonic emotional response. As a result, the preferred allocation of caregiving responsibilities depends not only on the total

caregiving demand, but also on asymmetries in attachment style, emotional reactivity, and perceived appeal.

Moreover, the analysis of equilibrium involvement and relative deterioration reveals that fairness-based criteria, such as equal percentage losses for both partners, may lead to suboptimal outcomes at the couple level. Configurations that appear equitable often coincide with scenarios of maximal total emotional loss, whereas more asymmetric caregiving arrangements can preserve higher levels of overall involvement, although at the cost of uneven individual sacrifices.

Taken together, these results suggest that, while caregiving demands can protect couples from fragile dynamics, they also reshape the emotional balance of the relationship in nontrivial ways. The model thus highlights how robustness, satisfaction, and fairness cannot generally be optimized simultaneously, and how couples may be forced to navigate difficult compromises when adapting to the demands of parenthood.

Finally, it is worth emphasizing that the model does not prescribe a single optimal outcome, but rather delineates a space of possible trade-offs. Depending on which parameters can be effectively modified, such as the distribution of caregiving responsibilities or the total caregiving, couples may prioritize different objectives. Some configurations favour robustness at the expense of emotional intensity, others preserve higher levels of involvement while tolerating asymmetries or bistability.

From this perspective, the model suggests that couples are not passively subjected to the effects of parenthood, but can actively navigate among different outcomes, consistent with empirical evidence reported in the literature (see, e.g., [2]). The choice of how to allocate caregiving responsibilities, in particular, emerges as a key control mechanism through which couples may decide whether to prioritize stability, equity, or the preservation of emotional involvement, according to their preferences and constraints.

# 4 | Couples of insecure and secure synergic individuals

We have seen that, in the absence of the synergic mechanism introduced in Section 1.4, the dynamics of a romantic couple cannot exhibit sustained oscillations, regardless of the individuals' attachment styles. In such settings, the system always converges to a equilibrium, possibly depending on initial conditions. Nevertheless, it is not difficult to imagine the existence of turbulent love stories, characterized by recurrent phases of emotional closeness and distancing (an experience that many individuals may recognize). Motivated by this observation, in this chapter we investigate the emergence of periodic romantic regimes and analyze how such dynamics are affected by the transition to parenthood. A formal proof of the non-existence of periodic regimes for non-synergic couples composed exclusively of secure individuals can be found in [38].

In this chapter, we restrict our analysis to the first quadrant of the phase portrait, thereby excluding configurations characterized by negative emotional involvement between the partners, in order to focus specifically on the emergence of cyclic behavior in emotionally positive relational regimes. As a consequence, issues of robustness and fragility associated with such configurations are not addressed. In particular, we begin with the childless case, in line with the approach adopted in the previous chapter. We then examine how the introduction of a child modifies the dynamics, and compare the resulting levels of emotional involvement with those obtained in the childless case. Finally we investigate the effects of oscillatory caregiving patterns on couple dynamics.

We consider a couple in which partner 1 is insecurely attached and non-synergic, while partner 2 is securely attached and synergic. For the sake of clarity, we report here the model used in the analysis, explicitly displaying the synergic term:

$$\begin{cases} \dot{x}_1 = -\alpha_1 x_1 + \gamma_1 A_2 + \begin{cases} \beta_1 x_2 e^{-k_1(1+\epsilon N h_1)x_2} & \text{if } x_2 \geq 0 \\ \frac{e^{x_2}-e^{-x_2}}{\frac{e^{x_2}}{R_1^+}-\frac{e^{-x_2}}{R_1^-(1+\epsilon N h_1)^{-1}}} & \text{if } x_2 < 0 \end{cases} \\ \dot{x}_2 = -\alpha_2 x_2 + \frac{e^{x_1}-e^{-x_1}}{\frac{e^{x_1}}{R_2^+}-\frac{e^{-x_1}}{R_2^-}} + \gamma_2 A_1 \begin{cases} 1 & \text{if } x_2 < 0 \\ (1+\frac{s x_2^m}{\sigma^m + x_2^m}) & \text{if } x_2 \geq 0 \end{cases} \end{cases} \tag{4.1}$$

Here, the parameter $R_1^+$ is required to satisfy a continuity condition on the derivative at $x_2 = 0$, yelding:

$$R_1^+ = \frac{1}{\frac{1}{R_1^-} + \frac{2}{\beta_1}}$$

For the theoretical background on bifurcation analysis, we refer to [30, 47], while a more comprehensive treatment of cyclic dynamics in romantic relationships can be found in [38].

## 4.1. Couples without children

As in the previous chapters, we first consider the childless case ($N = 0$), in order to determine under which conditions the couple exhibits cyclic dynamics and to establish a baseline behaviour of the couple for comparison with the parenthood scenario.

The parameter values leading to periodic behavior are reported in Table 4.1, while the corresponding trajectories are illustrated in Figure 4.1.

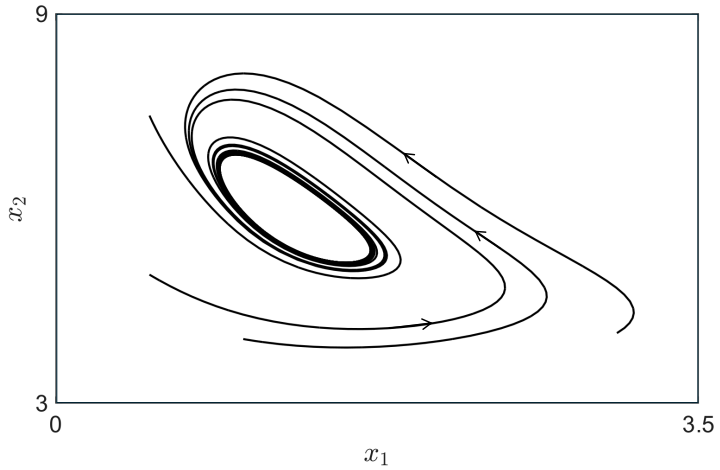


Figure 4.1: Trajectories approaching a limit cycle in the phase plane (Table 4.1).

| Parameter | Value |
|---|---|
| $\alpha_1$ | 0.1 |
| $\alpha_2$ | 0.1 |
| $\gamma_1$ | 1 |
| $\gamma_2$ | 1 |
| $A_1$ | 0.032 |
| $A_2$ | 0.045 |
| $\beta$ | 5 |
| $k$ | 1 |
| $R_1^-$ | $-1.5$ |
| $R_2^+$ | 0.5 |
| $R_2^-$ | $-0.05$ |
| $s$ | 20 |
| $\sigma$ | 6 |
| $m$ | 8 |

Table 4.1: Parameter values for model 4.1.

As previously discussed, the simultaneous presence of insecurity and synergism may give rise to cyclic dynamics, although this outcome is not guaranteed [21, 38]. For this reason, we perform a bifurcation analysis in the $(A_1, A_2)$ parameter space in order to identify the combinations of appeals that lead to the emergence of oscillations. The results of the bifurcation analysis are shown in Figure 4.2. A supercritical Hopf bifurcation curve $(H^-)$ is detected, marking the transition from a stable equilibrium to a periodic regime. Crossing this curve, the stable equilibrium loses stability and a stable limit cycle emerges around it, with a small initial amplitude that gradually increases as parameters vary [30, 47]. The Hopf curve terminates at two bifurcation points: a Generalized Hopf $(GH)$ on one side and a Bogdanov-Takens $(BT)$ on the other.

From the Generalized Hopf point, two additional bifurcation curves originate. Moving from left to right, the first corresponds to a Fold bifurcation of limit cycles $(LPC)$, generating two cycles around the equilibrium, an outer stable one and an inner unstable one. The second corresponds to a subcritical Hopf bifurcation $(H^+)$. In contrast to the previously described supercritical Hopf, the unstable cycle collapses onto the equilibrium, which becomes unstable, leading to a configuration characterized by an unstable equilibrium surrounded by a stable cycle. Since these two curves are nearly overlapping, small variations in the appeal parameters may result in an abrupt transition to cyclic dynamics.

From the Bogdanov–Takens point, three bifurcation curves originate: two saddle–node curves and one homoclinic curve. Moving from left to right, the first saddle–node bifurcation ($NS^-$) generates a saddle point and a stable equilibrium. In this parameter region, the system is characterized by the coexistence of a stable limit cycle surrounding an unstable equilibrium, together with the newly created equilibria. This saddle–node curve nearly coincides with the homoclinic curve (*hom*); crossing it, a stable cycle collides with a stable equilibrium and disappears. As a result, the system moves to a configuration with three equilibria: a stable node, an unstable node, and a saddle. Finally, the second saddle–node bifurcation curve ($NS^+$) corresponds to the collision of a saddle and an unstable equilibrium (a repellor).

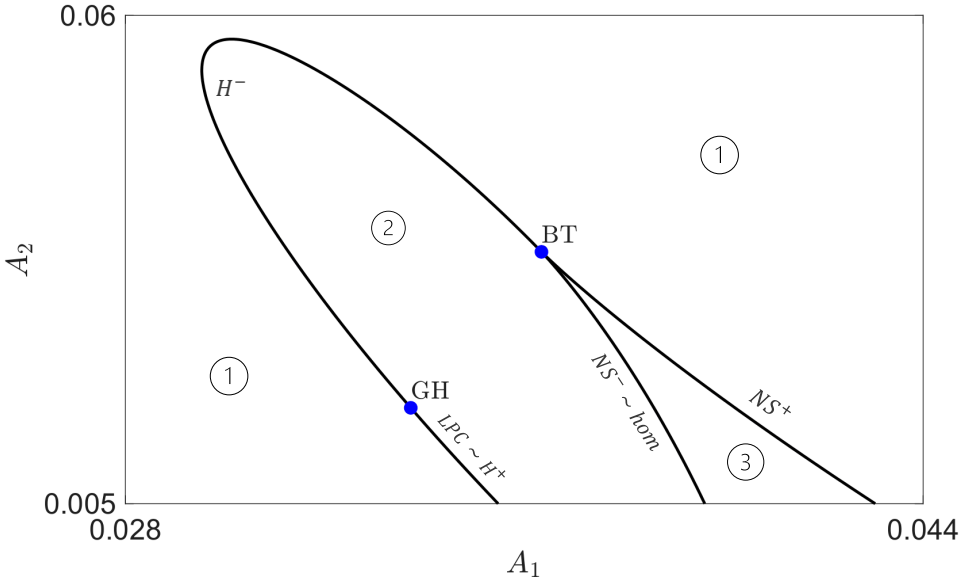


Figure 4.2: Bifurcation diagram on the $(A_1, A_2)$ parameter space.

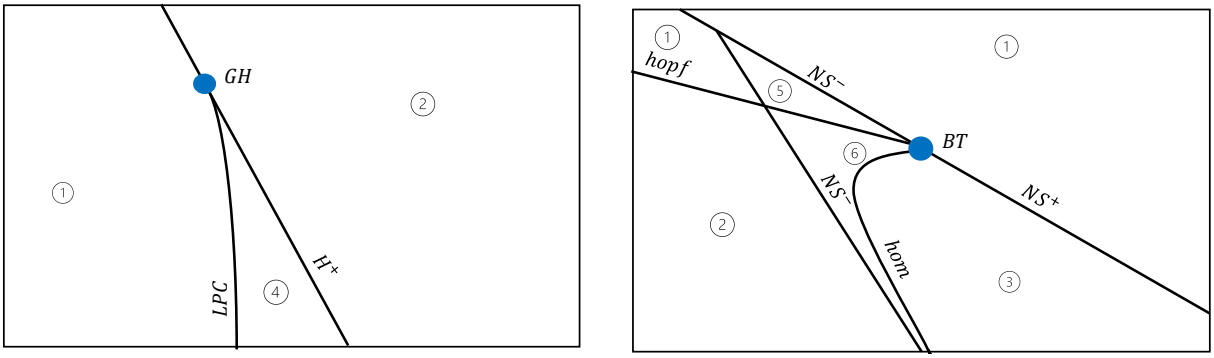


Figure 4.3: Zoomed-in regions near the bifurcation points.

It is worth emphasizing that the two zoomed panels, namely, the enlargement around the

Bogdanov–Takens point and that around the Generalized Hopf point, are intended as qualitative sketches. Their purpose is purely illustrative, aiming to facilitate the reader's understanding of the underlying bifurcation structure and the associated dynamical regimes.

In addition, Figure 4.4 illustrates the qualitative behavior associated with each numbered region of the bifurcation diagram. Solid dots denote stable equilibria, empty dots denote unstable equilibria (repellors), diamonds represent saddle points, solid circles indicate stable limit cycles, and dashed circles correspond to unstable limit cycles.

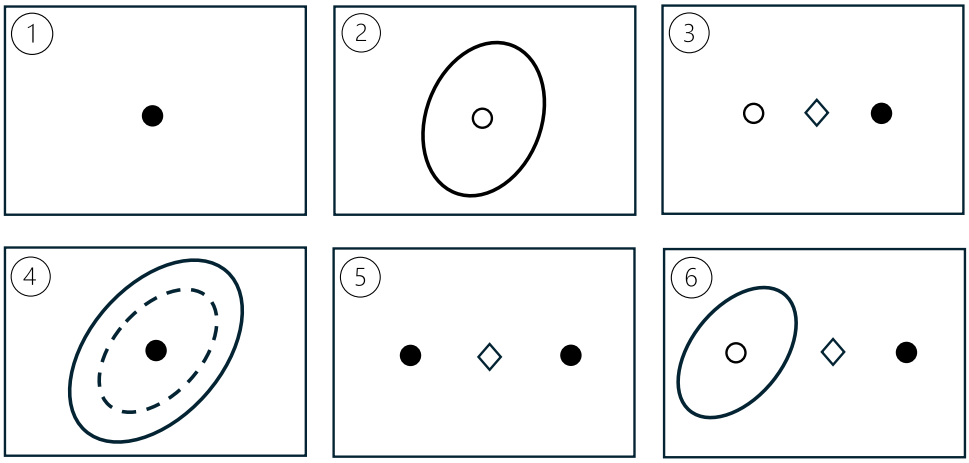


Figure 4.4: Qualitative behaviour of the regions indicated in Figure 4.2 and Figure 4.3.

## 4.2. The effect of the transition to parenthood

We now introduce a child and the associated caregiving demands into a couple that, in the childless case, exhibits cyclic dynamics. The aim is to investigate whether and how the introduction of parenthood affects the persistence of oscillations or, possibly, promoting a transition toward a stationary regime. We then compare the resulting time-averaged levels of emotional involvement (computed over the cycle) and the equilibrium levels in the $(\epsilon, N)$ parameter space with those of the corresponding levels of the childless case.

Specifically, we refer to the parameter set reported in Table 4.1, corresponding to a configuration in which $A_2 > A_1$, and perform a bifurcation analysis in the $(\epsilon, N)$ parameter space. The resulting bifurcation curve is shown in Figure 4.5. Below the curve, the system exhibits cyclic dynamics $(C)$, while above it the dynamics converge to a stationary equilibrium $(E)$. The curve corresponds to a supercritical Hopf bifurcation, implying that oscillations disappear smoothly as either $N$ or $\epsilon$ increase. In particular, the diagram suggests that a faster transition to stationarity occurs when partner 1 assumes a larger share of caregiving responsibilities. This finding is consistent with previous results obtained for

non-synergic individuals, where allocating a greater caregiving load to the less appealing, and therefore more reactive, partner tends to "stabilize" the dynamics. Interestingly, this mechanism persists even when partner 1 is insecurely attached.

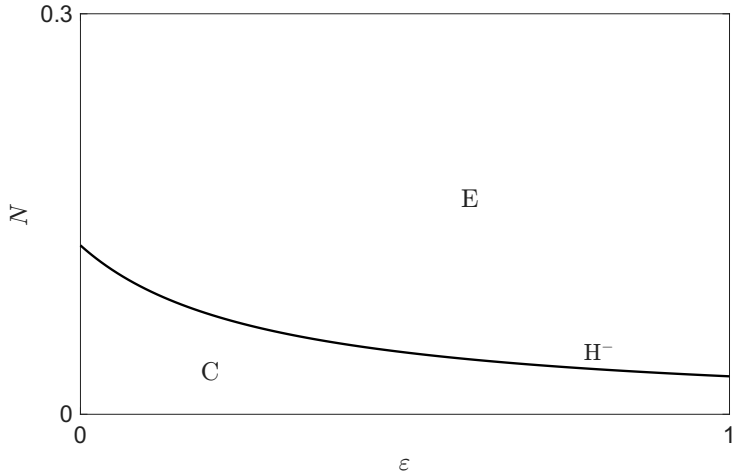


Figure 4.5: Bifurcation diagram on the $(\epsilon, N)$ parameter space. The cyclic regime $(C)$ lies below the curve, while the stationary regime $(E)$ lies above it. The parameters used are reported in Table 4.1.

From a dynamical perspective, this result suggests that caregiving responsibilities act as a damping mechanism on emotional oscillations. When the more reactive partner increases his involvement in caregiving, part of the emotions sustaining the cycle is effectively absorbed by the external demand represented by the child. As a consequence, the amplitude of emotional fluctuations progressively decreases, eventually restoring a stationary configuration. Although it may appear counterintuitive that an insecure individual contributes to "stabilization" when assuming greater responsibility, this effect can be interpreted as a redistribution of emotional energy toward the caregiving task. In this sense, parenthood may function as a structural constraint that reduces the intensity of reciprocal emotional amplification.

We now investigate the case in which $A_1 > A_2$, specifically $A_1 = 0.036$ and $A_2 = 0.01$. The corresponding bifurcation diagram is shown in Figure 4.6. In this configuration, the system undergoes a subcritical Hopf bifurcation, immediately followed by a fold of limit cycles. In contrast to the previous case, the transition from cyclic to stationary dynamics is abrupt: the stable limit cycle disappears suddenly rather than vanishing smoothly as in Figure 4.5. This outcome appears, at first glance, to contrast with the results obtained for non-synergic individuals. Here, partner 2 is effectively more reactive, since $A_1$ is larger and further amplified by the synergism. Nevertheless, the bifurcation diagram indicates

that assigning a larger share of caregiving responsibilities to partner 1 still facilitates an earlier transition to a stationary regime.

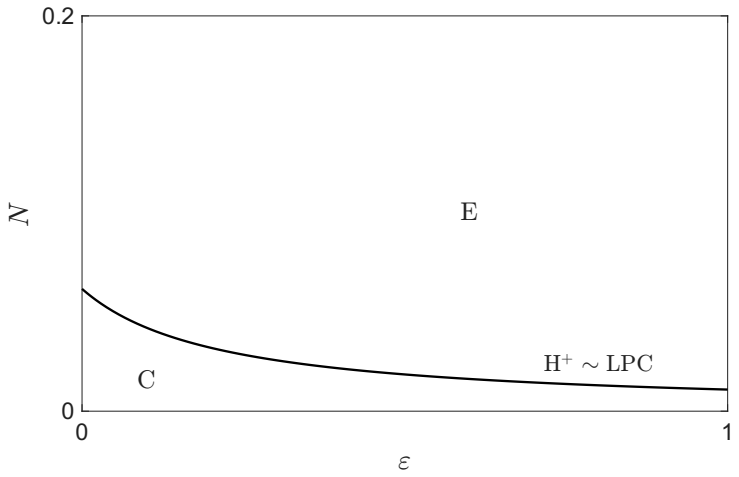


Figure 4.6: Bifurcation diagram on the $(\epsilon, N)$ parameter space. The cyclic regime $(C)$ lies below the curve, while the stationary regime $(E)$ lies above it. $A_1 = 0.036$, $A_2 = 0.01$; all the other parameters are as in Table 4.1.

Although partner 2 is synergic and the appeal of partner 1 is stronger and further amplified, the persistence of oscillations depends on the overall strength of the feedback loop between the partners. Caregiving does not alter the appeal mechanism itself, but reduces emotional responsiveness, so, when a larger share of caregiving responsibilities is assigned to partner 1, their effective reactivity decreases. As a consequence, the overall feedback intensity of the system is reduced and once the net reactivity falls below a critical threshold, the oscillatory regime can no longer be sustained and the dynamics collapse to an equilibrium. In this sense, the restoration of stationary behaviour is not achieved by weakening the synergic amplification directly, but by increasing dissipation within the feedback structure.

It is worth noting that a smooth transition from cyclic to stationary dynamics may also occur when $A_1 > A_2$. For instance, when $A_1 = 0.033$ and $A_2 = 0.025$, the bifurcation diagram displayed in Figure 4.7 shows that again the $(\epsilon, N)$ parameter space is crossed by a Hopf bifurcation, which in this case is supercritical. In contrast to the previously discussed configuration, the disappearance of oscillations now occurs gradually: as caregiving intensity increases, the amplitude of the limit cycle decreases continuously until the system converges to a stationary equilibrium. Consistently with the previous results, the diagram indicates that assigning a larger share of caregiving responsibilities to partner 1 promotes an earlier "stabilization" of the dynamics.

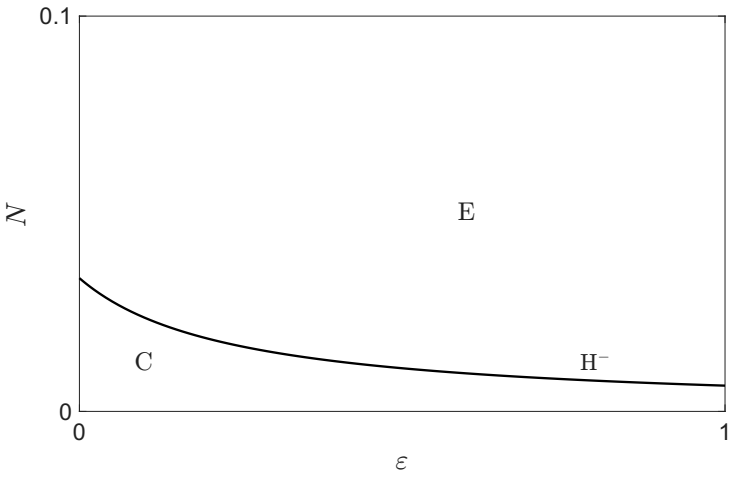


Figure 4.7: Bifurcation diagram on the $(\epsilon, N)$ parameter space. The cyclic regime $(C)$ lies below the curve, while the stationary regime $(E)$ lies above it. $A_1 = 0.033$, $A_2 = 0.025$; all the other parameters are as in Table 4.1.

As a final configuration, we consider a case in which the system starts from a stationary regime, enters a cyclic region in the $(\epsilon, N)$ parameter space, and eventually returns to a stationary behaviour. In this setting, we fix $A_1 = 0.0333$ and $A_2 = 0.05$, and the corresponding bifurcation diagram is shown in Figure 4.8. The lower Hopf bifurcation curve is supercritical, leading to a smooth transition from stationarity to cyclic dynamics as parameters vary. In contrast, the upper Hopf curve is subcritical and is immediately followed by a fold of limit cycles, producing an abrupt transition back to a stationary regime. Consistently with the previous bifurcation analyses in this section, the diagram indicates that when partner 2 assumes a larger share of caregiving responsibilities, the parameter region supporting cyclic dynamics becomes wider. Conversely, assigning a greater caregiving load to partner 1 reduces the extent of the oscillatory region, thereby facilitating the maintenance of stationarity. These results show that parenthood does not exert a uniformly stabilizing effect. While caregiving demands may suppress pre-existing oscillations, they can also induce cyclic behavior when the system initially lies near a bifurcation boundary. Parenthood therefore acts as a structural modifier of the dynamical landscape, potentially reshaping the qualitative regime of the couple. From a dynamical perspective, this configuration highlights the non-monotonic role of caregiving in the system. When the parameters lie near a bifurcation boundary, small variations in caregiving intensity or its distribution may push the system across stationarity limits. In this sense, parenthood does not simply add dissipation, but modifies the effective balance between responsiveness and damping.

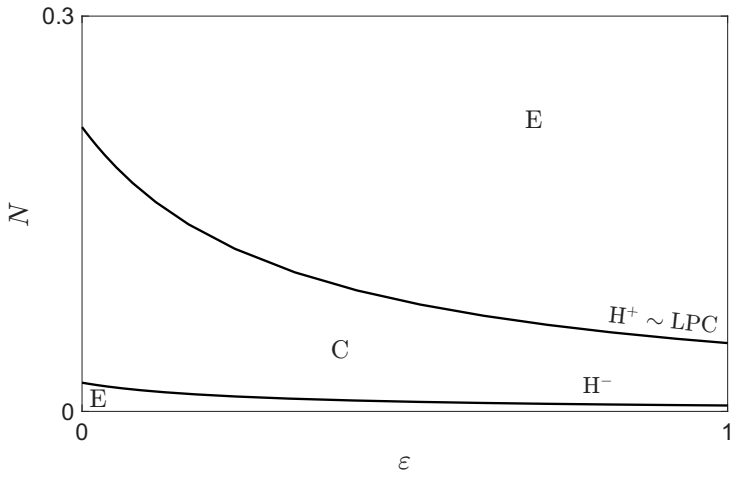


Figure 4.8: Bifurcation diagram on the $(\epsilon, N)$ parameter space. The cyclic regime $(C)$ lies between the curves, while the stationary regime $(E)$ lies outside them. $A_1 = 0.0333$, $A_2 = 0.05$; all the other parameters are as in Table 4.1.

We first analyze the levels of emotional involvement of both partners, $x_1$ and $x_2$ respectively, as functions of caregiving demand $N$ and of the allocation parameter $\epsilon$. We then analyze the levels of emotional involvement of both partners, $x_1$ and $x_2$, as well as the total level of affection within the couple, $(x_1 + x_2)$, in the $(\epsilon, N)$ parameter space. We then compare these levels with the corresponding values in the childless case in order to evaluate the net impact of caregiving on the couple's emotional balance. In regions characterized by cyclic dynamics, we compute time-averaged values of the state variables along the limit cycle, using an integral average. To account for the potential stress associated with persistent oscillations, we define an effective involvement by subtracting a weighted standard deviation from the mean value:

$$I_i = \langle x_i \rangle - \delta_i \sigma_i \tag{4.2}$$

where $\langle x_i \rangle$ denotes the temporal average of $x_i$ over the cycle, $\sigma_i$ is the corresponding standard deviation and $\delta_i \geq 0$ represents the sensitivity of partner $i$ to oscillatory variability. For simplicity, we assume the same value of $\delta$ for both partners, although the model could accommodate heterogeneous sensitivities.

The white curve in the figures represents the Hopf bifurcation, specified in each case as supercritical or subcritical. The black curve, when present, identifies the locus of points where both partners experience the same percentage decrease in emotional involvement. In this configuration, however, such a curve does not appear, as there are no parameter values for which the two partners undergo the same relative variation in involvement. This

indicates that the introduction of caregiving produces structurally differentiated effects on the partners.

We start from the couple characterized by the parameter values reported in Table 4.1, setting $\delta = 0$. Figure 4.9 shows the evolution of $I_1$ and $I_2$ as functions of $N$. As can be observed, the curves are not perfectly continuous due to the numerical approximation in the cyclic region. Nevertheless, an almost monotonic behaviour can be identified: $I_1$ increases with $N$, while $I_2$ decreases. At first glance, this result may appear counterintuitive, given that partner 1 is insecurely attached and might be expected to experience lower involvement under additional relational demands. However, from a dynamical perspective, the increase in his involvement can be interpreted as a consequence of the shift toward a stationary configuration. When caregiving responsibilities are concentrated on partner 2, the overall feedback intensity of the system is reduced, and oscillations are damped. The transition from a cyclic to a stationary regime allows partner 1 to maintain a more stable and sustained level of emotional involvement, rather than experiencing alternating phases of high and low engagement. In this sense, the apparent increase reflects not an amplification of reactivity, but rather a structural reorganization of the interaction toward a more sustained emotional state.

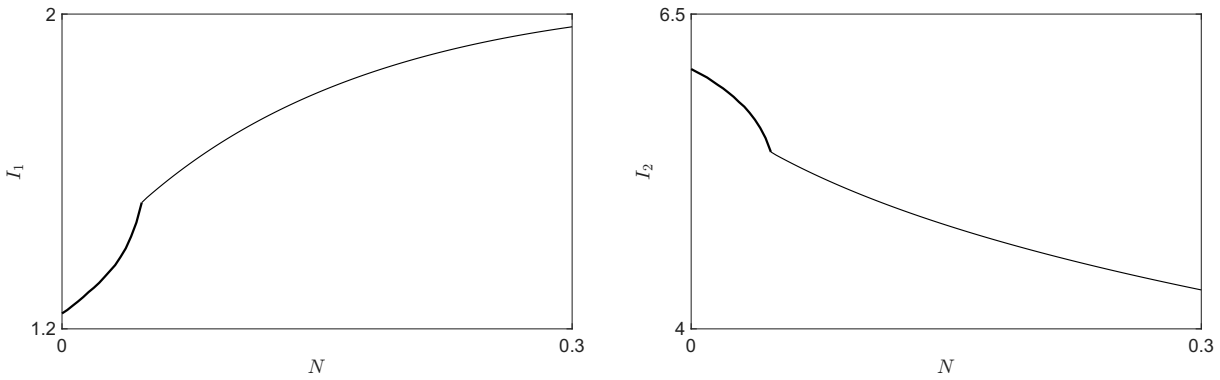


Figure 4.9: Evolution of $I_1$ and $I_2$ with respect to $N$, for $\epsilon = 0.5$. The thick line characterizes a limit cycle.

Figure 4.10 shows the evolution of the emotional involvement of both partners as function of $\epsilon$. Again, a seemingly counterintuitive behaviour emerges: both partners exhibit higher involvement when they assume a larger share of the caregiving responsibilities, contrary to what might be expected. One possible interpretation is that actively engaging in caregiving may increase perceived agency and relational commitment, which, in turn, reinforces emotional involvement.

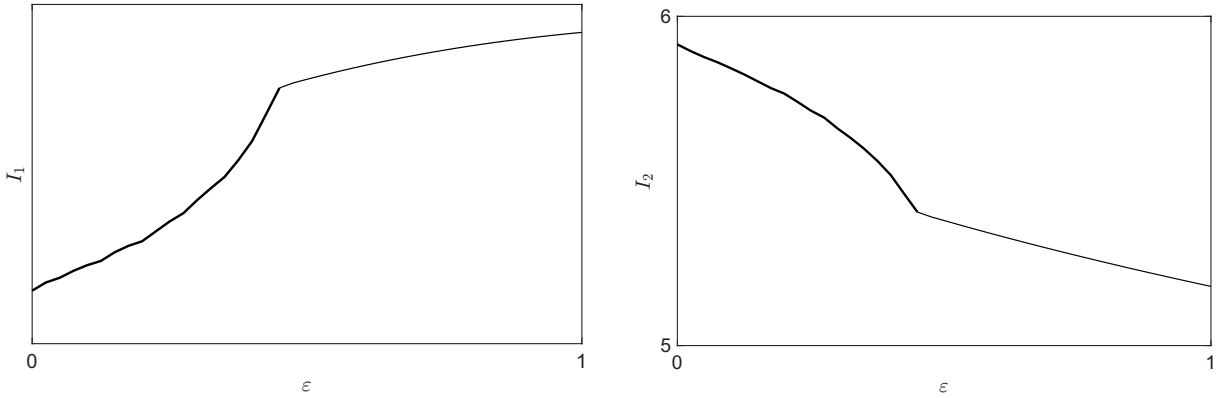


Figure 4.10: Evolution of $I_1$ and $I_2$ with respect to $\epsilon$, for $N = 0.05$. The thick line characterizes a limit cycle.

Now, keeping $\delta = 0$, we investigate all the combinations $(\epsilon, N)$. Figure 4.11 displays the equilibrium levels (or the mean values along the cycle, computed according to Equation (4.2)) of the state variables in the $(\epsilon, N)$ parameter space.

Considering partner 1 (Figure 4.11a), and consistently with Figure 4.9, we observe that the introduction of a child may increase his level of emotional involvement, particularly when caregiving responsibilities are predominantly assigned to partner 2, except for very low values of $N$ (see Figure 4.10). Moreover, for sufficiently high caregiving demands, when partner 2 bears most of the responsibilities, partner 1 reaches higher involvement levels. This behaviour is consistent with findings on insecurely attached individuals, who may experience heightened stress when exposed to excessive responsibilities and therefore benefit from a redistribution of caregiving load.

A different mechanism operates for partner 2. As shown in Figure 4.11b, the cyclic regime corresponds to higher levels of emotional involvement for him. In this case, oscillations include phases of particularly elevated engagement that raise the mean level above the stationary equilibrium. When caregiving responsibilities increase and the system converges to a fixed point, these high-intensity phases vanish, leading to a lower average involvement. Thus, while stabilization benefits partner 1 by removing detrimental low states, it reduces partner 2's average involvement by eliminating peak emotional amplification. Moreover, for fixed values of $N$, partner 2 benefits from assuming a larger share of caregiving responsibilities rather than delegating them to partner 1. At the same time, his involvement decreases smoothly as $N$ increases, reflecting the progressive impact of caregiving demands. Finally, examinationg the total involvement (Figure 4.11c), we observe that the cyclic regime does not correspond to the worst collective outcome in this case, as it still guarantees relatively high levels of overall affection. However, the highest

total involvement is attained for sufficiently large values of $N$ in the stationary regime, particularly when partner 2 assumes the full caregiving load. In contrast, configurations with $\epsilon$ between 0.5 and 1 appear to be less favorable for the couple as a whole.

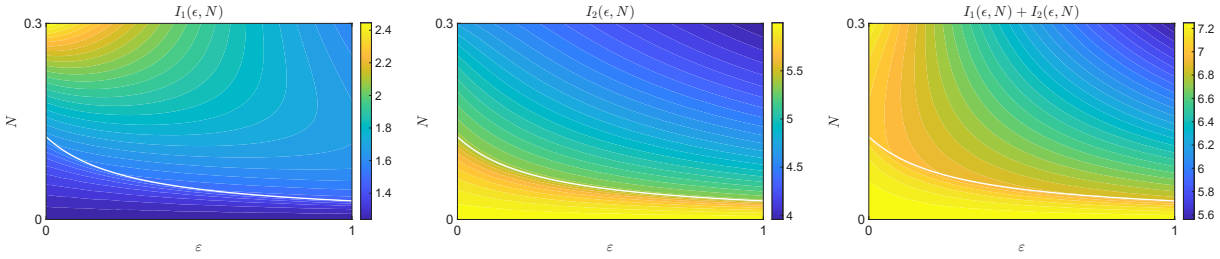


(a) (b) (c)

Figure 4.11: Evolution of individual and collective emotional involvement in the $(\epsilon, N)$ parameter space: (a) involvement $I_1$; (b) involvement $I_2$; (c) total involvement $(I_1 + I_2)$.

Now we compare the levels of emotional involvement in the $(\epsilon, N)$ parameter space with the corresponding values in the childless case, in order to evaluate the percentage variations induced by caregiving. Consistently with the previous figures, Figure 4.12 shows that partner 1 systematically experiences an increase in involvement relative to the childless configuration, whereas partner 2 undergoes a decrease across the parameter space. This confirms that the "stabilizing" effect of caregiving, which suppresses oscillations, benefits the insecure partner while reducing the average engagement of the synergic one. Regarding the total involvement (Figure 4.12c), a positive variation is observed only in the upper-left region of the parameter space, corresponding to sufficiently high values of $N$ and caregiving predominantly assigned to partner 2. In all other configurations, the total affection either remains approximately unchanged or decreases relative to the childless regime. Parenthood therefore redistributes emotional involvement asymmetrically across the partners. While the bifurcation analysis suggests that assigning a larger share of caregiving responsibilities to partner 1 promotes stabilization of the dynamics, this allocation is not necessarily optimal in terms of individual involvement for partner 2. Indeed, partner 2 benefits from the cyclic regime, which provides higher average levels of emotional engagement. This highlights a structural tension between dynamical stability and individual satisfaction: the caregiving distribution that minimizes oscillations does not coincide with the configuration that maximizes involvement for both partners.

We now repeat the analysis, initially setting $\delta = 0$, for the couple characterized by the parameter values reported in Table 4.1, fixing $A_1 = 0.036$ and $A_2 = 0.01$, corresponding to the configuration in which a subcritical Hopf bifurcation occurs, followed closely by a fold of limit cycles. For the sake of brevity, we omit the case $A_1 = 0.033$ and $A_2 = 0.025$,

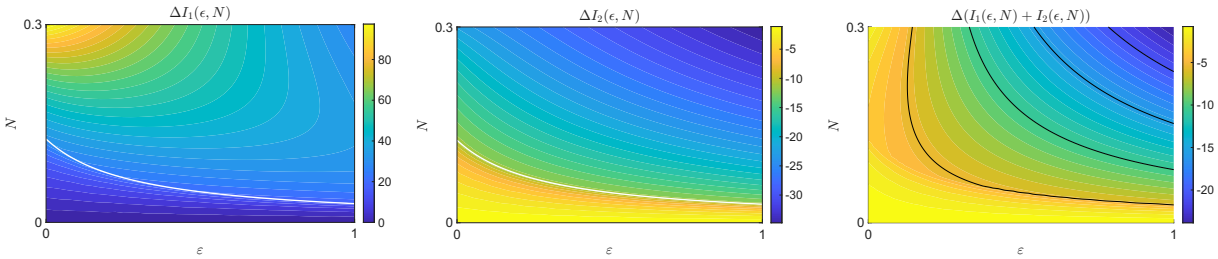


Figure 4.12: Comparison between the cases with and without a child in the $(\epsilon, N)$ parameter space: (a) variation in involvement $\Delta I_1$; (b) variation in involvement $\Delta I_2$; (c) variation in total involvement $\Delta(I_1 + I_2)$.

since it displays a supercritical Hopf bifurcation and analogous smooth behavior as the previous configuration. We begin by showing, in Figure 4.13, the evolution of $I_1$ and $I_2$, that is, the mean values of the state variables in this case (since $\delta = 0$), as functions of $N$ with $\epsilon = 0.5$. Here, the effect of the bifurcations is clearly visible. When the bifurcation curves are crossed, the stable limit cycle disappears abruptly, leaving only the equilibrium. As a consequence, partner 1 experiences a sudden increase in involvement, while partner 2 undergoes a sharp decrease.

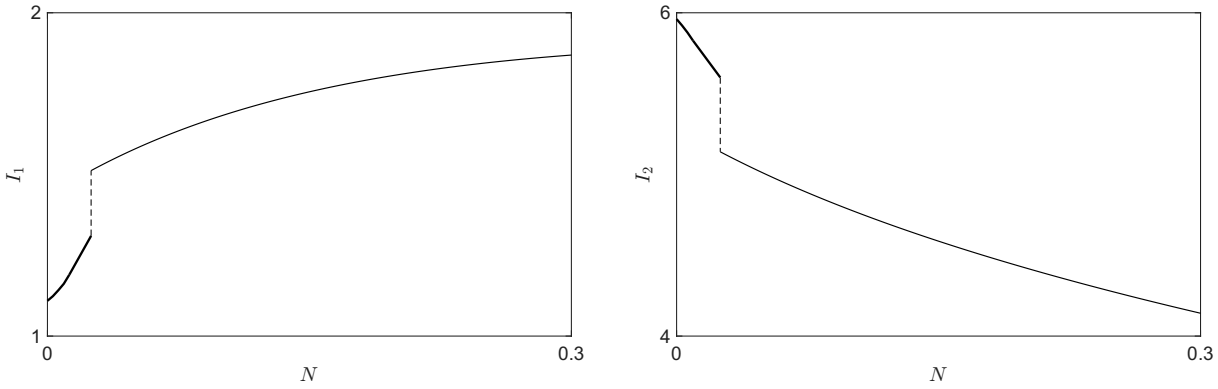


Figure 4.13: Evolution of $I_1$ and $I_2$ with respect to $N$, for $\epsilon = 0.5$. The thick line characterizes a limit cycle.

Similarly, Figure 4.14 shows the evolution of $I_1$ and $I_2$ as functions of $\epsilon$, with $N = 0.025$. Here again, an abrupt transition can be observed changing the allocation of caregiving responsibilities. Overall, the qualitative behaviour is consistent with that of the previous configuration: the insecure partner benefits, in terms of involvement, from exiting the cyclic region, whereas the secure partner does not. Moreover, for both partners, higher involvement levels are attained when they assume a larger share of caregiving respon-

sibilities, at least in terms of the effective involvement measure considered here. The main difference lies in the abrupt nature of the transition, which is a consequence of the subcritical Hopf bifurcation, closely followed by a fold of limit cycles.

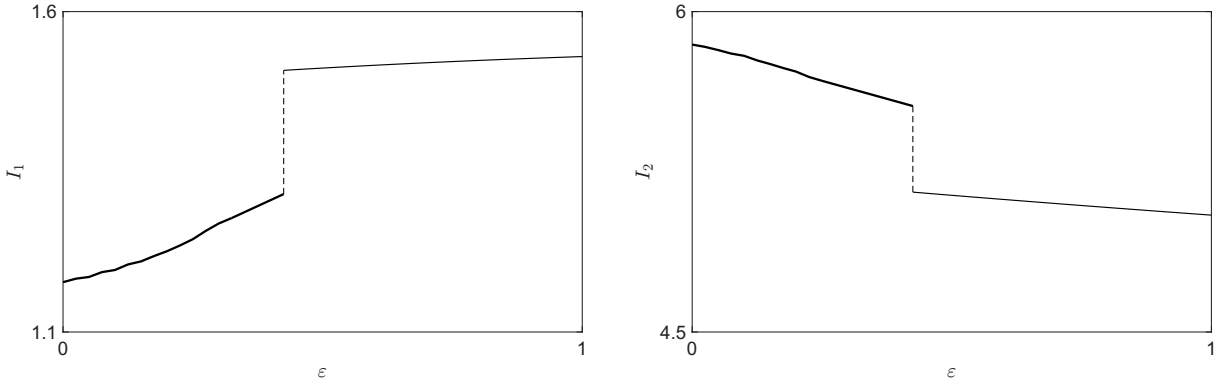


Figure 4.14: Evolution of $I_1$ and $I_2$ with respect to $\epsilon$, for $N = 0.025$. The thick line characterizes a limit cycle.

Figure 4.15 shows a behavior broadly consistent with the previous graphs: due to the bifurcations, the transition between cyclic and stationary regimes produces an abrupt change in the levels of emotional involvement. This discontinuity is particularly evident in Figure 4.15b and Figure 4.15c. For partner 2 and for the couple as a whole, the cyclic regime corresponds to higher levels of involvement, which decrease sharply once the system crosses the bifurcation boundary and converges to a stationary equilibrium. In contrast, for partner 1 the cyclic configuration represents the least favorable scenario. As in the previous case, the highest total involvement for the couple is attained in the upper-left region of the $(\epsilon, N)$ parameter space, where caregiving is predominantly assigned to partner 2. This configuration highlights how the nature of the bifurcation directly affects not only "stability" properties, but also the distribution of emotional benefits within the couple. In the presence of a subcritical Hopf bifurcation closely followed by a fold of limit cycles, small variations in caregiving intensity may lead to abrupt changes in average involvement levels, producing a sudden redistribution of emotional advantages between the partners. In contrast to the supercritical case discussed previously, where involvement levels adjust gradually as parameters vary, this structure introduces a threshold effect: once the bifurcation boundary is crossed, the disappearance of the cycle entails an immediate reduction of the high-involvement phases that benefit partner 2 and the couple as a whole.

This suggests that in such configurations, the emotional consequences of caregiving redistribution may be significantly more sensitive to parameter variations, reinforcing the idea that parenthood can reshape relational outcomes in a discontinuous manner.

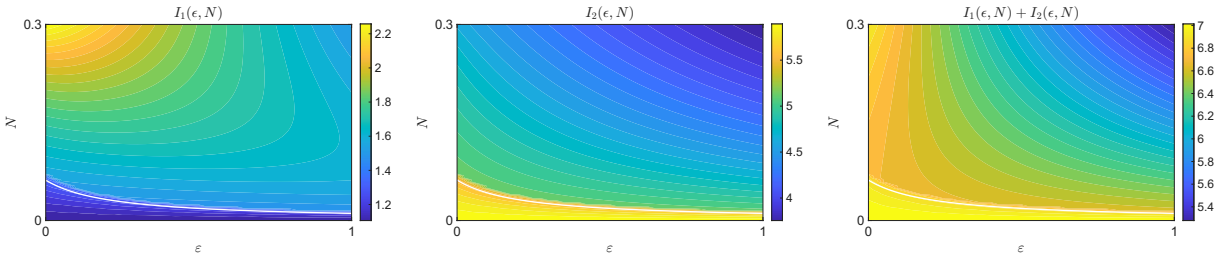


(a) (b) (c)

Figure 4.15: Evolution of individual and collective emotional involvement in the $(\epsilon, N)$ parameter space: (a) involvement $I_1$; (b) involvement $I_2$; (c) total involvement $(I_1 + I_2)$.

In Figure 4.16 we compare the involvement levels with those of the childless configuration. As in the previous case, we observe that partner 1 consistently experiences an increase in involvement, whereas partner 2 undergoes a decrease. The qualitative pattern therefore remains unchanged with respect to the redistribution of emotional gains and losses. However, in the present configuration, the bifurcations introduce a sharper contrast between regimes. The transition from cyclic to stationary dynamics produces a discontinuous variation in the percentage change of involvement, reinforcing the asymmetry between the partners.

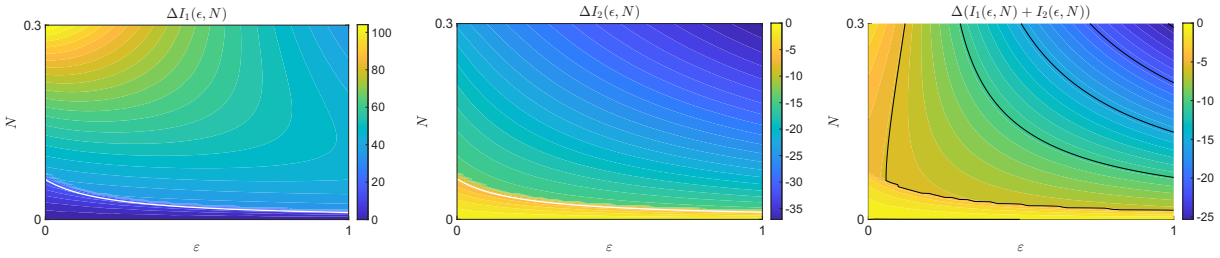


(a) (b) (c)

Figure 4.16: Comparison between the cases with and without a child in the $(\epsilon, N)$ parameter space: (a) variation in involvement $\Delta I_1$; (b) variation in involvement $\Delta I_2$; (c) variation in total involvement $\Delta(I_1 + I_2)$.

We now consider the same configuration with $\delta = 1$, that is, assuming that both partners are sensitive to variability induced by cyclic dynamics, in order to assess how this affects the effective involvement. Figure 4.17 displays the involvement of both partners as functions of $N$, with $\epsilon = 0.5$. As before, an abrupt change is observed at the bifurcation point. However, the qualitative interpretation differs for partner 2: rather than experiencing a deterioration, he exhibits a local increase in effective involvement precisely at the bifurcation, followed by a gradual decrease as $N$ increases further. When variability is explicitly

penalized in the involvement measure, the cyclic region no longer appears advantageous for either partner. In particular, partner 2 attains the highest effective involvement immediately after the bifurcation, whereas partner 1 exhibits a pattern similar to the previous case.

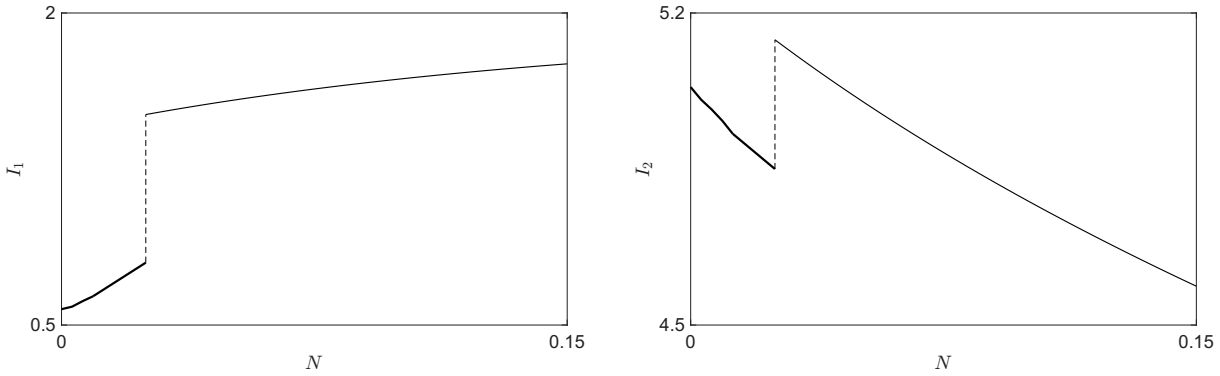


Figure 4.17: Evolution of $I_1$ and $I_2$ with respect to $N$, for $\epsilon = 0.5$. The thick line characterizes a limit cycle.

Figure 4.18 shows the evolution of the involvements as functions of $\epsilon$ with $N = 0.025$. For partner 1, the behaviour is similar to the case $\delta = 0$, since the cyclic region was already not advantageous for him. For partner 2, however, the result is reversed: once variability is taken into account, the cyclic regime is no longer preferable. Instead, he attains the highest effective involvement immediately after the bifurcation.

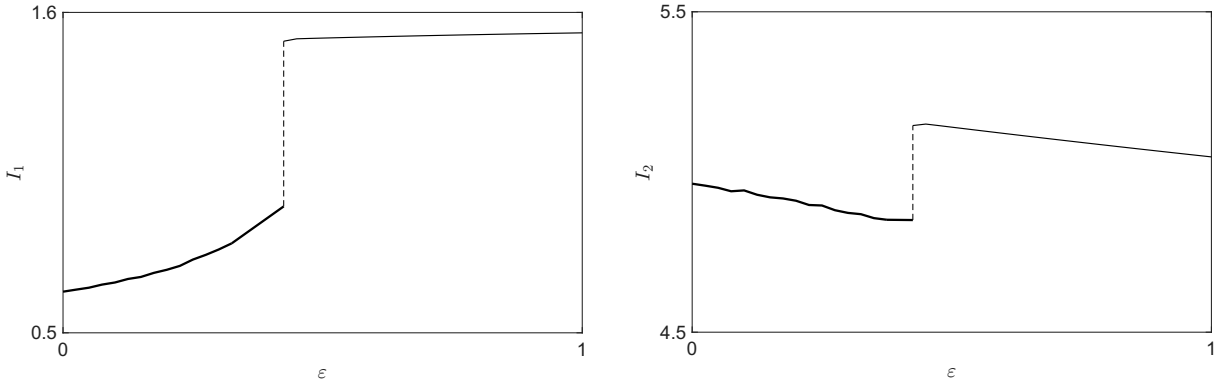


Figure 4.18: Evolution of $I_1$ and $I_2$ with respect to $\epsilon$, for $N = 0.025$. The thick line characterizes a limit cycle.

To complete the comparison between neglecting and accounting for oscillations, we also report the evolution of involvement in the $(\epsilon, N)$ parameter space. Figure 4.19 confirms the previous findings, showing a strong penalization of the cyclic region once variability

is taken into account, particularly evident for partner 1 (Figure 4.19a). For partner 2 (Figure 4.19b) and for the couple as a whole (Figure 4.19c), the qualitative behaviour changes: the cyclic region is now penalized and no longer appears favourable, especially in terms of total involvement.

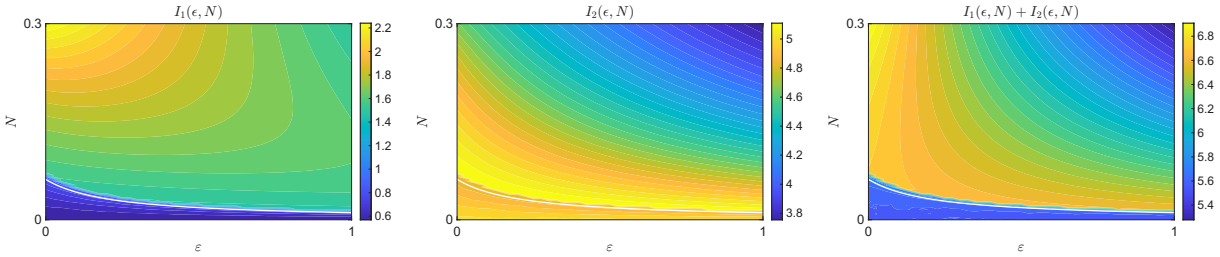


(a) (b) (c)

Figure 4.19: Evolution of individual and collective emotional involvement in the $(\epsilon, N)$ parameter space: (a) involvement $I_1$; (b) involvement $I_2$; (c) total involvement $(I_1 + I_2)$.

Figure 4.20c reports the comparison with the childless configuration. We still observe a general improvement for partner 1 (Figure 4.20a), with the most favourable situation located in the upper-left corner of the $(\epsilon, N)$ parameter space, corresponding to a stationary regime in which partner 2 assumes most of the caregiving responsibilities. Partner 2 (Figure 4.20b), on the other hand, generally experiences a decrease in involvement, although he performs better immediately above the bifurcation curve. For the couple as a whole (Figure 4.20c), the cyclic region corresponds to a net increase in total involvement. This is likely due to the fact that, in that region, the gain in involvement of partner 1 outweighs the decrease experienced by partner 2. Nevertheless, when considering the partners individually, the cyclic region does not represent the most favourable configuration.

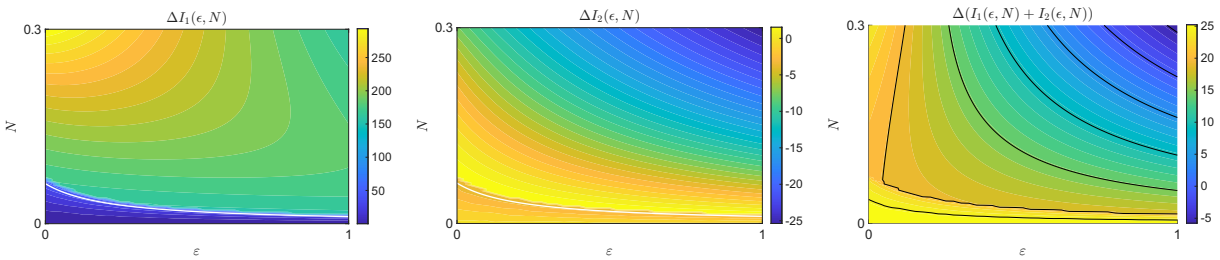


(a) (b) (c)

Figure 4.20: Comparison between the cases with and without a child in the $(\epsilon, N)$ parameter space: (a) variation in involvement $\Delta I_1$; (b) variation in involvement $\Delta I_2$; (c) variation in total involvement $\Delta(I_1 + I_2)$.

These results suggest that the evaluation of cyclic dynamics crucially depends on how emotional involvement is measured. When only the mean level is considered, the cyclic regime may appear advantageous in some parameter regions. However, once variability is explicitly penalized, reflecting partners who are sensitive to recurrent oscillations, the same regime becomes less desirable, and stationary configurations are generally preferred. In this sense, the comparison highlights that the perceived quality of a relational configuration depends not only on its average intensity, but also on its temporal variability.

Finally, we consider the configuration corresponding to the parameter values reported in Table 4.1, with $A_1 = 0.0333$ and $A_2 = 0.05$, in which both a supercritical and a subcritical Hopf bifurcation, the latter being closely followed by a fold of limit cycles, are present. We report here the analysis for $\delta = 0$, omitting the case $\delta = 1$, as it leads to qualitatively similar conclusions to those obtained in the previous configuration.

Figure 4.21 shows the variation in involvements as function of increasing $N$, with $\epsilon = 0.5$. The transition across the bifurcation curves is clearly visible: first, a smooth change occurs when crossing the supercritical Hopf bifurcation, followed by an abrupt variation when crossing the subcritical one and the associated fold of limit cycles. In line with previous findings, partner 1's involvement increases, whereas partner 2's decreases.

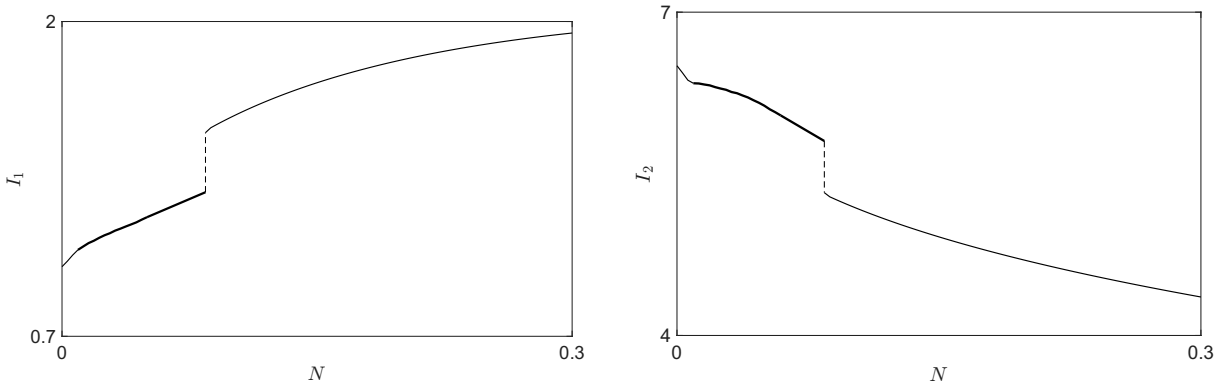


Figure 4.21: Evolution of $I_1$ and $I_2$ with respect to $N$, for $\epsilon = 0.5$. The thick line characterizes a limit cycle.

We then analyze how the involvements vary as functions of $\epsilon$, with $N = 0.1$. In this case, both bifurcations cannot be observed, since there is no fixed value of $N$ for which varying $\epsilon$ allows the system to cross both Hopf bifurcation curves. What is clearly visible, however, is the crossing of the subcritical Hopf bifurcation together with the fold of limit cycles. Consistently with the previous findings, both partners attain higher involvement when they assume a larger share of caregiving responsibilities. Moreover, partner 2 still prefers the cyclic region.

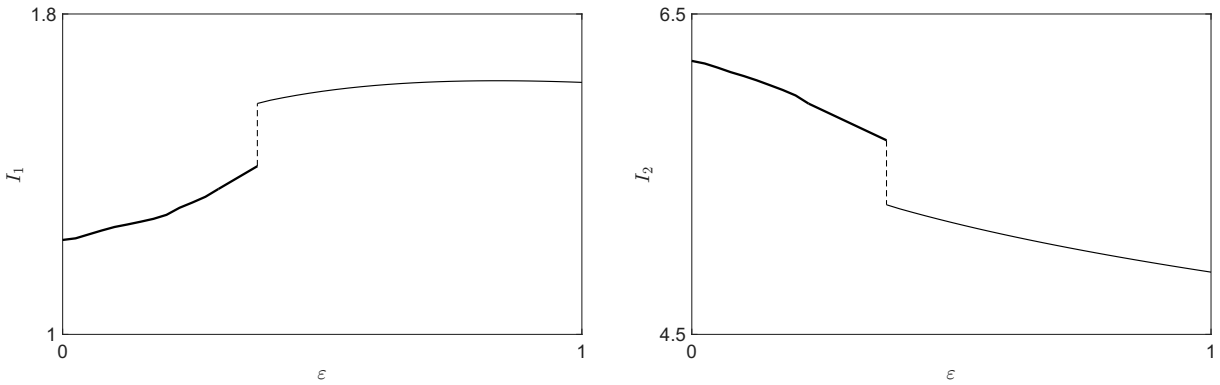


Figure 4.22: Evolution of $I_1$ and $I_2$ with respect to $\epsilon$, for $N = 0.1$. The thick line characterizes a limit cycle.

Since the lower Hopf bifurcation is supercritical, while the upper Hopf is subcritical, as shown in Figure 4.23, the combined effects of these two bifurcations are clearly reflected in the equilibrium levels (or the mean values along the cycle, computed according to Equation (4.2)) of involvement. The supercritical Hopf produces a smooth variation of involvement as the system enters or exits the cyclic regime, whereas the subcritical Hopf, together with the associated fold of limit cycles, leads to an abrupt change in the equilibrium levels, which is particularly evident in Figure 4.23b and Figure 4.23c.

As in the previous configurations, partner 1's level of involvement generally increases as caregiving intensity $N$ grows. In particular, the highest involvement levels are attained in the region below the first (supercritical) Hopf bifurcation, where the dynamics are stationary. Moreover, partner 1 benefits most when caregiving responsibilities are predominantly assigned to partner 2, especially for sufficiently large values of $N$. In this region, which corresponds to the upper-left corner in Figure 4.23a, the "stabilizing" effect of caregiving and the redistribution of emotional responsiveness combine to produce the most favorable configuration for him. This suggests that the progressive increase in caregiving demand acts as a stabilizing factor that, for partner 1, enhances sustained emotional involvement, particularly when he is not primarily responsible for the caregiving load. In line with previous findings, for partner 1 the region under the catastrofic bifurcation is the best configuration, always preferring to take the caregiving responsibilities. A different pattern emerges when focusing on partner 2. For him, the cyclic regime corresponds to higher levels of involvement, and the transition across the subcritical Hopf bifurcation and the associated fold of limit cycles produces a pronounced and abrupt reduction in engagement. In particular, once the system crosses the upper bifurcation boundary and the cycle disappears, the loss of the high-involvement phases results in a sudden decrease in emotional intensity. This confirms that partner 2 benefits from the oscillatory dynamics

and is penalized by the abrupt stabilization induced by the subcritical transition. Considering the total involvement (Figure 4.23c), we observe that the cyclic region maintains an approximately constant average level of affection, which does not represent the worst outcome for the couple. In fact, the least favorable configuration for total involvement occurs when partner 1 assumes most of the caregiving load in the stationary regime. This case clearly illustrates how the coexistence of supercritical and subcritical bifurcations generates a layered dynamical structure, in which smooth and abrupt transitions coexist and have distinct quantitative consequences on emotional involvement for each partner and for the couple as a whole.

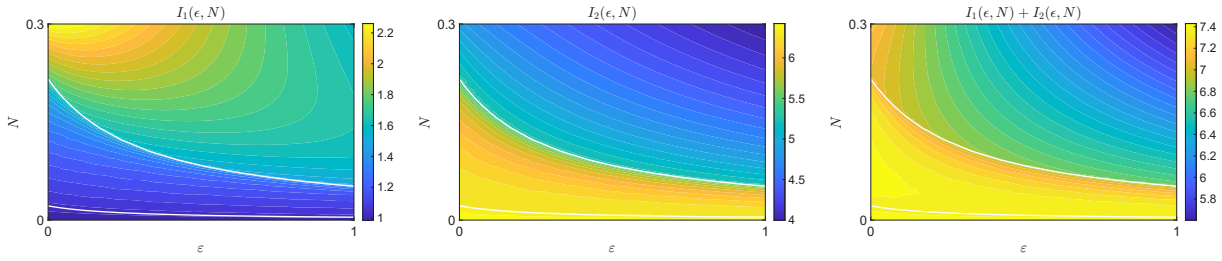


(a) (b) (c)

Figure 4.23: Evolution of individual and collective emotional involvement in the $(\epsilon, N)$ parameter space: (a) involvement $I_1$; (b) involvement $I_2$; (c) total involvement $(I_1 + I_2)$.

As a final step, we compare this configuration with the childless case (Figure 4.24). The qualitative pattern remains consistent with the previous analyses. In particular, partner 1 experiences a positive variation in emotional involvement across the $(\epsilon, N)$ parameter space (Figure 4.24a), whereas partner 2 benefits from the cyclic regime, which minimizes his involvement loss (Figure 4.24b). Once the system crosses the upper bifurcation boundary and converges to stationary configuration, partner 2's involvement decreases more markedly. Regarding the total involvement (Figure 4.24c), the variation remains close to zero within the cyclic region, indicating that oscillatory dynamics preserve overall affection levels relative to the childless case. The most favorable configuration for the couple as a whole is attained in the upper-left region of the parameter sapce, where caregiving intensity is high and predominantly assigned to partner 2.

The analysis carried out in this section shows that introducing a child through constant caregiving demands profoundly reshapes the dynamical structure of the couple. The presence of the parameters $N$ and $\epsilon$ does not merely shift involvement levels, but may alter the qualitative regime of the system by inducing or suppressing cyclic behavior.

The results highlight three main features. First, the qualitative nature of the bifurcation,

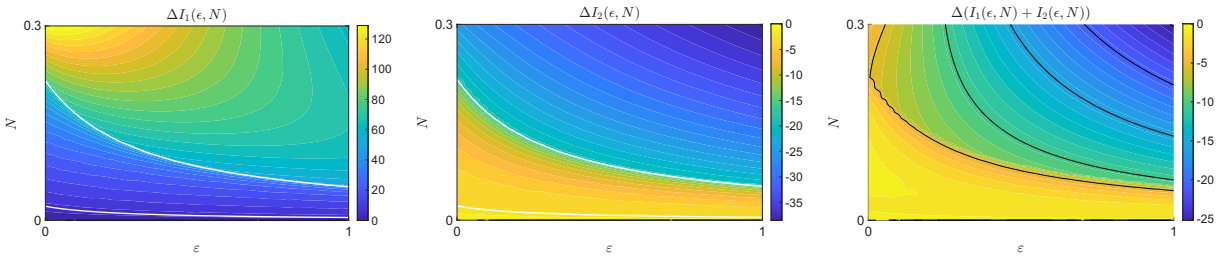


(a) (b) (c)

Figure 4.24: Comparison between the cases with and without a child in the $(\epsilon, N)$ parameter space: (a) variation in involvement $\Delta I_1$; (b) variation in involvement $\Delta I_2$; (c) variation in total involvement $\Delta(I_1 + I_2)$.

supercritical or subcritical, strongly affects how involvement varies with caregiving parameters, with the subcritical Hopf systematically followed by a nearly coincident fold of limit cycles. In the presence of a supercritical Hopf bifurcation, transitions between cyclic and stationary regimes are gradual, leading to smooth variations in average involvement. By contrast, a subcritical Hopf bifurcation, combined with a fold of limit cycles, generates abrupt regime shifts, producing discontinuous changes in emotional levels across the bifurcation boundary. Second, the redistribution of caregiving responsibilities generates structurally asymmetric outcomes, systematically benefiting one partner while penalizing the other. Third, stationarity and individual involvement do not generally coincide, revealing a tension between minimizing oscillations and maximizing emotional intensity. This tension becomes even more evident when accounting for sensitivity to variability through the parameter $\delta$. When oscillations are not penalized ($\delta = 0$), cyclic regimes may appear advantageous in terms of average involvement. However, once variability is explicitly incorporated into the evaluation of emotional engagement ($\delta > 0$), stationary configurations often become preferable, as recurrent fluctuations reduce effective involvement. The perceived desirability of a regime therefore depends not only on its mean intensity, but also on the partners' sensitivity to oscillatory variability. Although a stationary regime may intuitively appear preferable, as it eliminates emotional fluctuations, our analysis shows that this is not always the case from the perspective of involvement levels. In several configurations, cyclic dynamics yield higher average emotional engagement for one partner, or even for the couple as a whole, while stabilization may reduce peak involvement. Hence, the disappearance of oscillations should not be automatically interpreted as an improvement in relational quality.

Overall, parenthood acts as a structural perturbation of the relational system, capable of modifying both "stability" properties and the distribution of emotional benefits. In the

configurations examined so far, caregiving has been modeled as a constant demand. In the next section, we extend the analysis by allowing the child's needs to vary over time, thereby introducing an additional source of dynamical forcing into the system.

## 4.3. The effect of the transition to parenthood under oscillatory caregiving demands

In the previous Section, caregiving demands were modeled as constant over time. We now extend the analysis by considering a configuration in which the child's needs vary periodically, introducing an explicit temporal modulation in the caregiving load. Such a scenario is far from unrealistic. In everyday life, caregiving intensity often fluctuates due to external factors such as school schedules, the presence of a nanny or grandparents, seasonal arrangements (e.g., summer camps), or other institutional settings that alternate periods of lower and higher demands. These variations naturally generate oscillatory patterns in the time devoted to childcare. In this Section, we therefore investigate the effects of periodic caregiving demands on the emotional dynamics of the couple. It is worth emphasizing that, even if the present analysis focuses on oscillations in the overall caregiving load, an analogous approach could be adopted by keeping the total demand constant while allowing the distribution of responsibilities to vary periodically (for instance, in situations where one partner temporarily lives in another city for work-related reasons). In both cases, the system is subject to a time-dependent external forcing that may interact with its intrinsic dynamics.

We model the caregiving demands $N$ as a time-dependent quantity characterized by a mean value $\bar{N}$, a pulsation $\omega$ and an oscillation amplitude $\rho \in [0, 1]$. In particular, we assume that $N(t)$ varies periodically around its mean value with amplitude $\rho$ and pulsation $\omega$, so that the period is $T = \frac{2\pi}{\omega}$. These quantities are explicitly represented in Figure 4.25.

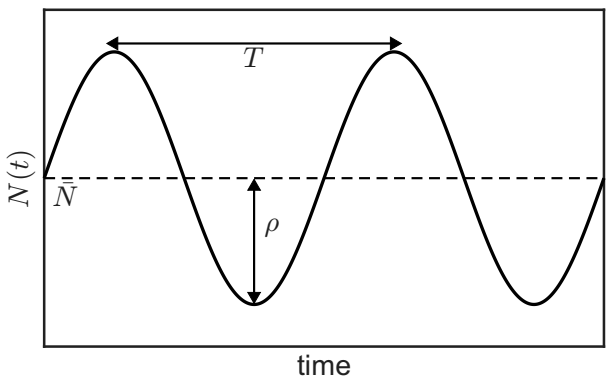


Figure 4.25: Example of periodic caregiving demands.

We begin by considering a configuration in which *endogenous* oscillations are already present, meaning that the cyclic behavior arises from the intrinsic structure of the system. For clarity, we report the corresponding parameter set in Table 4.2. These parameters generate the configuration previously analyzed in Section 4.2, for which the bifurcation diagram is reported in Figure 4.8.

Starting from this intrinsically oscillatory regime, we introduce an *exogenous* periodic forcing in the caregiving demand, defined as $N(t) = \bar{N}(1+\rho \sin(\omega t))$, where the oscillation is externally imposed and does not arise from the internal dynamics of the couple. We first consider small values of the amplitude $\rho$, and then progressively increasing it in order to assess its influence on the dynamics. Subsequently, we consider a stationary configuration located outside the cyclic region of the parameter space and introduce a periodic caregiving signal, in order to analyze how a stable stationary regime responds to an external time-dependent forcing. In each analysis, the mean value is fixed at $\bar{N} = N$, while the pulsation $\omega$, the oscillation amplitude $\rho$, and any modifications to the parameter set reported in Table 4.2 are specified explicitly.

| **Parameter** | **Value** |
|---|---|
| $\alpha_1$ | 0.1 |
| $\alpha_2$ | 0.1 |
| $\gamma_1$ | 1 |
| $\gamma_2$ | 1 |
| $A_1$ | 0.0333 |
| $A_2$ | 0.05 |
| $\beta$ | 5 |
| $k$ | 1 |
| $R_1^-$ | $-1.5$ |
| $R_2^+$ | 0.5 |
| $R_2^-$ | $-0.05$ |
| $s$ | 20 |
| $\sigma$ | 6 |
| $m$ | 8 |
| $N$ | 0.1245 |
| $\epsilon$ | 0.2 |

Table 4.2: Parameter values for model 4.1.

To analyze this setting, we first examine the temporal evolution of the state variables.

We then represent the corresponding attractor in the $(x_1, x_2)$-phase plane and construct its Poincarè map. The Poincaré map is obtained by sampling the state variables $(x_1, x_2)$ at discrete time instants separated by the forcing period. More precisely, we record the values of the system at times $t_k = \frac{2k\pi}{\omega}$, corresponding to each completed period of the external forcing. The resulting sequence of points (stroboscopic map) in the phase plane provides a discrete representation of the long-term dynamics under periodic forcing. For a more detailed theoretical discussion about periodic, quasi-periodic and chaos regimes, we refer to [30, 47].

As anticipated, we begin the analysis by considering a couple that already exhibits endogenous cyclic dynamics, using the set parameter in Table 4.2. We then introduce a periodic forcing in the caregiving demand with small amplitude $\rho = 0.1$ and pulsation $\omega = 0.12$, in order to investigate how the intrinsic oscillatory regime responds to a low-intensity external modulation. Figure 4.26 displays the temporal evolution of the state variables $x_1(t)$ and $x_2(t)$. The observed dynamics are neither purely periodic nor chaotic. Instead, the trajectories exhibit a quasi-periodic regime: although the oscillatory pattern appears recurrent over time, successive peaks do not coincide exactly, and the waveform does not repeat with a single fixed period. This behavior arises from the interaction between two frequencies: the intrinsic frequency of the endogenous oscillations and the frequency $\omega$ of the external periodic forcing. Since these frequencies are not rationally related, the system does not synchronize with the forcing, and no closed periodic orbit is formed.

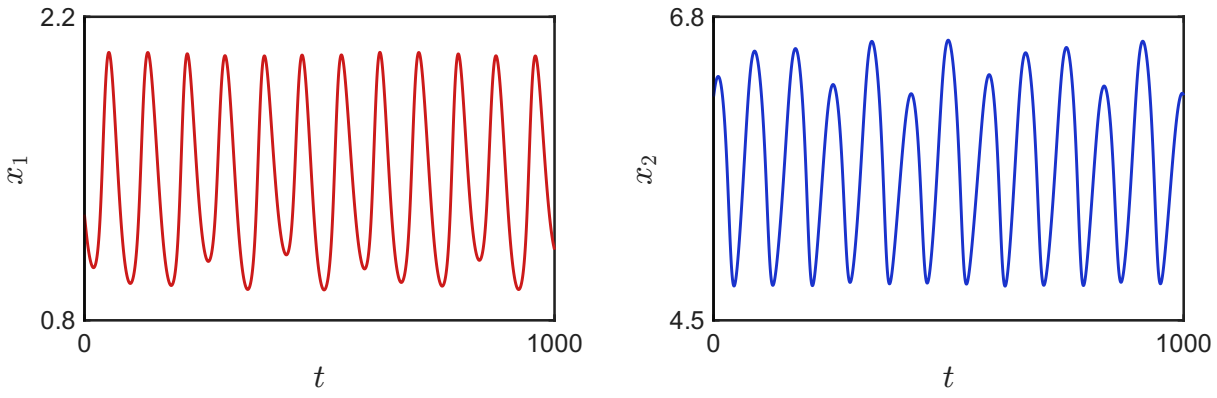


Figure 4.26: Time series of $x_1(t)$ (left) and $x_2(t)$ (right). $\rho = 0.1$ and $\omega = 0.12$.

As illustrated in Figure 4.27a, the long-term attractor of the system corresponds to a quasi-periodic behaviour. In the $(x_1, x_2)$ phase plane, the motion evolves on a torus: the trajectory winds around this toroidal surface, wrapping around it in a non-repeating manner. Unlike a periodic orbit, it never closes onto itself, it continues to wind around the torus indefinitely, progressively filling it in a dense way without retracing the same closed

path. This interpretation is further supported by the Poincaré map, shown in Figure 4.27b. By sampling the system at time instants separated by the forcing period $T = \frac{2\pi}{\omega}$ (stroboscopic map), the discrete points lie along a closed curve, which is the signature of quasi-periodic motion on a torus.

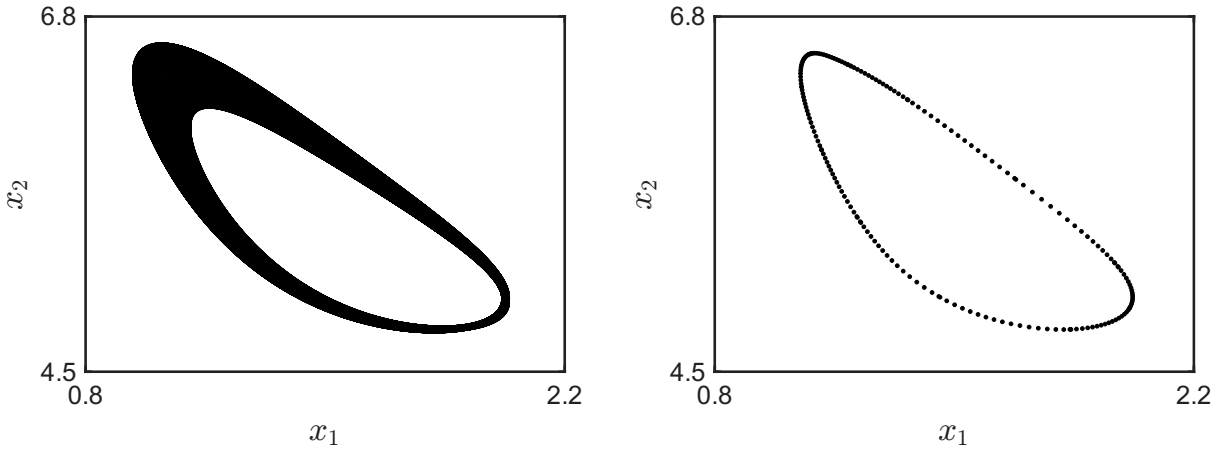


(a) Torus in the $(x_1, x_2)$-phase plane.

(b) Poincaré section showing a closed curve.

Figure 4.27: Quasi-periodic dynamics under periodic caregiving forcing, with $\rho = 0.1$ and $\omega = 0.12$.

These results show that when a small-amplitude periodic forcing is introduced into a system that already exhibits endogenous oscillations, the long-term dynamics may evolve toward a quasi-periodic regime. In this configuration, the trajectory does not repeat itself exactly, as in a periodic orbit, but neither does it display sensitive dependence on initial conditions or irregular behavior typical of chaos. Instead, the motion remains structured and bounded, governed by the interaction of two frequencies. The emergence of an invariant torus can therefore be interpreted as an intermediate dynamical organization between strict periodicity and chaotic motion. While periodic dynamics correspond to complete synchronization and temporal regularity, and chaos reflects strong unpredictability and instability, quasi-periodic motion preserves coherence without exact repetition. From a relational perspective, this regime may represent a configuration in which the couple maintains an organized emotional structure, but with a modulation induced by fluctuating caregiving demands. The dynamics are neither fully "stabilized" nor disrupted; instead, they reflect a continuous adaptation to external oscillations. In this sense, the toroidal attractor suggests a balance between intrinsic relational rhythms and exogenous influences, where the couple's internal dynamics are not destroyed by the forcing, but reshaped into a more complex yet still coherent pattern. It indicates that small oscillatory caregiving demands can modulate, without "destabilizing", the emotional interaction between partners.

If we now increase the forcing amplitude to $\rho = 0.282$, while keeping the other parameters fixed, the system undergoes a qualitative transition and chaotic dynamic emerges.

Figure 4.28 displays the temporal evolution of the two state variables. In contrast to the quasi-periodic case, no regular or recurrent pattern can be identified. The oscillations appear irregular, with amplitudes and intervals between peaks varying unpredictably over time. However, it is important to note that chaos cannot be conclusively established solely from time-series inspection. At first glance, chaotic and quasi-periodic signals may appear similar, as both lack exact repetition. The distinguishing feature of chaos lies in its sensitive dependence on initial conditions and the geometric structure of its attractor, rather than in the mere absence of periodicity.

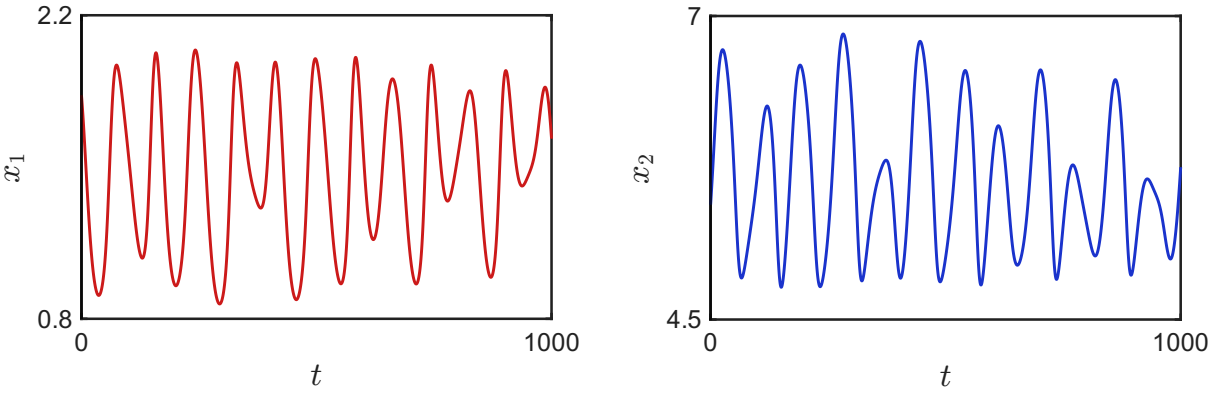


Figure 4.28: Time series of $x_1(t)$ (left) and $x_2(t)$ (right). $\rho = 0.282$ and $\omega = 0.12$.

We further examine the geometric structure of the attractor in Figure 4.29a. In contrast to the quasi-periodic case, the torus is no longer visible, instead, the attractor loses its regular smooth structure and is replaced by an irregular set confined to a bounded region of the $(x_1, x_2)$-phase plane. The trajectory does not lie on a closed curve nor on a smooth surface. Rather, it appears to wander unpredictably within a well-defined region, without settling into periodic or quasi-periodic motion. This irregular geometry, combined with boundedness, is characteristic of a chaotic attractor. The chaotic nature of the dynamics becomes more evident when analyzing the corresponding Poincaré map, illustrated in Figure 4.29b. In contrast to the quasi-periodic regime, where the sampled points lie on a smooth closed curve corresponding to a torus, the Poincaré section in the present case does not produce a finite set of points (as in periodic motion) nor a "continuous" curve. Instead, the points appear scattered within a bounded region of the phase plane, forming a complex geometric structure. This scattered distribution is indicative of a strange attractor: although the motion remains confined to a limited region, the discrete points

generated by the Poincaré map do not organize into a smooth manifold. Therefore, the Poincaré map clearly distinguishes the chaotic regime from the quasi-periodic one, revealing that the loss of the torus corresponds to the emergence of irregular dynamics driven by strong external forcing.

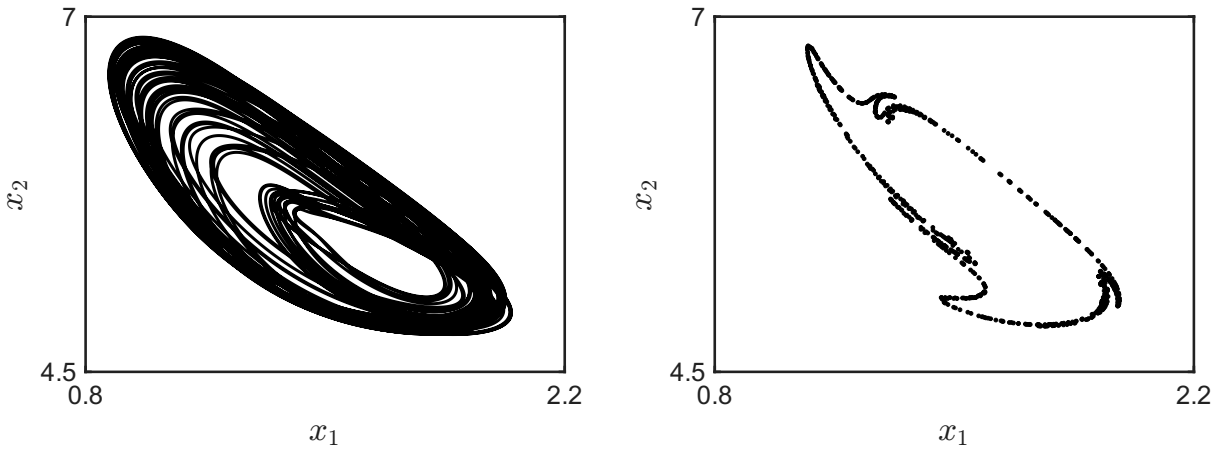


(a) Strange attractor in the $(x_1, x_2)$-phase plane.

(b) Poincaré section showing a scattered set characteristic of chaos.

Figure 4.29: Chaotic dynamics under strong periodic caregiving forcing, with $\rho = 0.282$ and $\omega = 0.12$.

These results show that increasing the amplitude of oscillatory caregiving demands may induce qualitative transitions in the dynamical behavior of the system. As the forcing amplitude grows, the intrinsic oscillatory regime first loses its simple periodic structure and evolves into a quasi-periodic motion on a torus. In this intermediate configuration, the emotional dynamics become more complex, yet remain organized and bounded. For sufficiently large amplitudes, however, the invariant torus breaks down and chaotic dynamics emerge. In this regime, the temporal evolution of mutual involvement becomes highly irregular and sensitive to initial conditions. Although the motion remains confined within a bounded region of the phase plane, long-term predictability is lost. This progression suggests that oscillatory caregiving demands act as a modulation parameter that can progressively reshape the relational dynamics, moving the system from regular oscillations to increasingly complex regimes. In the present case, chaos arises through the destruction of a quasi-periodic torus.

The analysis and the figures presented above are obtained by initializing the system directly on the attractor, thus eliminating the transient phase. For completeness, we also report in Figure 4.30 the temporal evolution of the two state variables when the system starts from a periodic regime and, at a given time $t$, a large-amplitude periodic caregiving

modulation is introduced. This scenario may be interpreted as the onset of regularly varying external demands, for instance due to changes in the child's daily routine (e.g., the beginning of school attendance). The system initially displays periodic oscillations, which are then replaced by chaotic motion following the activation of the external modulation.

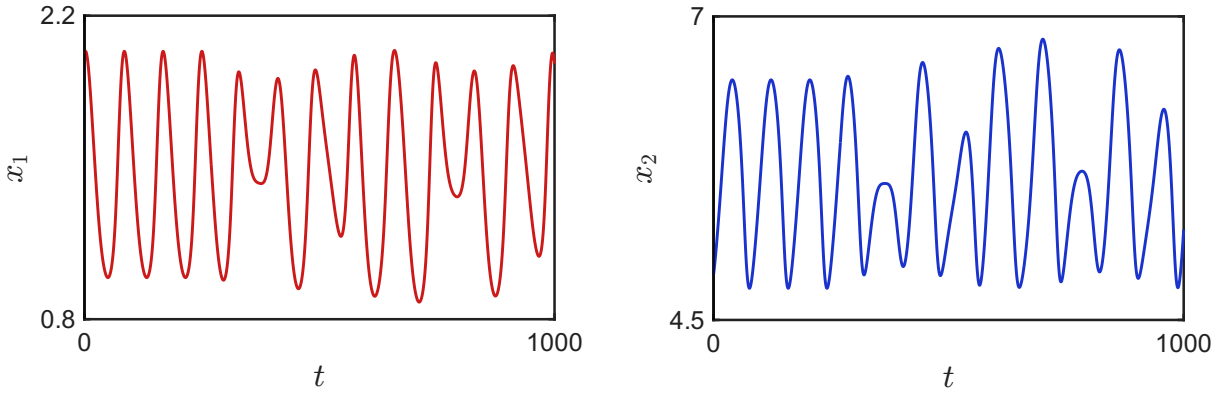


Figure 4.30: Time series of $x_1(t)$ (left) and $x_2(t)$ (right). Beginning of chaotic behaviour after introducing periodic caregiving with $\rho = 0.282$ and $\omega = 0.12$.

As a final step, we consider a configuration in which, under constant caregiving demands, the system lies in a stationary regime characterized by a stable equilibrium. Specifically, we adopt the parameter set reported in Table 4.2 with $N = 0.08$ and $\epsilon = 0.8$, for which the autonomous system exhibits no intrinsic oscillations. We then introduce a strong periodic modulation in the caregiving demand, with amplitude $\rho = 0.8$ and pulsation $\omega = 0.2$, and analyze the resulting dynamics.

As shown in Figure 4.31, the temporal evolution of the involvement variables becomes irregular and highly variable. Unlike the quasi-periodic regime observed previously, no structured modulation pattern can be identified, and successive oscillations differ significantly in amplitude and timing.

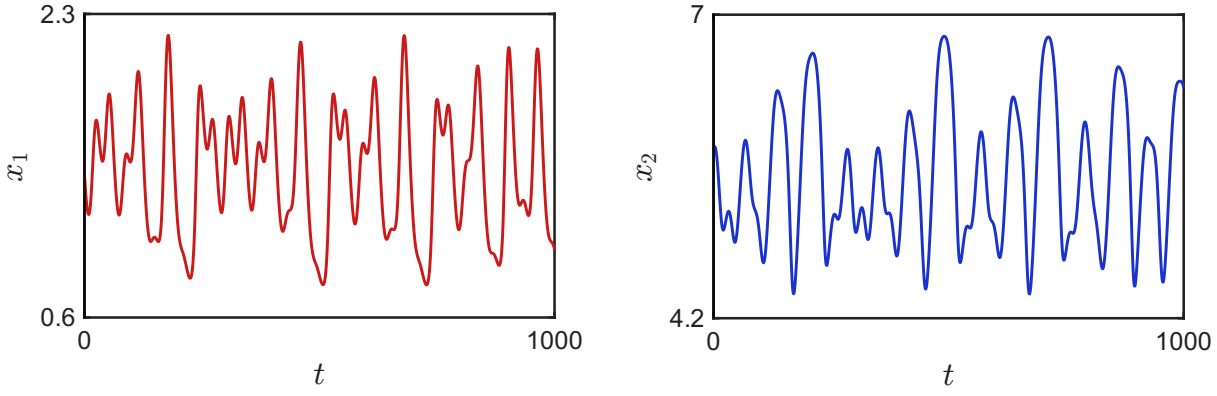


Figure 4.31: Time series of $x_1(t)$ (left) and $x_2(t)$ (right). $\rho = 0.8$ and $\omega = 0.2$.

To better characterize the regime, we examine the geometric structure of the attractor in the $(x_1, x_2)$-phase plane (Figure 4.32a). The trajectory no longer converges to a fixed point nor organizes along a smooth curve. Instead, it evolves within a bounded region, forming an irregular set without closed trajectories, which suggests the presence of a strange attractor. The chaotic nature of the dynamics is further supported by the corresponding Poincaré map in Figure 4.32b. When the system is sampled at intervals equal to the forcing period, the discrete points do not collapse to a finite set nor lie on a smooth closed curve. Rather, they form a scattered structure within a bounded region, consistent with chaotic dynamics driven by strong external forcing.

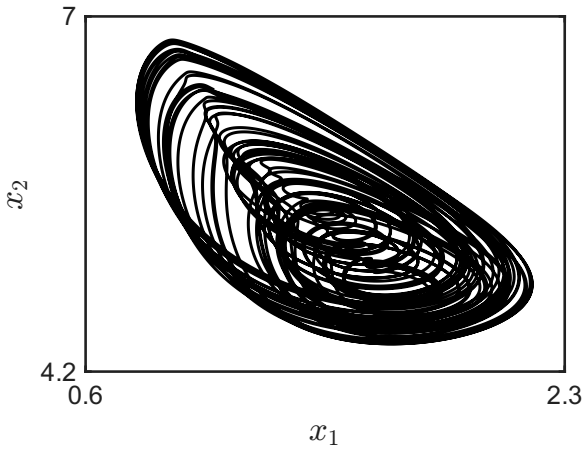


(a) Strange attractor in the $(x_1, x_2)$-phase plane.

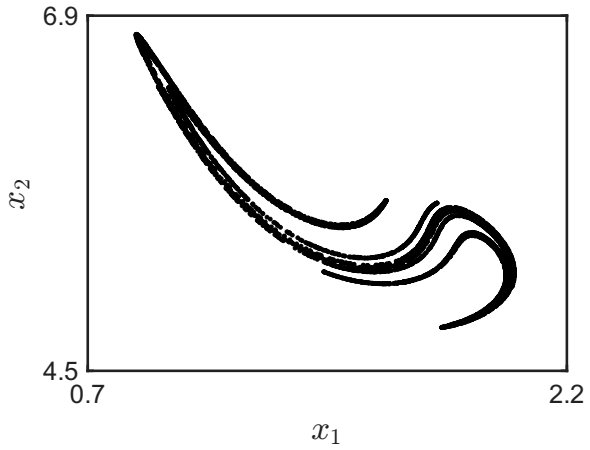


(b) Poincaré section showing a scattered set characteristic of chaos.

Figure 4.32: Chaotic dynamics under strong periodic caregiving forcing, with $\rho = 0.8$ and $\omega = 0.2$.

This last result shows that, even in the absence of endogenous oscillations, sufficiently strong exogenous periodic forcing may drive the system into a chaotic regime. In other words, intrinsic periodicity is not a necessary condition for the emergence of complex and unpredictable dynamics: external modulation alone can generate chaos. The recurrent oscillations in caregiving demands act as a nonlinear forcing mechanism that continuously perturbs the emotional interaction between the partners. When the amplitude of this modulation is large enough, the system is no longer able to maintain a stable equilibrium or a regular oscillatory pattern, and the interaction becomes highly sensitive to initial conditions, leading to irregular and effectively unpredictable fluctuations in mutual involvement. From a relational perspective, this suggests that strong and persistent variability in caregiving demands may destabilize emotional coordination, even when the couple would otherwise exhibit stable stationary behavior. Thus, oscillatory caregiving

demands can act not only as a source of modulation or enrichment of existing dynamics, but also as a mechanism capable of generating qualitative "instability" in an otherwise "stable" relational system.

As in the previous case of transition from a periodic regime to chaos, we now display the temporal evolution of a system initially in a stationary regime, to which a strong external modulation is introduced. In Figure 4.33, the dynamics initially correspond to a stable equilibrium, visible as a constant value over time. Once the periodic forcing is activated, the trajectory departs from the equilibrium and evolves toward a chaotic regime.

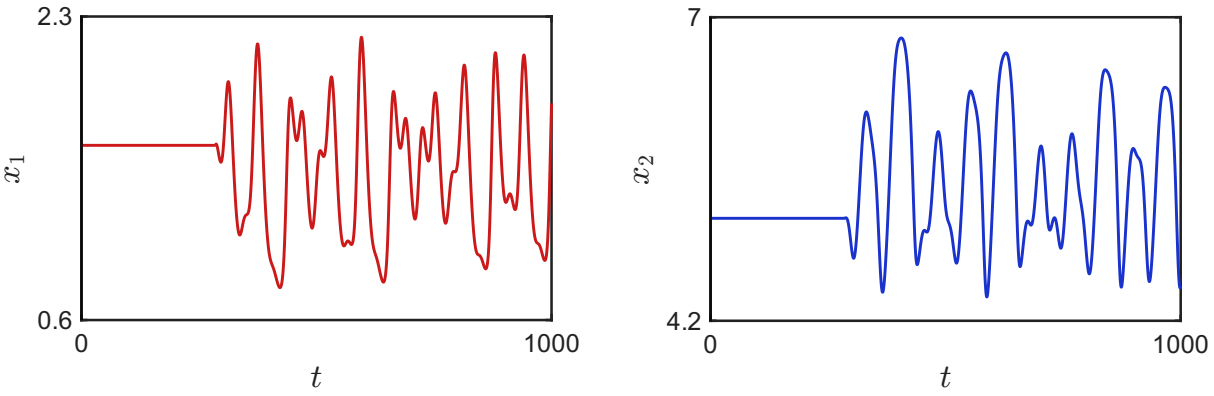


Figure 4.33: Time series of $x_1(t)$ (left) and $x_2(t)$ (right).

The analysis developed in this section shows that allowing caregiving demands to vary periodically introduces a qualitatively new layer of dynamical complexity into the model. When external modulation is weak, the interaction between intrinsic oscillations and periodic forcing may generate quasi-periodic motion on an invariant torus, preserving bounded and structured dynamics while eliminating exact periodicity. As the amplitude of the forcing increases, the torus may break down, giving rise to chaotic attractors characterized by irregular yet deterministic evolution. Remarkably, strong periodic modulation can also induce chaotic behavior in configurations that, under constant caregiving demands, exhibit a stable equilibrium. This demonstrates that complex dynamics need not originate from intrinsic oscillatory mechanisms: time-dependent external forcing alone may produce rich and highly sensitive responses in the emotional interaction between partners.

Taken together with the results obtained under constant caregiving demands, this chapter highlights how the transition to parenthood can reshape the relational dynamics of a couple in multiple ways. Constant caregiving modifies mean equilibrium levels and may alter the qualitative regime through bifurcations, while oscillatory caregiving acts as a time-dependent forcing capable of generating periodic, quasi-periodic, or chaotic responses. Importantly, different dynamical regimes correspond to distinct patterns of

emotional coordination. Periodic motion reflects regular and synchronized oscillations; quasi-periodic dynamics introduce structured but non-repeating modulation; chaotic attractors produce bounded yet highly irregular fluctuations. These regimes differ not only in their geometric properties in phase space, but also in their implications for predictability and temporal coherence of mutual involvement. Overall, this chapter shows that both the intensity and the temporal variability of caregiving demands can significantly reshape the behavior of the couple. Parenthood, within this framework, is not associated with a single deterministic outcome, but rather with a spectrum of possible dynamical regimes, whose emergence depends on both individual characteristics and the temporal structure of caregiving demands.

# 5 | Conclusions and future developments

In this work, we presented a modified version of the love dynamics model introduced in [38], incorporating caregiving demands $N$ and the sharing of responsibilities $\epsilon$ in order to account for the transition to parenthood. By embedding these parameters into the original dynamical framework, we extended the analysis from dyadic romantic interaction to a setting in which external demands reshape the emotional exchange between partners. The model was tested across different couple configurations (secure-secure, insecure-secure, and insecure-secure synergic) under constant caregiving demands. The case of time-varying caregiving was investigated specifically for the insecure-secure synergic configuration, where the coexistence of intrinsic asymmetry and nonlinear effects allows for a richer spectrum of dynamical behaviors.

Empirical research suggests that the transition to parenthood does not lead to a unique relational outcome [10, 15, 24, 27, 39]. Our theoretical results are consistent with this perspective. Rather than identifying a single dynamical pattern, the model highlights how caregiving intensity and its distribution affect equilibrium levels of emotional involvement and the qualitative robustness of the couple.

For non-synergic individuals, increasing caregiving demands generally reduces both individual and collective levels of involvement when demands are constant. However, important differences emerge depending on attachment style. In particular, in asymmetric configurations involving an insecure partner, involvement may increase for the insecure individual when caregiving responsibilities are predominantly assumed by the secure partner. This counterintuitive effect reflects how caregiving load modifies emotional responsiveness differently across attachment profiles. Thus, the impact of increasing $N$ cannot be understood independently of the relational structure and individual characteristics of the partners. The distribution of responsibilities, however, plays a more subtle role: while certain allocations promote robustness or convergence to a stationary regime, they do not necessarily maximize emotional engagement for both partners. The model therefore sug-

gests that the transition to parenthood involves a structural trade-off between stability, equity, and intensity of emotional engagement. In particular, couples may face alternative configurations depending on their relational priorities: they may choose allocations that produce similar proportional reductions of involvement, leading to greater equity and, in some cases, robustness; alternatively, they may favor asymmetric distributions that preserve higher total emotional involvement at the cost of imbalance between partners. Importantly, the allocation that equalizes losses does not always coincide with the one that maximizes total involvement. Hence, the model highlights that different caregiving strategies correspond to different relational objectives, and that the optimal configuration depends on whether the couple prioritizes equity, total emotional intensity, or qualitative robustness of the interaction.

In couples characterized by the coexistence of insecurity and synergism, periodic variations in caregiving demands introduce an additional level of dynamical complexity. Weak oscillatory modulation can transform periodic dynamics into quasi-periodic motion on tori, preserving bounded and organized interaction while eliminating exact repetition. Strong modulation may generate chaotic attractors, even in configurations that are stationary under constant demands. These results highlight the importance not only of caregiving intensity but also of its temporal variability.

Overall, the thesis shows that caregiving parameters can significantly reshape the behavior of the couple. Parenthood, within this framework, is neither inherently "stabilizing" nor "destabilizing"; rather, it reshapes the geometry of the dynamical system, potentially leading to stationary, oscillatory, quasi-periodic, or chaotic regimes depending on the interaction between attachment styles and caregiving structure.

Despite its explanatory potential, the model remains simplified: it is deterministic, limited to two state variables, and treats caregiving demands as externally imposed rather than emerging from a broader family system.

Future developments may include the introduction of stochastic perturbations, adaptive redistribution of responsibilities, or the modeling of the child as an additional dynamic agent interacting dynamically with both parents. Further research could also integrate social and environmental influences into the dynamical framework. An essential next step is empirical validation. Longitudinal studies, such as those already conducted in the literature (e.g., [14]), following couples over several years during and after the transition to parenthood, could provide data suitable for confronting the model with observed relational trajectories. Repeated assessments through structured questionnaires or diary-based measures could approximate variables related to emotional involvement, perceived

robustness or fragility, and possible oscillatory patterns in interaction quality. Such data would allow parameter estimation and qualitative evaluation of the predicted regimes.

From a theoretical perspective, the model could also be extended by incorporating additional attachment profiles, such as ambivalent or disorganized attachment [1, 6], whose interaction patterns may generate qualitatively different dynamics. Moreover, future work could explicitly account for demographic and contextual factors that influence the transition to parenthood, including age, gender differences, socioeconomic status, and financial conditions [4, 26], that may act as additional control parameters shaping the structure of relational dynamics.

By combining attachment theory with nonlinear dynamical systems, this thesis offers a conceptual bridge between mathematical modeling and the psychological study of intimate relationships. The results suggest that major life transitions, such as parenthood, may be understood not as events leading to a single predictable outcome, but as structural perturbations capable of generating a spectrum of relational trajectories.

# Bibliography

[1] M. D. S. Ainsworth, M. C. Blehar, E. Waters, and S. N. Wall. *Patterns of attachment.* 1978.

[2] J. Belsky and J. J. Kelly. The transition to parenthood. 1994.

[3] J. Belsky, G. B. Spanier, and M. Rovine. Stability and change in marriage across the transition to parenthood. *Journal of Marriage and Family*, 45:567–577, 1983.

[4] I. Bogdan, M. N. Turliuc, and O. S. Candel. Transition to parenthood and marital satisfaction: A meta-analysis. *Frontiers in Psychology*, 13, 7 2022. ISSN 16641078. doi: 10.3389/fpsyg.2022.901362.

[5] C. Borg. The romantic love narrative of a couple who are also parents to a disabled child. Technical report, 2019.

[6] J. Bowlby. *Attachment and loss. Volume I: Attachment.* Basic Books, a member of the Perseus Books Group, 1969. ISBN 0465005438.

[7] J. Bowlby. *Attachment and loss. Volume II: Separation anxiety and anger.* Basic Books, 1973. ISBN 0465076912.

[8] J. Bowlby. *Attachment and Loss. Volume III: Loss sadness and depression.* 1980.

[9] D. A. Cohn, D. H. Silver, C. P. Cowan, P. A. Cowan, and J. Pearson. Working models of childhood attachment and couple relationships. *Journal of Family Issues*, 13:432–449, 1992. ISSN 15525481.

[10] C. P. Cowan and P. A. Cowan. *When partners become parents : the big life change for couples.* Lawrence Erlbaum Associates, Mahwah, NJ, 2000 - 1992. ISBN 9780805835595.

[11] C. P. Cowan, P. A. Cowan, G. Heming, E. Garrett, W. S. Coysh, H. Curtis-Boles, and A. J. Boles III. Transitions to parenthood: His, hers, and theirs. *Journal of family issues*, 6(4):451–481, 1985.

[12] A. Dhooge, W. Govaerts, Y. A. Kuznetsov, H. G. Meijer, and B. Sautois. New features

of the software matcont for bifurcation analysis of dynamical systems. *Mathematical and Computer Modelling of Dynamical Systems*, 14:147–175, 4 2008. ISSN 13873954.

[13] B. D. Doss and G. K. Rhoades. The transition to parenthood: Impact on couples' romantic relationships. *Current Opinion in Psychology*, 13:25–28, 2017. ISSN 2352250X.

[14] B. D. Doss, G. K. Rhoades, S. M. Stanley, and H. J. Markman. The effect of the transition to parenthood on relationship quality: An 8-year prospective study. *Journal of Personality and Social Psychology*, 96:601–619, 3 2009. ISSN 00223514.

[15] E. D. Dyer. Parenthood as crisis: A re-study. 25:196–201, 1963.

[16] M. E. Feinberg, M. Xia, G. M. Fosco, R. E. Heyman, and S. M. Chow. Dynamical systems modeling of couple interaction: a new method for assessing intervention impact across the transition to parenthood. *Prevention Science*, 18:887–898, 2017. ISSN 13894986.

[17] J. Fillo, J. A. Simpson, W. S. Rholes, and J. L. Kohn. Dads doing diapers: Individual and relational outcomes associated with the division of childcare across the transition to parenthood. *Journal of Personality and Social Psychology*, 108:298–316, 2015. ISSN 00223514.

[18] J. Gottman, C. Swanson, and J. Murray. The mathematics of marital conflict: Dynamic mathematical nonlinear modeling of newly wed marital interaction. *Journal of Family Psychology*, 13:3–19, 1999.

[19] J. Gottman, C. Swanson, and K. Swanson. A general systems theory of marriage: Nonlinear difference equation modeling of marital interaction. 2002.

[20] J. M. Gottman, J. D. Murray, C. C. Swanson, R. Tyson, and K. R. Swanson. *The Mathematics of Marriage: Dynamic Nonlinear Models*. 2002.

[21] A. Gragnani, S. Rinaldi, and G. Feichtinger. Cyclic dynamics in romantic relationships. *International Journal of Bifurcation and Chaos*, 07:2611–2619, 1997.

[22] D. Griffin and K. Bartholomew. Models of the self and other: Fundamental dimensions underlying measures of adult attachment. *Journal of Personality and Social Psychology*, 1994.

[23] N. K. Grote and M. S. Clark. Perceiving unfairness in the family: Cause or consequence of marital distress? *Journal of Personality and Social Psychology*, 80:281–293, 2001. ISSN 00223514.

[24] L. S. Hackel and D. N. Ruble. Changes in the marital relationship after the first baby is born: predicting the impact of expectancy disconfirmation. *Journal of personality and social psychology*, 62 6:944–57, 1992.

[25] R. Hidaka, I. Sobue, M. Yano, R. Ito, and T. Kobayashi. Development of a japanese version of the index of sexual satisfaction for use in couples with young children. *Behavioral Sciences*, 12, 2022. ISSN 2076328X.

[26] E. S. Kluwer. From partnership to parenthood: A review of marital change across the transition to parenthood. *Journal of Family Theory & Review*, 2:105–125, 2010. ISSN 1756-2570.

[27] E. S. Kluwer and M. D. Johnson. Conflict frequency and relationship quality across the transition to parenthood. *Journal of Marriage and Family*, 69:1089–1106, 2007. ISSN 00222445.

[28] E. S. Kluwer, J. A. M. Heesink, and E. V. D. Vliert. The marital dynamics of conflict over the division of labor. *Journal of Marriage and Family*, 59:635–653, 1997.

[29] J. L. Kohn, S. W. Rholes, J. A. Simpson, A. M. L. Martin, S. S. Tran, and C. L. Wilson. Changes in marital satisfaction across the transition to parenthood: The role of adult attachment orientations. *Personality and Social Psychology Bulletin*, 38:1506–1522, 11 2012. ISSN 01461672.

[30] Y. A. Kuznetsov. *Elements of Applied Bifurcation Theory*. 2004.

[31] E. E. Lemasters. Parenthood as crisis. Technical report, 1957.

[32] G. Levinger. Toward the analysis of close relationships. *Journal of Experimental Social Psychology*, 16(6):510–544, 1980. ISSN 0022-1031.

[33] S. K. Nelson, K. Kushlev, T. English, E. W. Dunn, and S. Lyubomirsky. In defense of parenthood: Children are associated with more joy than misery. *Psychological Science*, 24:3–10, 2013. ISSN 14679280.

[34] W. S. Rholes, J. A. Simpson, L. Campbell, and J. Grich. Adult attachment and the transition to parenthood. *Journal of Personality and Social Psychology*, 81:421–435, 2001. ISSN 00223514.

[35] S. Rinaldi and A. Gragnani. Love dynamics between secure individuals: A modeling approach. *Nonlinear Dynamics, Psychology, and Life Sciences*, 2, 1998.

[36] S. Rinaldi and A. Gragnani. Minimal models for dyadic processes: A review. *The Complex Matters of th Mind*, 1998.

[37] S. Rinaldi, F. D. Rossa, and F. Dercole. Love and appeal in standard couples. *International Journal of Bifurcation and Chaos*, 20:2443–2451, 2010. ISSN 02181274.

[38] S. Rinaldi, F. D. Rossa, F. Dercole, A. Gragnani, and P. Landi. *Modeling love dynamics*. World Scientific, 2016. ISBN 9789814696319.

[39] C. S. Russell. Transition to parenthood: Problems and gratifications. *Journal of Marriage and Family*, 36:294–302, 1974.

[40] E. Scharfe and K. Bartholomew. Reliability and stability of adult attachment patterns. *Personal Relationships*, 1:23–43, 1994. ISSN 14756811.

[41] A. F. Shapiro, J. M. Gottman, and S. Carrère. The baby and the marriage: Identifying factors that buffer against decline in marital satisfaction after the first baby arrives. *Journal of Family Psychology*, 14:59–70, 2000. ISSN 08933200.

[42] J. A. Simpson and W. S. Rholes. Adult attachment orientations and well-being during the transition to parenthood, 2019. ISSN 2352250X.

[43] J. A. Simpson, S. W. Gangestad, and M. Lerma. Perception of physical attractiveness: Mechanisms involved in the maintenance of romantic relationships. *Journal of Personality and Social Psychology*, 59:1192–1201, 1990.

[44] J. C. Sprott. Dynamical models of love. *Nonlinear Dynamics, Psychology, and Life Sciences*, 8, 2004.

[45] R. Sternberg and M. Barnes. *The Psychology of Love*. Yale University Press, 1988. ISBN 9780300039504.

[46] S. H. Strogatz. Love affairs and differential equations. Technical report, 1988.

[47] S. H. Strogatz. *Nonlinear Dynamics and Chaos*. 1994.

[48] O. Taubman-Ben-Ari. *Pathways and barriers to parenthood: Existential concerns regarding fertility, pregnancy, and early parenthood*. Springer International Publishing, 2019. ISBN 9783030248642.

# List of Figures

# List of Tables